Critical phenomena in complex networks

S. N. Dorogovtsev* and A. V. Goltsev†

Departamento de Física, Universidade de Aveiro, 3810-193 Aveiro, Portugal and A. F. Ioffe Physico-Technical Institute, 194021 St. Petersburg, Russia

J. F. F. Mendes‡

Departamento de Física, Universidade de Aveiro, 3810-193 Aveiro, Portugal

(Published 6 October 2008)

The combination of the compactness of networks, featuring small diameters, and their complex architectures results in a variety of critical effects dramatically different from those in cooperative systems on lattices. In the last few years, important steps have been made toward understanding the qualitatively new critical phenomena in complex networks. The results, concepts, and methods of this rapidly developing field are reviewed. Two closely related classes of these critical phenomena are considered, namely, structural phase transitions in the network architectures and transitions in cooperative models on networks as substrates. Systems where a network and interacting agents on it influence each other are also discussed. A wide range of critical phenomena in equilibrium and growing networks including the birth of the giant connected component, percolation, k-core percolation, phenomena near epidemic thresholds, condensation transitions, critical phenomena in spin models placed on networks, synchronization, and self-organized criticality effects in interacting systems on networks are mentioned. Strong finite-size effects in these systems and open problems and perspectives are also discussed.

DOI: 10.1103/RevModPhys.80.1275 PACS number(s): 64.60.Bd, 64.60.aq, 64.60.ah, 89.75.Fb

CONTENTS

*sdorogov@fis.ua.pt
†goltsev@fis.ua.pt
‡jfmendes@fis.ua.pt

I. INTRODUCTION

By definition, complex networks are networks with more complex architectures than classical random graphs with their "simple" Poissonian distributions of connections. The great majority of real-world networks, including the World Wide Web, the Internet, basic cellular networks, and many others, are complex ones. The complex organization of these nets typically implies a skewed distribution of connections with many hubs, strong inhomogeneity, and high clustering, as well as nontrivial temporal evolution. These architectures are quite compact (with a small degree of separation between vertices), infinitely dimensional (which is a fundamental property of various networks) small worlds.

Physicists have intensively studied the structural properties of complex networks since the end of the 1990s, but the current focus is essentially on cooperative systems defined on networks and on dynamic processes taking place on networks. In recent years, it was revealed that the extreme compactness of networks together with their complex organization result in a wide spectrum of nontraditional critical effects and intriguing singularities. We review the progress made in the understanding of the unusual critical phenomena in networked systems.

One should note that the current interest in critical effects in networks can be explained not only by numerous important applications. Critical phenomena in disordered systems were among the hottest fundamental topics of condensed-matter theory and statistical physics at the end of the 20th century. Complex networks imply a new type of strong disorder, almost unknown in condensed matter, where fluctuations of structural characteristics of vertices (e.g., the number of neighbors) may far exceed their mean values. One should add to this large-scale inhomogeneity, which is significant in many complex networks, statistical properties of vertices may strongly differ in different parts of a network.

The first studies of a critical phenomenon in a network were by Solomonoff and Rapoport (1951) and Erdős and Rényi (1959), who introduced classical random graphs and described the structural phase transition of the emergence of a giant connected component. These simplest random graphs were widely used by physicists as substrates for various cooperative models.

Another basic small-world substrate in statistical mechanics and condensed-matter theory is the Bethe lattice (an infinite regular tree) and its diluted variations. The Bethe lattice usually allows exact analytical treatment, and, typically, each new cooperative model is inspected on this network (as well as on the infinite fully connected graph).

Studies of critical phenomena in complex networks essentially use approaches developed for these two fundamental, related classes of networks: classical random graphs and the Bethe lattices. In these graphs and many others, small and finite loops (cycles) are rare and not essential; the architectures are locally treelike, which is a simplifying feature that is extensively exploited. One may say that the existing analytical and algorithmic approaches already allow one to exhaustively analyze any locally treelike network and to describe cooperative models on it. Moreover, the tree ansatz works well even in numerous situations for loopy and clustered networks. We discuss various techniques based on this stan-

dard approximation. It is these techniques, including, in particular, the Bethe-Peierls approximation, that are the main instruments for studying the critical effects in networks.

Critical phenomena in networks include a wide range of issues: structural changes in networks, the emergence of critical—scale-free—network architectures, various percolation phenomena, epidemic thresholds, phase transitions in cooperative models defined on networks, critical points of diverse optimization problems, transitions in coevolving couples—a cooperative model and its network substrate, transitions between different regimes in processes taking place on networks, and many others. We show that many of these critical effects are closely related and universal for different models and may be described and explained in the framework of a unified approach.

The outline of this review is as follows. In Sec. II, we describe basic models of complex networks. Section III contains a discussion of structural phase transitions in networks: the emergence of the giant connected component of a complex random network and various related percolation problems. In Sec. IV, we describe condensation phenomena, where a finite fraction of edges, triangles, etc. are attached to a single vertex. Section V overviews the main critical effects in disease spreading. Sections VI, VII, and VIII discuss the Ising, Potts, and *XY* models on networks. We use the Ising model to introduce the main techniques of analyzing interacting systems in networks. A comprehensive description of this analytical apparatus is given by Dorogovtsev *et al.* (2007), which also discusses a number of issues omitted here. Section IX contains a general phenomenological approach to critical phenomena in networks. In Secs. X and XI, we discuss the specifics of synchronization and self-organized criticality on networks. Section XII describes a number of other critical effects in networks. In Sec. XIII, we indicate open problems and perspectives of this field. Note that for a few interesting problems, as yet uninvestigated for complex networks, we discuss only the classical random graph case.

II. MODELS OF COMPLEX NETWORKS

In this section, we introduce basic networks, which are used as substrates for models, and basic terms. For more details, see the books and reviews of Albert and Barabási (2002), Dorogovtsev and Mendes (2002, 2003), Bollobás and Riordan (2003), Newman (2003a), Pastor-Satorras and Vespignani (2004), Boccaletti *et al.* (2006), Durrett (2006), and Caldarelli (2007).

A. Structural characteristics of networks

A random network is a statistical ensemble, where each member—a particular configuration of vertices and edges—is realized with some prescribed probability (statistical weights). Each graph of N vertices may be described by its adjacency $N\times N$ matrix (a_{ij}), where $a_{ij}=0$ if edges between vertices i and j are absent, and $a_{ij}>0$ otherwise. In simple graphs, $a_{ij}=0,1$. In weighted networks, the adjacency matrix elements are non-negative numbers that may be noninteger—the weights of edges. The simplest characteristic of a vertex in a graph is its degree q, which is the number of its nearest neighbors. In physics this is often called connectivity. In directed graphs, at least some of the edges are directed, and one should introduce in and out degrees. For random networks, a vertex degree distribution $P(q)$ is the first statistical measure.

The presence of connections between the nearest neighbors of a vertex i is described by its clustering coefficient $C(q_i)\equiv t_i/[q_i(q_i-1)/2]$, where t_i is the number of triangles (loops of length 3) attached to this vertex and $q_i(q_i-1)/2$ is the maximum possible number of such triangles. Note that, in general, the mean clustering $\langle C\rangle \equiv\Sigma_q P(q)C(q)$ should not coincide with the clustering coefficient (transitivity) $C\equiv\langle t_i\rangle/\langle q_i(q_i-1)/2\rangle$, which is three times the ratio of the total number of triangles in the network and the total number of connected triples of vertices. A connected triple here is a vertex with its two nearest neighbors. A triangle can be treated as three connected triples, which explains the coefficient 3.

A loop (simple cycle) is a closed path visiting each vertex only once. By definition, trees are graphs without loops.

For each pair of vertices i and j connected by at least one path, one can introduce the shortest path length, the intervertex distance ℓ_{ij}, the corresponding number of edges in the shortest path. The distribution of intervertex distances $\mathcal{P}(\ell)$ describes the global structure of a random network, and the mean intervertex distance $\bar{\ell}(N)$ characterizes the "compactness" of a network. In finite-dimensional systems, $\bar{\ell}(N)\sim N^{1/d}$. We, however, mostly discuss networks with the small-world phenomenon—the small worlds, where $\bar{\ell}$ increases with the total number of vertices N more slowly than any positive power, i.e., $d=\infty$ (Watts, 1999). Typically, in networks, $\bar{\ell}(N)\sim\ln N$ (Albert *et al.*, 1999).

Another important characteristic of a vertex (or edge) is its betweenness centrality (or, which is the same, *load*), which is the number of shortest paths between other vertices that run through this vertex (or edge). In stricter terms, the betweenness centrality $b(v)$ of vertex v is defined as follows. Let $s(i,j)>0$ be the number of shortest paths between vertices i and j. Let $s(i,v,j)$ be the number of these paths passing through vertex v. Then $b(v)\equiv\Sigma_{i\neq v\neq j}s(i,v,j)/s(i,j)$. A betweenness centrality distribution is introduced for a random network.

A basic notion is a giant connected component analogous to the percolation cluster in condensed matter. This is a set of mutually reachable vertices and their interconnections, containing a finite fraction of vertices of an infinite network. Note that, in physics, the infinite-network limit, $N\to\infty$, is also called the thermodynamic limit. The relative size of the giant component (the relative number of its vertices) and the size distribution of

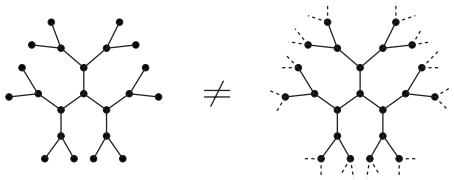

FIG. 1. Cayley tree (on the left) vs the Bethe lattice (on the right).

finite connected components describe the topology of a random network.

B. Cayley tree versus Bethe lattice

Two different regular graphs are extensively used as substrates for cooperative models. Both are small worlds if the degree of their vertices exceeds 2. In the (regular) Cayley tree, explained in Fig. 1, a finite fraction of vertices are dead ends. These vertices form a sharp border of this tree. There is a central vertex, equidistant from the boundary vertices. The presence of the border essentially determines the physics of interacting systems on the Cayley tree.

The Bethe lattice is an infinite regular graph (see Fig. 1). All vertices in a Bethe lattice are topologically equivalent, and boundaries are absent. Note that, in the thermodynamic limit, the random regular graphs asymptotically approach Bethe lattices (Johnston and Plecháč, 1998). The random regular graph is a maximally random network of vertices of equal degree. The graph is constructed of vertices with the same number (degree) of stubs by connecting pairs of the stubs in all possible ways.

C. Equilibrium random trees versus growing ones

Remarkably, random connected trees (i.e., consisting of a single connected component) may or may not be small worlds (Burda *et al.*, 2001; Bialas *et al.*, 2003). The equilibrium random connected trees have extremely extended architectures characterized by the fractal (Hausdorff) dimension $d_h=2$, i.e., $\bar{\ell}(N)\sim N^{1/2}$. These random trees are the statistical ensembles that consist of all possible connected trees with N labeled vertices, taken with equal probability; see Fig. 2, left side. The degree distributions of these networks are rapidly decreasing, $P(q)=e^{-1}/(q-1)!$. However, one may arrive at scale-free degree distributions $P(q)\sim q^{-\gamma}$ by, for example, introducing special degree-dependent statistical weights of different members of these ensembles. In this case, if $\gamma\geqslant 3$, then $d_h=2$, and if $2<\gamma<3$, then the fractal dimension is $d_h=(\gamma-1)/(\gamma-2)>2$.

In contrast to this, growing (causal, recursive) random connected trees are small worlds. These trees are constructed by sequential attachment of new (labeled) vertices; see Fig. 2, right side. The rule of this attachment or, alternatively, specially introduced degree-dependent weights for different realizations, determines the resulting degree distributions. The mean intervertex distance in these graphs $\bar{\ell}\sim\ln N$. Thus, even with identical degree distributions, equilibrium and growing random trees have quite different geometries.

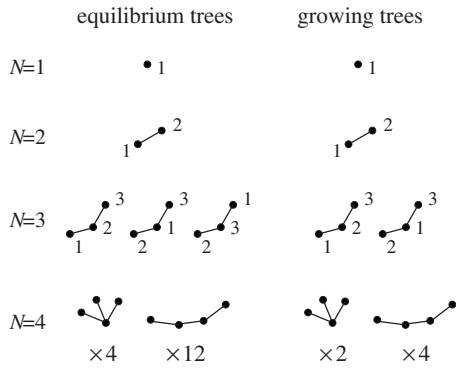

FIG. 2. Statistical ensembles of equilibrium random connected trees (left-hand side) and growing connected trees (right-hand side) for $N=1,2,3,4$. The ensemble of equilibrium trees consists of all possible connected trees of N labeled vertices, where each tree is taken with the same weight. The ensemble of growing (causal) trees is the following construction. Its members are all possible connected trees of size N that can be made by sequential attachment of new labeled vertices. Each of these trees of N vertices is taken with the same weight. Notice that at $N=3$ one of the labeled graphs of the equilibrium ensemble is absent in the ensemble of growing trees. At $N=4$, the numbers of isomorphic graphs is indicated in both ensembles. (By definition, isomorphic graphs differ from each other only by vertex labels.) Already at $N=4$ the equilibrium random tree is less compact, since the probability of realization of the chain is higher in this case.

D. Classical random graphs

Two of the simplest models of random networks are so close (asymptotically coincident in the thermodynamic limit) that they are together called classical random graphs. The Gilbert model, or the G_{np} model (Solomonoff and Rapoport, 1951; Gilbert, 1959), is a random graph where an edge between each pair of N vertices is present with a fixed probability p.

Slightly more difficult for analytical treatment is the Erdős-Rényi model (Erdős and Rényi, 1959), which is also called the G_{nm} model, and is a statistical ensemble where all members—all possible graphs with a given numbers of vertices N and edges M—have equal probability of realization. The relationship between the Erdős-Rényi and the Gilbert models is given by the following equalities for the mean degree: $\langle q\rangle=2M/N=pN$. If $\langle q\rangle/N\to 0$ as $N\to\infty$, a network is *sparse*, i.e., it is far more sparse than a fully connected graph. So the Gilbert model is sparse when $p(N\to\infty)\to 0$.

Classical random graphs are maximally random graphs under a single constraint—a fixed mean degree $\langle q\rangle$. Their degree distribution is Poissonian, $P(q)=e^{-\langle q\rangle}\langle q\rangle^q/q!$.

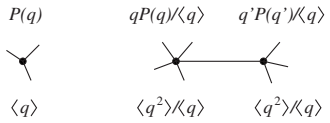

FIG. 3. Distribution of connections and the mean degree of a randomly chosen vertex (on the left) differ sharply from those of end vertices of a randomly chosen edge (on the right).

E. Uncorrelated networks with arbitrary degree distributions

We emphasize that in a random network, the degree distribution of the nearest neighbors $P_{\mathrm{NN}}(q)$ (or the degree distribution of an end vertex of a randomly chosen edge) does not coincide with the vertex degree distribution $P(q)$. In general random networks,

$$P_{\mathrm{NN}}(q) = qP(q)/\langle q\rangle, \quad \langle q\rangle_{\mathrm{NN}} = \langle q^2\rangle/\langle q\rangle > \langle q\rangle; \tag{1}$$

see Fig. 3. These simple relations play a key role in the theory of complex networks.

By definition, in uncorrelated networks correlations are absent. In particular, there are no correlations between degrees of the nearest neighbors. That is, the joint distribution of degrees of the nearest-neighbor vertices factors into the product

$$P(q,q') = qP(q)q'P(q')/\langle q\rangle^2. \tag{2}$$

Thus, the architectures of uncorrelated networks are determined by their degree distributions. The Erdős-Rényi and Gilbert models are simple uncorrelated networks. Below we list the models of complex uncorrelated networks, which are actually very close to each other in the thermodynamic limit. In this limit, all these networks are locally treelike (if they are sparse, of course), with only infinite loops.

1. Configuration model

Direct generalization of the Erdős-Rényi graphs is the famous configuration model formulated by Bollobás (1980); see also Bender and Canfield (1978). In graph theory, these networks are also called random labeled graphs with a given degree sequence. The configuration model is the statistical ensemble, whose members are realized with equal probability. These members are all possible graphs with a given set $\{N_q = NP(q)\}$, $q = 0,1,2,3,\ldots$, where N_q is the number of vertices of degree q. In simple terms, the configuration model provides maximally random graphs with a given degree distribution $P(q)$.

This construction may also be portrayed in more graphic terms. (i) Attach stubs (edge halves) to N vertices according to a given sequence of numbers $\{N_q\}$. (ii) Pair randomly chosen stubs together into edges. Since stubs of the same vertex may be paired together, the configuration model, in principle, allows a number of loops of length 1 as well as multiple connections. Fortunately, these may be neglected in many problems.

Using Eq. (1) gives $z_2 = \langle q^2\rangle - \langle q\rangle$ for the mean number of the second nearest neighbors of a vertex. That is, the mean branching coefficient of the configuration model and, generally, of an uncorrelated network is

$$B = z_2/z_1 = (\langle q^2\rangle - \langle q\rangle)/\langle q\rangle, \tag{3}$$

where $z_1 = \langle q\rangle$. Consequently, the mean number of the ℓth nearest neighbors of a vertex is $z_\ell = z_1(z_2/z_1)^{\ell-1}$. So the mean intervertex distance is $\bar{\ell}(N) \cong \ln N/\ln(z_2/z_1)$ (Newman *et al.*, 2001).

The distribution of the intervertex distances in the configuration model is quite narrow. Its relative width approaches zero in the thermodynamic limit. In other words, in this limit almost all vertices of the configuration model are mutually equidistant (Dorogovtsev *et al.*, 2003a). We emphasize that this remarkable property is valid for a wide class of networks with the small-world phenomenon.

The configuration model was generalized to bipartite networks (Newman *et al.*, 2001). By definition, a bipartite graph contains two kinds of vertices, and only vertices of different kinds may be interlinked. In short, the configuration model of a bipartite network is a maximally random bipartite graph with two given degree distributions for two types of vertices.

2. Static model

Direct generalization of the Gilbert model is the static one (Goh *et al.*, 2001; see also Chung and Lu, 2002, Soderberg, 2002, and Caldarelli *et al.*, 2002). These are graphs with a given sequence of desired degrees. The desired degrees $\{d_i\}$ play the role of "hidden variables" defined on vertices $i = 1,2,\ldots,N$. Pairs of vertices (ij) are connected with probabilities $p_{ij} = 1 - \exp(-d_i d_j/N\langle d\rangle)$. The degree distribution of the resulting network $P(q)$ tends to a given distribution of desired degrees at sufficiently large q. It is important that at small enough d_i the probability $p_{ij} \cong d_i d_j/N\langle d\rangle$. The exponential function keeps the probability below 1 even if $d_i d_j > N\langle d\rangle$, which is possible if the desired degree distribution is heavy tailed.

3. Statistical mechanics of uncorrelated networks

It is also easy to generate random networks using a standard thermodynamic approach; see Burda *et al.* (2001), Bauer and Bernard (2002), and Dorogovtsev *et al.* (2003b). In particular, assuming that the number of vertices is constant, one may introduce "thermal" hopping of edges or their rewiring. These processes lead to relaxational dynamics in the system of edges connecting vertices. The final state of this relaxation process (an equilibrium statistical ensemble) may be treated as an "equilibrium random network." This network is uncorrelated if the rate or probability of rewiring depends only on degrees of host vertices and on degrees of targets, and, in addition, if rewirings are independent. The resulting diverse degree distributions are determined by two factors: a specific degree-dependent rewiring and the mean vertex degree in the network. Note that, if multiple connections are allowed, this construction is es-

sentially equivalent to the simple balls-in-boxes (or backgammon) model (Bialas *et al.*, 1997, 2000), where the ends of edges (balls) are statistically distributed among vertices (boxes).

4. Cutoffs of degree distributions

Heavy-tailed degree distributions $P(q)=\langle N(q)\rangle/N$ in finite networks inevitably end with a rapid drop at large degrees (the cutoff). Here $\langle N(q)\rangle$ is the number of vertices of degree q in a random network, averaged over all members of the corresponding statistical ensemble. Knowledge of the size dependence on the cutoff position $q_{\rm cut}(N)$ is critically important for estimating various size effects in complex networks. The difficulty is that the form of $q_{\rm cut}(N)$ is highly model dependent.

We present here estimates of $q_{\rm cut}(N)$ in uncorrelated scale-free networks, where $P(q)\sim q^{-\gamma}$. The results depend essentially on (i) whether exponent γ is above or below 3, and (ii) whether multiple connections are allowed in the network.

In the range $\gamma\geqslant 3$, the resulting estimates are the same in networks with multiple connections (Burda *et al.*, 2001) and without them (Dorogovtsev *et al.*, 2005). In this range, calculation of a degree distribution taking into account all members of a statistical network ensemble leads to $q_{\rm cut}(N)\sim N^{1/2}$. The total number of members in an equilibrium network ensemble (e.g., for the configuration model) is large, say, of the order of $N!$. However, in empirical research or simulations, ensembles under investigation have rather small numbers n of members—a whole ensemble may consist of a single empirically studied map or of a few runs in a simulation. Often, only a single network configuration is used as a substrate in simulations of a cooperative model. In these measurements, a natural cutoff of an observed degree distribution arises (Cohen *et al.*, 2000; Dorogovtsev *et al.*, 2001c). Its degree, much lower than $N^{1/2}$, is estimated from the following condition. In the n studied ensemble members, a vertex degree exceeding $q_{\rm cut}$ should occur once: $nN\int_{q_{\rm cut}(N)}^{\infty}dq\,P(q)\sim 1$. This gives the actually observable cutoff

$$q_{\rm cut}(N,\gamma\geqslant 3)\sim(nN)^{1/(\gamma-1)} \tag{4}$$

if $n\ll N^{(\gamma-3)/2}$, which is a typical situation, and $q_{\rm cut}(N,\gamma\geqslant 3)\sim N^{1/2}$ otherwise.

In the range $2<\gamma<3$, the cutoff depends essentially on the kind of uncorrelated network. If in an uncorrelated network multiple connections are allowed, then $q_{\rm cut}(N,2<\gamma<3)\sim N^{1/(\gamma-1)}$. In uncorrelated networks without multiple connections, $q_{\rm cut}(N,2<\gamma<3)\sim N^{1/2}\ll N^{1/(\gamma-1)}$ (Burda and Krzywicki, 2003), although see Dorogovtsev *et al.* (2005) for a different estimate for a specific model without multiple connections. For discussion of the cutoff problem in the static model in this range of exponent γ, see Lee *et al.* (2006).

Seyed-allaei *et al.* (2006) found that in scale-free uncorrelated networks with exponent $\gamma<2$, the cutoff is $q_{\rm cut}(N,1<\gamma<2)\sim N^{1/\gamma}$. They showed that the mean degree of these networks increases with N, namely, $\langle q\rangle\sim N^{(2-\gamma)/\gamma}$.

For the sake of completeness, we mention here that in growing scale-free recursive networks $q_{\rm cut}(N,\gamma>2)\sim N^{1/(\gamma-1)}$ (Dorogovtsev *et al.*, 2001c; Krapivsky and Redner, 2002; Waclaw and Sokolov, 2007). Note that growing networks are correlated.

F. Equilibrium correlated networks

The simplest correlations in a network are those between degrees of the nearest-neighbor vertices. These correlations are described by the joint degree-degree distribution $P(q,q')$. If $P(q,q')$ is not factorized, unlike equality (2), the network is correlated (Maslov and Sneppen, 2002; Newman, 2002b).

Networks, that are maximally random under the constraint that their joint degree-degree distributions $P(q,q')$ are fixed, naturally generalize uncorrelated networks. That is, only these correlations are present. These networks are still sometimes analytically treatable. In the hierarchy of equilibrium network models, this is the next higher level, after classical random graphs and uncorrelated networks with an arbitrary degree distribution. Note that networks with these correlations are still locally treelike in the sparse network regime. In this sense, they may be treated as random Bethe lattices.

These networks may be constructed in the spirit of the configuration model. An alternative construction (networks with hidden variables) directly generalizes the static model. These are networks where (i) a random hidden variable h_i with distribution $P_h(h)$ is assigned to each vertex, and (ii) each pair of vertices (ij) is connected by an edge with probability $p(h_i,h_j)$ (Caldarelli *et al.*, 2002; Soderberg, 2002; Boguñá and Pastor-Satorras, 2003). The resulting joint degree-degree distribution is determined by $P_h(h)$ and $p(h,h')$ functions.

G. Loops in networks

The above-described equilibrium network models share the convenient locally treelike structure in the sparse network regime. The number of loops $\mathcal{N}_L$ with length L in a network allows us to quantify this property. We stress that the total number of loops in these networks is in fact very large. Indeed, the typical intervertex distance $\sim\ln N$, so that the number of loops with lengths $\gtrsim\ln N$ should be large. On the other hand, there are few loops of smaller lengths. In simple terms, if the second moment of the degree distribution is finite in the thermodynamic limit, then the number of loops of any given finite length is finite even in an infinite network. Consequently, the probability that a finite loop passes through a vertex is quite small, which explains the treelikeness.

In more precise terms, the number of loops in uncorrelated undirected networks is given by (Bianconi and

Capocci, 2003; Bianconi and Marsili, 2005)

$$\mathcal{N}_L \sim \frac{1}{2L}\left(\frac{\langle q^2\rangle - \langle q\rangle}{\langle q\rangle}\right)^L, \tag{5}$$

which is valid for sufficiently short (at least, for finite) loops, so that the clustering coefficient $C(k)=C=\langle C\rangle = (\langle q^2\rangle - \langle q\rangle)^2/N\langle q\rangle^3$ (Newman, 2003b). In addition, there are exponentially many, $\ln \mathcal{N}_L \propto N$, loops of essentially longer lengths (roughly speaking, longer than the network diameter). These "infinite loops," as they are longer than a correlation length for a cooperative system, do not violate the validity of the tree approximation. Moreover, without these loops (in perfect trees) phase transitions are often impossible, as, e.g., in the Ising model on a tree. The mean number of loops of length L passing through a vertex of degree k is $\mathcal{N}_L(k) \approx [k(k-1)/\langle q\rangle N][(L-1)/L]\mathcal{N}_{L-1}$. With degree distribution cutoffs represented in Sec. II.E.4, Eq. (5) leads to finite $\mathcal{N}_L$ in uncorrelated networks with $\gamma>3$, and to a large number of loops

$$\mathcal{N}_L \sim (1/2L)(a/\langle q\rangle)^L N^{L(3-\gamma)/2} \tag{6}$$

for $2<\gamma<3$ and $\langle q^2\rangle \cong aN^{(3-\gamma)/2}$, where a is a constant. For the statistics of loops in directed networks, see Bianconi *et al.* (2008). Note that Eqs. (5) and (6) indicate that even the sparse uncorrelated networks are actually loopy if $\gamma<3$. Nonetheless, we suppose that the tree ansatz still works even in this situation (see following discussion).

H. Evolving networks

Self-organization of nonequilibrium networks during their evolution (usually growth) is one of the traditional explanations of network architectures with a great role of highly connected hubs. One should also stress that nonequilibrium networks inevitably have a wide spectrum of correlations.

The simplest random growing network is a random recursive tree defined as follows. The evolution starts from a single vertex. At each time step, a new vertex is attached to a random existing one by an edge. The resulting random tree has an exponential degree distribution.

1. Preferential attachment

To arrive at a heavy-tailed degree distribution, one may use preferential attachment—vertices for linking are chosen with probability proportional to a special function $f(q)$ of their degrees (preference function). In particular, the scale-free networks are generated with a linear preference function.

A recursive network growing in the following way is rather representative. The growth starts with some initial configuration, and at each time step a new vertex is attached to preferentially chosen $m \geqslant 1$ existing vertices by m edges. Each vertex for attachment is chosen with probability proportional to a linear function of its degree, $q+A$, where the constant $A>-m$. In particular, if $A=0$ (the proportional preference), this is the Barabási-Albert model (Barabási and Albert, 1999), where the γ exponent of the degree distribution is 3. In general, for a linear preferential attachment, the degree distribution exponent is $\gamma=3+A/m$ (Dorogovtsev *et al.*, 2000; Krapivsky *et al.*, 2000).

Among these recursive networks, the Barabási-Albert model is a special case: it has anomalously weak degree-degree correlations for the nearest neighbors, and so it is frequently treated as "almost uncorrelated."

The idea of preferential attachment providing complex network architectures was well explored. The smooth variations of these diverse structures with various model parameters were extensively studied. For example, Szabó *et al.* (2003) described the variations of the degree-dependent clustering in simple generalizations of the Barabási-Albert model.

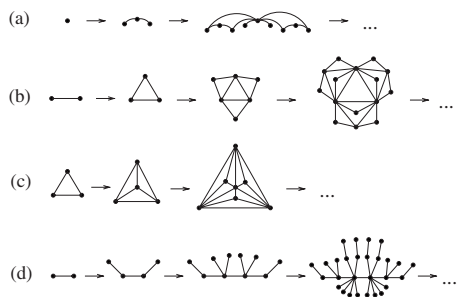

FIG. 4. Examples of deterministic small worlds: (a) Barabási *et al.* (2001), (b) Dorogovtsev and Mendes (2002) and Dorogovtsev *et al.* (2002a), (c) Andrade *et al.* (2005) and Doye and Massen (2005), and (d) Jung *et al.* (2002). The γ exponent for each of these four deterministic graphs is $1+\ln 3/\ln 2=2.585\ldots$.

2. Deterministic graphs

Deterministic graphs often provide the only possibility for analytical treatment of difficult problems. Moreover, using these graphs, one may mimic complex random networks surprisingly well. Figure 4 demonstrates a few simple scale-free deterministic graphs, which show the small-world phenomenon and whose discrete degree distributions have a power-law envelope.

I. Small-world networks

The small-world networks introduced by Watts and Strogatz (1998) are superpositions of finite-dimensional lattices and classical random graphs, thus combining their properties. One of the variations of the Watts-Strogatz model is explained in Fig. 5: randomly chosen pairs of vertices in a one-dimensional lattice are connected by shortcuts. There is a smooth crossover from a lattice to a small-world geometry with an increasing number of shortcuts. Remarkably, even with extremely low relative numbers of shortcuts, these networks demonstrate the small-world phenomenon.

Kleinberg (1999, 2000) used an important generalization of the Watts-Strogatz model. In the Kleinberg net-

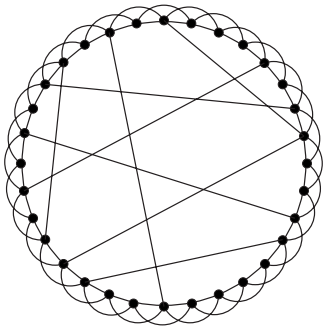

FIG. 5. A simple variation of the Watts-Strogatz model (Watts and Strogatz, 1998; Watts, 1999). Adapted from Newman, 2000.

work (the grid-based model with exponent α), the probability that a shortcut connects a pair of vertices separated by Euclidean distance r decreases as $r^{-\alpha}$. The resulting network geometry depends critically on the value of the exponent α.

We end this section with a short remark. In solid-state physics, boundary conditions play an important role. We stress that as a rule the networks under discussion have no borders, so the question of boundary conditions is meaningless here. There are very few exceptions, e.g., the Cayley tree.

III. THE EMERGENCE OF A GIANT COMPONENT

This is a basic structural transition in the network architecture. Numerous critical phenomena in cooperative models on networks can be explained by taking into account the specifics of this transition in complex networks. The emergence of a giant connected component corresponds to the percolation threshold notion in condensed matter. The study of random graphs began with the discovery and description of this transition (Solomonoff and Rapoport, 1951; Erdős and Rényi, 1959). Remarkably, it takes place in sparse networks, at $\langle q \rangle \sim$const, which makes this range of mean degrees most interesting.

A. Tree ansatz

The majority of analytical results for cooperative models on complex networks were obtained in the framework of the tree approximation. This ansatz assumes the absence of finite loops in a network in the thermodynamic limit and allows only infinite loops. The allowance of the infinite loops is of primary importance since they greatly influence the critical behavior. Indeed, without loops, that is, on perfect trees, the ferromagnetic order, say, in the Ising model, occurs only at zero temperature. Also, the removal of even a vanishingly small fraction of vertices or edges from a perfect tree eliminates the giant connected component.

The tree ansatz allows one to use the convenient techniques of random branching processes. On the other hand, in the framework of this ansatz, equilibrium networks are actually equivalent to random Bethe lattices.

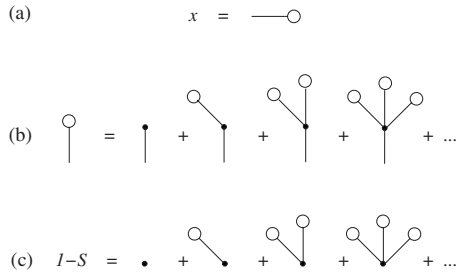

FIG. 6. (a) Graphic notation for the probability x that, following a randomly chosen edge to one of its end vertices, we arrive at a finite connected component. (b) Equation (8) or, equivalently, Eq. (10) in graphic form. (c) Graphic representation of Eq. (9) and of equivalent Eq. (11) for the relative size S of the giant connected component.

B. Organization of uncorrelated networks

The mathematical solution to the problem of organizing arbitrary uncorrelated networks as a system of connected components was proposed by Molloy and Reed (1995, 1998). Callaway *et al.* (2000) and Newman *et al.* (2001) represented and developed these ideas using the apparatus and language of physics. Here we describe these fundamental results and ideas in simple terms. We refer the reader to Newman *et al.* (2001) and Newman (2003c) for details of this theory based on the generating function technique.

1. Evolution of the giant connected component

The theory of uncorrelated networks [we discuss the configuration model, which is completely described by the degree distribution $P(q)$ and size N] is based on the following simplifying features:

(i) The sole characteristic of a vertex in these networks is its degree. In any other respect, the vertices are statistically equivalent—there are no borders or centers, or older or younger vertices in these models. The same is true for edges.

(ii) The tree ansatz is valid.

(iii) Equations (1) and (2) are valid (see Fig. 3).

Feature (i) allows one to introduce the probability x that, following a randomly chosen edge to one of its end vertices, he or she arrives at a finite connected component. In stricter terms, choose a random edge; choose its random end; then x is the probability that after removing this edge, the chosen end vertex will belong to a finite connected component. A graphic representation of x is introduced in Fig. 6(a). The probability that an edge belongs to one of the finite components is, graphically,

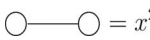

(7)

This is the probability that, by following an edge in any direction, we arrive at finite trees. Thus $1-x^2$ is a frac-

tion of edges that are in the giant connected component. This simple relation enables us to measure x. Using features (i), (ii), and (iii) leads to the following self-consistent equation for x and expression for the probability $1-S$ that a vertex belongs to a finite connected component:

$$x = \sum_q \frac{qP(q)}{\langle q \rangle} x^{q-1}, \tag{8}$$

$$1 - S = \sum_q P(q) x^q. \tag{9}$$

In particular, Eq. (9) is explained as follows. A vertex belongs to a finite connected component if and only if following every emanating edge in the direction from this vertex we arrive at a finite tree. The probability of this event is x^q for a vertex of degree q. For a randomly chosen vertex, we must sum over q the products of x^q and the probability $P(q)$. One can see that S is the relative size of the giant connected component. Figures 6(b) and 6(c) present and explain these formulas in graphic form. Note that if $P(q=0,1)=0$, then Eq. (8) has the only solution $x=1$, and so $S=1$, i.e., the giant connected component coincides with the network. Using the generating function of the degree distribution $\varphi(z) \equiv \Sigma_q P(k) z^q$ and the notation $\varphi_1(z) \equiv \varphi'(z)/\varphi'(1) = \varphi'(z)/\langle q \rangle$ gives

$$x = \phi_1(x), \tag{10}$$

$$S = 1 - \phi(x). \tag{11}$$

These relations demonstrate the usefulness of the generating function technique in network theory. The deviation $1-x$ plays the role of the order parameter. If Eq. (8) has a nontrivial solution $x<1$, then the network has the giant connected component. The size of this component can be found by substituting the solution of Eq. (8) or (10) into Eq. (9) or (11). Remarkably, the resulting S is obtained by only considering finite connected components [which are (almost) surely trees in these networks]; see Fig. 6. Knowing the size of the giant connected component and the total number of finite components, one can find the number of loops in the giant component. For the calculation of this number, see Lee *et al.* (2004c). Applying generating function techniques in a similar way, one may also describe the organization of connected components in the bipartite uncorrelated networks; see Soderberg (2002).

Analysis of Eq. (8) shows that an uncorrelated network has a giant connected component when the mean number of second nearest neighbors of a randomly chosen vertex $z_2 = \langle q^2 \rangle - \langle q \rangle$ exceeds the mean number of nearest neighbors: $z_2 > z_1$. This is the Molloy-Reed criterion,

$$\langle q^2 \rangle - 2\langle q \rangle > 0 \tag{12}$$

(Molloy and Reed, 1995). For the Poisson degree distribution, i.e., for the classical random graphs, $z_2 = \langle q \rangle^2$, and so the point of emergence of the giant connected component is $z_1 = 1$. In the Gilbert model, this corresponds to the critical probability $p_c(N \to \infty) \cong 1/N$ that a pair of vertices is connected. These relations explain the importance of the sparse network regime, where this transition takes place. The Molloy-Reed criterion shows that the divergence of the second moment of the degree distribution guarantees the presence of the giant connected component.

Exactly at the point of emergence of the giant connected component, the mean size of a finite component to which a randomly chosen vertex belongs diverges as follows:

$$\langle s \rangle = \langle q \rangle^2 / (2\langle q \rangle - \langle q^2 \rangle) + 1 \tag{13}$$

(Newman *et al.*, 2001). This formula is given for the phase without the giant connected component. In this problem, $\langle s \rangle$ plays the role of susceptibility. Usually, it is convenient to express the variation of the giant component near the critical point and other critical properties in terms of the deviation of one parameter, e.g., the mean degree $\langle q \rangle$, from its critical value, $\langle q \rangle_c$. Usually, the resulting singularities in terms of $\langle q \rangle - \langle q \rangle_c$ are the same as in terms of $p - p_c$ in the percolation problem on complex networks (p is the concentration of undeleted vertices; see below). Note that, in scale-free networks with fixed exponent γ, one may vary the mean degree by changing the low-degree part of a degree distribution.

2. Percolation on uncorrelated networks

What happens with a network if a random fraction $1-p$ of its vertices (or edges) is removed? In this site (or bond) percolation problem, the giant connected component plays the role of the percolation cluster, which may be destroyed by decreasing p. Two equivalent approaches to this problem are possible. The first (Cohen *et al.*, 2000) uses the following idea. (i) Find the degree distribution of the damaged network, which is $\tilde{P}(q) = \Sigma_{r=q}^{\infty} P(r) C_r^q p^q (1-p)^{r-q}$ for both the site and bond percolation. (ii) Since the damaged network is obviously still uncorrelated, Eqs. (8) and (9) with this $\tilde{P}(q)$ describe the percolation.

The second approach is technically more convenient: derive direct generalizations of Eqs. (8) and (9) with the parameter p and the degree distribution $P(q)$ of the original, undamaged network (Callaway *et al.*, 2000). Simple arguments, similar to those illustrated by Fig. 6, immediately lead to

$$x = 1 - p + p \sum_q \frac{qP(q)}{\langle q \rangle} x^{q-1}, \tag{14}$$

$$1 - S = 1 - p + p \sum_q P(q) x^q. \tag{15}$$

Although Eq. (14) is valid for both the site and bond percolation, Eq. (15) is valid only for site percolation. For the bond percolation problem, use Eq. (9). One can see that the giant connected component is present when

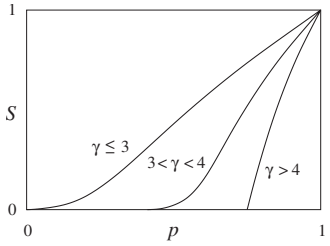

FIG. 7. Effect of the heavy-tailed architecture of a network on the variation of its giant connected component under random damage. The relative size of the giant connected component S is shown as a function of the concentration p of the retained vertices in the infinite network.

$$pz_2 > z_1, \tag{16}$$

that is, the percolation threshold is at

$$p_c = z_1/z_2 = \langle q\rangle/(\langle q^2\rangle - \langle q\rangle). \tag{17}$$

So, in particular, $p_c=1/\langle q\rangle$ for classical random graphs, and $p_c=1/(q-1)$ for random regular graphs. Equations (16) and (17) show that it is impossible to eliminate the giant connected component in an infinite uncorrelated network if the second moment of its degree distribution diverges—the network is ultraresilient against random damage or failures (Albert *et al.*, 2000; Cohen *et al.*, 2000). In scale-free networks, this occurs if $\gamma\leqslant 3$. Callaway *et al.* (2000) considered a more general problem, where the probability $p(q)$ that a vertex is removed depends on its degree. As is natural, the removal of highly connected hubs from a scale-free network (intentional damage) effectively destroys its giant connected component (Albert *et al.*, 2000; Cohen *et al.*, 2001).

Near the critical point, the right-hand side of Eq. (14) for the order parameter $1-x$ becomes nonanalytic if higher moments of the degree distribution diverge. This leads to unusual critical singularities in these percolation problems and to unusual critical phenomena at the emergence of the giant connected component in networks with heavy-tailed degree distributions (Cohen *et al.*, 2002, 2003a). For the sake of convenience, let the infinite uncorrelated network be scale-free. In this case, the critical behavior of the size S of the giant connected component is as follows (Cohen *et al.*, 2002).

(i) If $\gamma>4$, i.e., $\langle q^3\rangle<\infty$, then $S\propto p-p_c$, which is the standard mean-field result, also valid for classical random graphs.

(ii) If $3<\gamma<4$, then $S\propto(p-p_c)^{1/(\gamma-3)}$, i.e., the β exponent equals $1/(\gamma-3)$.

(iii) If $\gamma=3$, then $p_c=0$ and $S\propto p\exp(-2/p\langle q\rangle)$.

(iv) If $2<\gamma<3$, then $p_c=0$ and $S\propto p^{1+1/(3-\gamma)}$.

These results are shown in Fig. 7. We stress that the unusual critical exponents are only a consequence of a fat-tailed degree distribution, and the theory is essentially of a mean-field nature. Note that we discuss only unweighted networks, where edges have unit weights. For percolation on weighted networks, see Braunstein, Buldyrev, Cohen, *et al.* (2003), Braunstein *et al.* (2004), and Li *et al.* (2007), and references therein. In weighted networks, one can naturally introduce a mean length of the path along edges with the minimum sum of weights $\bar{\ell}_{\rm opt}$. Based on the percolation theory, Braunstein *et al.* showed that in the Erdős-Rényi graphs with a wide weight distribution, the optimal path length $\bar{\ell}_{\rm opt}\sim N^{1/3}$.

Numerous variations of percolation on networks may be considered. In particular, one may remove vertices from a network with a degree-dependent probability (Albert *et al.*, 2000; Callaway *et al.*, 2000; Gallos *et al.*, 2005).

The probability that a vertex of degree q belongs to the giant connected component is $1-x^q$ [compare with Eq. (9)], so that it is high for highly connected vertices. Here x is the physical root of Eq. (8) for the order parameter. The degree distribution of vertices in the giant connected component (GCC) is

$$P_{\rm GCC}(q) = P(q)(1-x^q)\Big/\left[1-\sum_q P(q)x^q\right]. \tag{18}$$

Therefore at the point of emergence ($x\to 1$) of the giant connected component, the degree distribution of its vertices is proportional to $qP(q)$. Thus, in networks with slowly decreasing degree distributions, the giant connected component near its point of creation consists mostly of vertices with high degrees.

Cohen *et al.* (2001, 2003a) found that at the emergence point, the giant connected component does not have a small-world geometry (that is, with a diameter growing with the number of vertices N more slowly than any positive power of N) but a fractal one. Its fractal dimension (the chemical dimension d_l in their notations) equals $d_l(\gamma>4)=2$ and $d_l(3<\gamma<4)=(\gamma-2)/(\gamma-3)$. That is, the mean intervertex distance in the giant connected component (of size n) at the point of its disappearance is large, $\bar{\ell}\sim n^{d_l}$. To be clear, suppose that we are destroying a small world by deleting its vertices. Then precisely at the moment of destruction, a tiny remnant of the network has a much greater diameter than the original compact network. It is important that this remnant is an equilibrium tree with a degree distribution characterized by exponent $\gamma-1$. Indeed, recall that in Sec. II.C we indicated that equilibrium connected trees have a fractal structure. So substituting $\gamma-1$ for γ in the expression for the fractal dimension of equilibrium connected trees [Burda *et al.* (2001), see Sec. II.C], explains the form of $d_l(\gamma)$.

3. Statistics of finite connected components

The sizes of largest connected components $s^{(i)}$ depend on the number of vertices in a network N. Here the index $i=1$ is for the largest component, $i=2$ is for the second largest component, and so on. In the classical random graphs, $s^{(i)}(N)$ with a fixed i and $N\to\infty$ are as follows [for more details, see Borgs *et al.* (2001) and Bollobás and Riordan (2003)]: (i) for $p<p_c(1-CN^{-1/3})$, $s^{(i\geqslant 1)}(N)\sim\ln N$; (ii) within the so-called scaling window

$|p-p_c|<CN^{-1/3}$, $s^{(i\geqslant 1)}(N)\sim N^{2/3}$; (iii) for $p>p_c(1+CN^{-1/3})$, $s^{(1)}(N)\sim N$, $s^{(i>1)}(N)\sim \ln N$ (Bollobás, 1984). Here C denotes corresponding constants and $p=\langle q\rangle/N$.

In Sec. IX.B, we present a general phenomenological approach to finite-size scaling in complex networks. Applying this approach to scale-free networks with degree distribution exponent γ allows one to describe the sizes of the largest connected components: (i) if $\gamma>4$, the same formulas hold as for the classical random graphs; (ii) if $3<\gamma<4$, then $s^{(i\geqslant 1)}(N)\sim N^{(\gamma-2)/(\gamma-1)}$ within the scaling window $|p-p_c|<CN^{-(\gamma-3)/(\gamma-1)}$ (Kalisky and Cohen, 2006), and the classical results hold outside of the scaling window.

Similarly, one can write

$$p_c(N=\infty)-p_c(N)\sim N^{-(\gamma-3)/(\gamma-1)} \tag{19}$$

for the deviation of the percolation threshold in the range $3<\gamma<4$. (Note that p_c is well defined only in the $N\to\infty$ limit.) We discuss the size effect in networks with $2<\gamma<3$ in Sec. III.B.4.

We compare these results with the corresponding formulas for the standard percolation on lattices. If the dimension of a lattice is below the upper critical dimension for the percolation problem, $d<d_u=6$, then

$$s^{(i\geqslant 1)}(N)\sim N^{d_f/d} \tag{20}$$

within the scaling window $|p-p_c|<\text{const}\times N^{-1/(\nu d)}$. Here $d_f=(d+2-\eta)/2=\beta/\nu+2-\eta$ is the fractal dimension of the percolation cluster in the critical point measured in the d-dimensional space using a box-counting procedure, ν is the correlation length exponent, and η is the Fisher exponent. (The boxes in this box-counting procedure are based on an original, undamaged network.) Above the upper critical dimension, which is the case for small worlds, one must replace d in these formulas (and in scaling relations) by d_u and substitute the mean-field values of the critical exponents ν, η, and β, namely, use $\nu=\frac{1}{2}$ and $\eta=0$. For networks, the mean-field exponent $\beta=\beta(\gamma)$, and so, similarly to Hong, Ha, and Park (2007), we may formally introduce the upper critical dimension $d_u(\gamma)=2\beta/\nu+2-\eta=4\beta(\gamma)+2$ and the fractal dimension $d_f(\gamma)=\beta/\nu+2-\eta=2\beta(\gamma)+2$.

With the known order parameter exponent $\beta(\gamma)$ from Sec. III.B.2, this heuristic approach gives the fractal dimension

$$d_f(\gamma\geqslant 4)=4,\quad d_f(3<\gamma<4)=2(\gamma-2)/(\gamma-3) \tag{21}$$

(Cohen *et al.*, 2003a). Note that this fractal dimension d_f does not coincide with the "chemical dimension" d_l discussed above but rather $d_f=2d_l$. Similarly,

$$d_u(\gamma\geqslant 4)=6,\quad d_u(3<\gamma<4)=2(\gamma-1)/(\gamma-3) \tag{22}$$

(Cohen *et al.*, 2003a; Hong, Ha, and Park, 2007; Wu, Lagorio, Braunstein, *et al.*, 2007). With these $d_u(\gamma)$ and $d_f(\gamma)$, we reproduce the above formulas for finite-size networks.

The size distribution of connected components in the configuration model was derived using the generating function technique (Newman *et al.*, 2001; Newman, 2007). Let $\mathcal{P}(s)$ be the size distribution of a finite component to which a randomly chosen vertex belongs and $\mathcal{Q}(s)$ be the distribution of the total number of vertices reachable following a randomly chosen edge. $h(z)\equiv\Sigma_s\mathcal{P}(s)z^s$ and $h_1(z)\equiv\Sigma_s\mathcal{Q}(s)z^s$ are the corresponding generating functions. Then

$$h(z)=z\phi(h_1(z)), \tag{23}$$

$$h_1(z)=z\phi_1(h_1(z)) \tag{24}$$

(Newman *et al.*, 2001). To get $h(z)$ and its inverse transformation $\mathcal{P}(s)$, one should substitute the solution of Eq. (24) into Eq. (23).

Equations (23) and (24) have an interesting consequence for scale-free networks without a giant connected component. If the degree distribution exponent is $\gamma>3$, then in this situation the size distribution $\mathcal{P}(s)$ is also asymptotically a power law, $\mathcal{P}(s)\sim s^{-(\gamma-1)}$ (Newman, 2007). To arrive at this result, one must recall that if a function is a power law, $P(k)\sim k^{-\gamma}$, then its generating function near $z=1$ is $\varphi(z)=a(z)+C(1-z)^{\gamma-1}$, where $a(z)$ is an analytic function at $z=1$, and C is a constant. Substituting this $\varphi(z)$ into Eqs. (23) and (24) results in the nonanalytic contribution $\sim(1-z)^{\gamma-2}$ to $h(z)$. [One must also take into account that $h(1)=h_1(1)=1$ when a giant component is absent.] This corresponds to the power-law asymptotics of $\mathcal{P}(s)$. Remarkably, there is a qualitative difference in the component size distribution between undamaged networks and networks with randomly removed vertices or edges. In percolation problems for arbitrary uncorrelated networks, the power law for the distribution $\mathcal{P}(s)$ fails everywhere except a percolation threshold (see below).

In uncorrelated scale-free networks without a giant connected component, the largest connected component contains $\sim N^{1/(\gamma-1)}$ vertices (Durrett, 2006; Janson, 2007), where we assume $\gamma>3$. As is natural, this size coincides with the cutoff $k_{\text{cut}}(N)$ in these networks.

Near the critical point in uncorrelated scale-free networks with a giant connected component, the size distribution of finite connected components to which a randomly chosen vertex belongs is

$$\mathcal{P}(s)\sim s^{-\tau+1}e^{-s/s^*(p)}, \tag{25}$$

where $s^*(p_c)\to\infty$: $s^*(p)\sim(p-p_c)^{-1/\sigma}$ near p_c (Newman *et al.*, 2001). The size distribution of finite connected components is $\mathcal{P}_s(s)\sim\mathcal{P}(s)/s$. In uncorrelated networks with rapidly decreasing degree distributions, Eq. (25) is also valid in the absence of a giant connected component. Note that this situation includes randomly damaged scale-free networks: percolation. The distribution $\mathcal{P}(s)$ near the critical point in undamaged scale-free networks without a giant component looks as $\mathcal{P}(s)\sim s^{-\tau+1}$ at sufficiently small s, and $\mathcal{P}(s)\sim s^{-\gamma+1}$ at sufficiently large s ($\gamma>3$; in this region the inequality $\gamma>\tau$ is valid). The exponents τ, σ, and β satisfy the scaling relations $\tau-1=\sigma\beta+1=\sigma d_u/2=d_u/d_f$. We stress that the mean size of a finite connected component, i.e., the first moment of the distribution $\mathcal{P}_s(s)$, is finite at the critical point. A diver-

gent quantity (and an analog of susceptibility) is the mean size of a finite connected component to which a randomly chosen vertex belongs,

$$\langle s\rangle = \sum_s s\mathcal{P}(s) \sim |p-p_c|^{-\tilde{\gamma}}, \tag{26}$$

where $\tilde{\gamma}$ is the "susceptibility" critical exponent. This exponent does not depend on the form of the degree distribution. Indeed, the well-known scaling relation $\tilde{\gamma}/\nu = 2-\eta$ with $\nu=\frac{1}{2}$ and $\eta=0$ substituted leads to $\tilde{\gamma}=1$ within the entire region $\gamma>3$.

The resulting exponents for finite connected components in the scale-free configuration model are as follows: (i) for $\gamma>4$, the exponents are $\tau=\frac{5}{2}$, $\sigma=\frac{1}{2}$, $\tilde{\gamma}=1$, which are also valid for classical random graphs; (ii) for $3<\gamma<4$, $\tau=2+1/(\gamma-2)$, $\sigma=(\gamma-3)/(\gamma-2)$, $\tilde{\gamma}=1$ (Cohen *et al.*, 2003a).

The situation in the range $2<\gamma<3$ is not so clear. The difficulty is that in this interesting region, the giant connected component disappears at $p=0$, i.e., only with the disappearance of the network itself. Consequently, one cannot separate "critical" and noncritical contributions, and so scaling relations fail. In this range, (iii) i.e., for $2<\gamma<3$, $\langle s\rangle \propto p$, $\tau=3$, $\sigma=3-\gamma$. Note that the last two values imply a specific cutoff of the degree distribution, namely, $q_{\rm cut}\sim N^{1/2}$.

In principle, the statistics of connected components in the bond percolation problem for a network may be obtained by analyzing the solution of the p-state Potts model (Sec. VII) with $p=1$ placed on this net. Lee *et al.* (2004c) realized this approach for the static model.

The correlation volume of a vertex is defined as

$$V_i \equiv \sum_{\ell=0} z_\ell(i) b^\ell, \tag{27}$$

where z_ℓ is the number of the ℓth nearest neighbors of vertex i and b is a parameter characterizing the decay of correlations. The parameter b may be calculated for specific cooperative models and depends on their control parameters; see Sec. VI.C.4. In particular, if $b=1$, the correlation volume is reduced to the size of a connected component. We estimate the mean correlation volume in the uncorrelated network with the mean branching coefficient $B=z_2/z_1$: $\bar{V}\sim\Sigma_\ell(bB)^\ell$ (assume that the network has the giant connected component). So $\bar{V}(N\to\infty)$ diverges at and above the critical value of the parameter, $b_c=1/B$. At the critical point, $\bar{V}(b_c)=\Sigma_\ell 1\sim \ln N$. Since $B^{\bar{\ell}(N)}\sim N$, we obtain $\bar{V}\sim N^{\ln(bB)/\ln B}$ for $b>b_c$. Thus, as b increases from b_c to 1, the exponent of the correlation volume grows from 0 to 1.

The correlation volume takes into account remote neighbors with exponentially decreasing (if $b<1$) weights. A somewhat related quantity (the mean number of vertices at a distance less than $a\bar{\ell}(N)$ from a vertex, where $a\geqslant 1$) was analyzed by Lópes *et al.* (2007) in their study of limited path percolation. This number is of the order of N^δ, where the exponent $\delta=\delta(a,B)\leqslant 1$.

4. Finite-size effects

Practically all real-world networks are small, which makes the factor of finite size important. For example, empirically studied metabolic networks contain about 10^3 vertices. Even the largest artificial net (the World Wide Web, whose size will soon approach 10^{11} Web pages) shows qualitatively strong finite-size effects May and Lloyd, 2001; Dorogovtsev and Mendes, 2002; Boguñá *et al.*, 2004). To understand the strong effect of finite size in real scale-free networks, one must recall that the exponent $\gamma\leqslant 3$ in most of them, that is, the second moment of a degree distribution diverges in the infinite network limit.

Note that the tree ansatz may be used even in this region ($\gamma\leqslant 3$), where the uncorrelated networks are loopy. The same is true for at least the great majority of interacting systems on these networks. The reason for this surprising applicability is not yet clear.

We now demonstrate the "poor man's approach" to percolation on a finite-size (uncorrelated) network with $\gamma\leqslant 3$, where $p_c(N\to\infty)\to 0$. To be specific, we find the size dependence of the percolation threshold, $p_c(N)$. The idea of this estimate is quite simple. We use Eq. (17), which was derived for an infinite network, but with the finite network's degree distribution substituted. Then, if the cutoff of the degree distribution is $q_{\rm cut}\sim N^{1/2}$, we arrive at

$$p_c(N,2<\gamma<3)\sim N^{-(3-\gamma)/2}, \quad p_c(N,\gamma=3)\sim 1/\ln N. \tag{28}$$

These relations suggest the emergence of noticeable percolation thresholds even in large networks. In other words, the ultraresilience against random failures is effectively broken in finite networks.

Calculations of other quantities for percolation (and for a wide circle of cooperative models) on finite nets are analogous. Physicists, unlike mathematicians, routinely apply estimates of this sort to various problems defined on networks. Usually, these intuitive estimates work but evidently demand thorough verification. Unfortunately, a strict statistical mechanics theory of finite-size effects for networks is technically hard and was developed only for special models; see Sec. IV.A. For a phenomenological approach to this problem, see Sec. IX.B.

5. *k*-core architecture of networks

The k-core of a network is its largest subgraph whose vertices have degree at least k (Chalupa *et al.*, 1979; Bollobás, 1984). In other words, each of the vertices in the k-core has at least k nearest neighbors within this subgraph. The notion of the k-core naturally generalizes the giant connected component and offers a more comprehensive view of the network organization. The k-core of a graph may be obtained by the "pruning algorithm," which looks as follows (see Fig. 8). Remove from the graph all vertices of degrees less than k. Some of the remaining vertices may now have fewer than k edges.

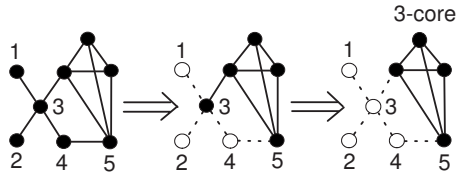

FIG. 8. Construction of the 3-core of a graph. First we remove vertices 1, 2, and 4 together with their links because they have degrees smaller than 3. In the obtained graph, vertex 3 has degree 1. By removing it, we get the 3-core of the graph.

Prune these vertices, and so on until no further pruning is possible. The result, if it exists, is the k-core. Thus, a network is hierarchically organized as a set of successively enclosed k-cores, similarly to a Russian nesting doll—"matrioshka." Alvarez-Hamelin *et al.* (2006) used this k-core architecture to produce a set of visualizations of diverse networks.

k-core (bootstrap) percolation implies the breakdown of the giant k-core at a threshold concentration of vertices or edges removed at random from an infinite network. Pittel *et al.* (1996) found the way to analytically describe the k-core architecture of classical random graphs. Fernholz and Ramachandran (2004) mathematically proved that the k-core organization of the configuration model is asymptotically exactly described in the framework of a simple tree ansatz.

We now discuss the k-core percolation in the configuration model with degree distribution $P(q)$ using arguments based on the tree ansatz (Dorogovtsev *et al.*, 2006a, 2006b; Goltsev *et al.*, 2006). The validity of the tree ansatz is nontrivial since in this theory it is applied to a giant k-core that has loops. Note that in treelike networks, $(k \geqslant 3)$-cores (if they exist) are giant—finite $(k \geqslant 3)$-cores are impossible. In contrast to the giant connected component problem, the tree ansatz applied to higher k-cores fails far from the k-core point of emergence. We assume that a vertex in the network is present with probability $p=1-Q$. In this locally treelike network, the giant k-core coincides with the infinite $(k-1)$-ary subtree. By definition, the m-ary tree is a tree where all vertices have branching at least m.

Let the order parameter in the problem R be the probability that a given end of an edge of a network is not the root of an infinite $(k-1)$-ary subtree. (Of course, R depends on k.) An edge is in the k-core if both ends of this edge are roots of infinite $(k-1)$-ary subtrees, which happens with the probability $(1-R)^2$. In other words,

$$(1-R)^2 = \frac{\text{number of edges in the } k\text{-core}}{\text{number of edges in the network}}, \tag{29}$$

which expresses the order parameter R in terms of observables. Figure 9 graphically explains this and the following two relations. A vertex is in the k-core if at least k of its neighbors are roots of infinite $(k-1)$-ary trees. So, the probability M_k that a random vertex belongs to the k-core (the relative size of the k-core) is given by

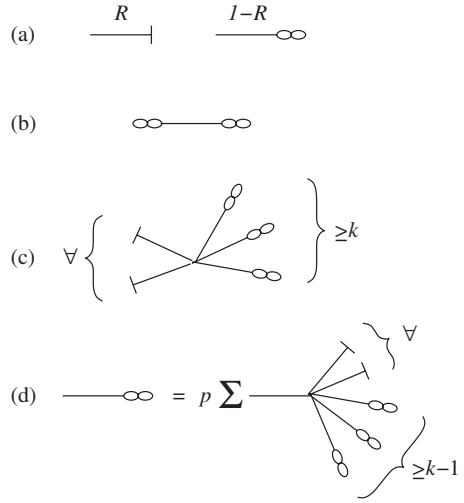

FIG. 9. Diagrammatic representation of Eqs. (29)–(31). (a) Graphic notations for the order parameter R and for $1-R$. (b) The probability that both ends of an edge are in the k-core, Eq. (29). (c) Configurations contributing to M_k, which is the probability that a vertex is in the k-core, Eq. (30). The symbol $\forall$ indicates that there may be any number of nearest neighbors that are not trees of infinite $(k-1)$-ary subtrees. (d) A graphic representation of Eq. (31) for the order parameter. Adapted from Goltsev *et al.*, 2006.

$$M_k = p \sum_{n \geqslant k} \sum_{q \geqslant n} P(q) C_n^q R^{q-n} (1-R)^n, \tag{30}$$

where $C_n^q = q!/(q-n)!n!$. To obtain the relative size of the k-core, one must substitute the physical solution of the equation for the order parameter into Eq. (30). We write the equation for the order parameter, noticing that a given end of an edge is a root of an infinite $(k-1)$-ary subtree if it has at least $k-1$ children that are roots of infinite $(k-1)$-ary subtrees. Therefore,

$$1-R = p \sum_{n=k-1}^{\infty} \sum_{i=n}^{\infty} \frac{(i+1)P(i+1)}{z_1} C_n^i R^{i-n} (1-R)^n. \tag{31}$$

This equation differs strongly from that for the order parameter in the ordinary percolation; compare with Eq. (14). The solution of Eq. (32) at $k \geqslant 3$ indicates a quite unusual critical phenomenon. The order parameter (and also the size of the k-core) has a jump at the critical point like a first-order phase transition. On the other hand, it has a square root critical singularity,

$$R_c - R \propto [p - p_c(k)]^{1/2} \propto M_k - M_{kc}; \tag{32}$$

see Fig. 10. This intriguing critical phenomenon is often called a hybrid phase transition (Parisi and Rizzo, 2006; Schwartz *et al.*, 2006) Equations (32) are valid if the second moment of the degree distribution is finite. Otherwise, the picture is similar to what we observed for ordinary percolation. In this range, the k-cores, even of high order, practically cannot be destroyed by the random removal of vertices from an infinite network.

The 2-core of a graph can be obtained from the giant connected component of this graph by pruning dangling

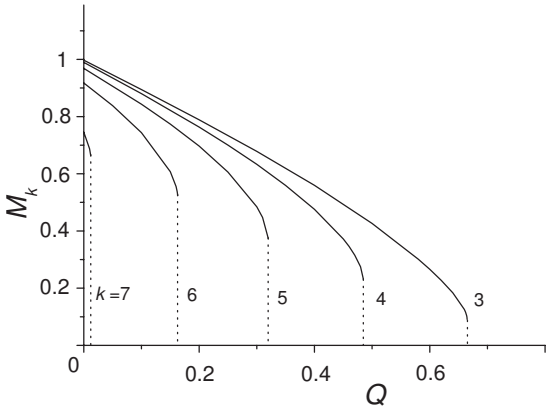

FIG. 10. Relative sizes of the k-cores M_k in classical random graphs with the mean degree $z_1=10$ versus the concentration $Q=1-p$ of randomly removed vertices. Adapted from Dorogovtsev *et al.*, 2006a.

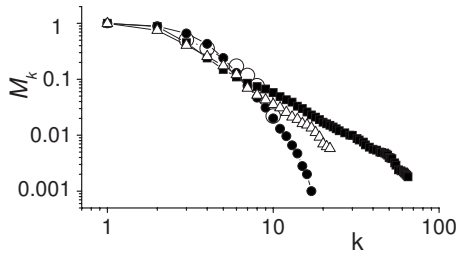

FIG. 11. Relative size of the k-cores vs k in several networks. ○, M_k calculated neglecting correlations, using the degree distribution of Internet router network, $N\approx 190\,000$. Adapted from Dorogovtsev *et al.*, 2006a. △, measurements for the autonomous system network [Cooperative Association for Internet Data Analysis (CAIDA) map], $N=8542$. Adapted from Alvarez-Hamelin *et al.*, 2008. ●, results for a maximally random scale-free ($\gamma=2.5$) network of 10^6 vertices, and ■, for a similar network but with a given strong clustering, $C=0.71$. Adapted from Serrano and Boguñá, 2006a.

branches. At $k=2$, Eq. (31) for the order parameter is identical to Eq. (14) for the ordinary percolation. Therefore, the creation point of the 2-core coincides with that of the giant connected component, and the phase transition is continuous. According to Eq. (30), the size M_2 of the 2-core is proportional to $(1-R)^2$ near the critical point, and so it is proportional to the square of the size of the giant connected component. This gives $M_2 \propto (p-p_c)^2$ if the degree distribution decays rapidly.

In stark contrast to ordinary percolation, the emergence of $(k>2)$-cores is not related to the divergence of corresponding finite components, which are absent in treelike networks. Then, is there any divergence associated with this hybrid transition? The answer is yes. To unravel the nature of this divergence, we introduce a new notion. The k-core's corona is a subset of vertices in the k-core (with their edges) that have exactly k nearest neighbors in the k-core, i.e., the minimum possible number of connections. One may see that the corona itself is a set of disconnected clusters. Let N_{crn} be the mean total size of corona clusters attached to a vertex in the k-core. It turns out that it is $N_{\mathrm{crn}}(p)$ that diverges at the creation point of the k-core,

$$N_{\mathrm{crn}}(p) \propto [p-p_c(k)]^{-1/2} \tag{33}$$

(Goltsev *et al.*, 2006; Schwartz *et al.*, 2006). Moreover, the mean intervertex distance in the corona clusters diverges by the same law as $N_{\mathrm{crn}}(p)$ (Goltsev *et al.*, 2006). It looks as if the corona clusters "merge together" exactly at the k-core percolation threshold and simultaneously disappear together with the k-core, which does not exist at $p>p_c(k)$.

Similarly to the mean size of a cluster to which a vertex belongs in ordinary percolation N_{crn} plays the role of susceptibility in this problem; see Schwartz *et al.* (2006) for more details. The exponent of the singularity in Eq. (33), namely, $\frac{1}{2}$, dramatically differs from the standard mean-field value of exponent $\tilde{\gamma}=1$ (see Sec. III.B.3). At this point, it is appropriate to mention a useful association. Recall the temperature dependence of the order parameter $m(T)$ in a first-order phase transition. In normal thermodynamics, metastable states cannot be realized. Nonetheless, consider the metastable branch of $m(T)$. One can find that near the end (T_0) of this branch, $m(T)=m(T_0)+\mathrm{const}\times[T_0-T]^{1/2}$, and the susceptibility $\chi(T)\propto(T_0-T)^{-1/2}$. Compare these singularities with those of Eqs. (32) and (33). The only essential difference is that, in contrast to the k-core percolation, in the ordinary thermodynamics this region is not approachable. Parallels of this kind have already been discussed by Aizenman and Lebowitz (1988).

Using Eqs. (30) and (31), we can find the k-core sizes M_k in the range $2<\gamma<3$,

$$M_k = p^{1/(3-\gamma)}(q_0/k)^{(\gamma-1)/(3-\gamma)}, \tag{34}$$

where q_0 is the minimal degree in the scale-free degree distribution (Dorogovtsev *et al.*, 2006a). The exponent of this power law agrees with the observed one in a real-world network—the Internet at the autonomous system level and the map of routers (Kirkpatrick, 2005; Carmi, Havlin, Kirkpatrick, *et al.*, 2006; Alvarez-Hamelin *et al.*, 2008). In the infinite scale-free networks of this kind, there is an infinite sequence of k-cores (34). These cores all have a practically identical architecture—their degree distributions asymptotically coincide with the degree distribution of the network in the range of high degrees.

The finiteness of networks restricts the k-core sequence with maximum number k_h for the highest k-core. Dorogovtsev *et al.* (2006a, 2006b) and Goltsev *et al.* (2006) estimated k_h substituting empirical degree distributions into the equations for uncorrelated networks. Unfortunately, the resulting k_h turned out to be several (three) times smaller than the observed values (Carmi *et al.*, 2007; Alvarez-Hamelin *et al.*, 2008). Later Serrano and Boguñá (2006a, 2006c) arrived at a more realistic k_h, taking into account high clustering (see Fig. 11). (They simulated a maximally random network with a given degree distribution and a given clustering.) There is also another way to diminish k_h: random damaging first de-

stroys the highest k-core, then the second highest, and so on.

C. Percolation on degree-degree correlated networks

In a random network, let only pair correlations between nearest-neighbor degrees be present. Then this network has a locally treelike structure, and one can analyze the organization of connected components (Newman, 2002b; Boguñá *et al.*, 2003b; Vázquez and Moreno, 2003). The network is completely described by the joint degree-degree distribution $P(q,q')$, see Sec. II.F (and by N). It is convenient to use a conditional probability $P(q'|q)$ that if an end vertex of an edge has degree q, then the second end has degree q'. In uncorrelated networks, $P(q'|q)=q'P(q')/\langle q\rangle$ is independent of q. Obviously, $P(q'|q)=\langle q\rangle P(q,q')/qP(q)$. The important quantity in this problem is the probability x_q that if an edge is attached to a vertex of degree q, then, following this edge to its second end, we will not appear in the giant connected component. For the sake of brevity, we discuss only the site percolation problem, where p is the probability that a vertex is retained. For this problem, equations for x_q and an expression for the relative size of the giant connected component take the following form:

$$x_q = 1 - p + p\sum_{q'} P(q'|q)(x_{q'})^{q'-1}, \tag{35}$$

$$1 - S = 1 - p + p\sum_{q} P(q)(x_q)^q \tag{36}$$

(Vázquez and Moreno, 2003), which naturally generalizes Eqs. (14) and (15). Solving the system of equations (35) gives the full set $\{x_q\}$. Substituting $\{x_q\}$ into Eq. (36) provides S. Newman (2002b) originally derived these equations in a more formal way, using generating functions, and numerically solved them for various networks. The resulting curve $S(p)$ was found to depend significantly on the type of correlations—whether the degree-degree correlations were assortative or disassortative. Compared to an uncorrelated network with the same degree distribution, the assortative correlations increase the resilience of a network against random damage, while the disassortative correlations diminish this resilience. See Noh (2007) for a similar observation in another network model with correlations.

Equation (35) shows that the emergence of the giant connected component is a continuous phase transition. The percolation threshold is found by linearizing Eq. (35) for small $y_q=1-x_q$, which results in the condition $\Sigma_{q'}C_{qq'}y_{q'}=0$, where the matrix elements $C_{qq'}=-\delta_{qq'}+p(q'-1)P(q'|q)$. With this matrix, the generalization of the Molloy-Reed criterion to the correlated networks is the following condition: if the largest eigenvalue of the matrix $C_{qq'}$ is positive, then the correlated network has a giant connected component. The percolation threshold may be obtained by equating the largest eigenvalue of this matrix to zero. In uncorrelated networks, this reduces to criterion (17).

Interestingly, the condition of ultraresilience against random damage does not depend on correlations. As in uncorrelated networks, if the second moment $\langle q^2\rangle$ diverges in an infinite network, the giant connected component cannot be eliminated by random removal of vertices (Boguñá *et al.*, 2003b; Vázquez and Moreno, 2003). Simple calculations show that the mean number z_2 of the second nearest neighbors of a vertex in a degree-degree correlated network diverges simultaneously with $\langle q^2\rangle$. It is this divergence of z_2 that guarantees the ultraresilience.

Percolation and optimal shortest path problems were also studied for weighted networks with correlated weights (Wu, Lagorio, Braunstein, *et al.*, 2007).

D. The role of clustering

The statistics of connected components in highly clustered networks, with numerous triangles (i.e., the clustering coefficient C does not approach zero as $N\to\infty$), is a difficult and poorly studied problem. An important step to resolving this problem has been made by Serrano and Boguñá (2006a, 2006b, 2006c). They studied constructions of networks with given degree distributions and given mean clusterings of vertices of degree q, $C(q)$. It turns out that only if $C(q)<1/(q-1)$ is it possible to build an uncorrelated network with a given pair of characteristics: $P(q)$ and $C(q)$. Since clustering of this kind does not induce degree-degree correlations, the regime $C(q)<1/(q-1)$ was conventionally called "weak clustering." [When $C(q)<1/(q-1)$, then the number of triangles based on an edge in the network is one or zero.] On the other hand, if $C(q)$ is higher than $1/(q-1)$ at least at some degrees ("strong clustering") then the constructed networks necessarily have at least correlations between the degrees of the nearest neighbors.

Serrano and Boguñá (2006a, 2006b, 2006c) made a simplifying assumption that triangles in a network cannot have joint edges and neglected long loops. This assumption allowed them to use a variation of the "tree ansatz." In particular, they studied the bond percolation problem for these networks. The conclusions of this work are as follows:

(i) If the second moment of the degree distribution is finite, weak clustering makes the network less resilient to random damage—the percolation threshold (in terms of $Q=1-p$, where Q is the fraction of removed edges) decreases; see Fig. 12. In contrast, strong clustering moves the percolation threshold in the opposite direction, although small damage (low Q) noticeably diminishes the giant connected component.

(ii) If the second moment of the degree distribution diverges, neither weak nor strong clustering can

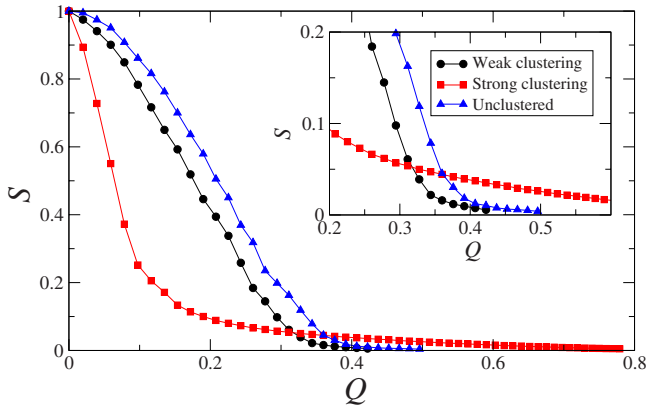

FIG. 12. (Color online) Bond percolation on unclustered and strongly and weakly clustered scale-free networks. The exponent $\gamma=3.5$. The relative size S of the giant connected component is shown as a function of the concentration $Q=1-p$ of removed edges. From Serrano and Boguñá, 2006c.

destroy the giant connected component in an infinite network.

Newman (2003b) proposed a different approach to highly clustered networks. He used the fact that a one-mode projection of a bipartite uncorrelated network has high clustering, while the original bipartite network has a locally treelike structure. (In this projection, two vertices of, say, type 1, are nearest neighbors if they have at least one joint vertex of type 2.) This feature allows one to describe properties of the clustered one-partite network with a tunable clustering and a tunable degree distribution by applying the tree ansatz to the bipartite network. For details (applications to percolation and epidemic processes) see Newman (2003b).

E. Giant component in directed networks

The structure of the giant connected component in uncorrelated directed networks was studied by Dorogovtsev *et al.* (2001a). By definition, edges of directed networks are directed, so that the configuration model is described by the joint in- and out-degree distribution $P(q_i,q_o)$. Directed networks have a far more complex organization and topology of the giant connected components than undirected ones. This organization may include specifically interconnected giant subcomponents with different points of emergence. Applying the tree ansatz, they found the emergence points of various giant components and obtained their sizes for an arbitrary $P(q_i,q_o)$; see also Schwartz *et al.* (2002). For a more detailed description of the giant components in directed networks, see Serrano and De Los Rios (2007).

Boguñá and Serrano (2005) generalized this theory to uncorrelated networks that contain both directed and undirected connections. These networks are characterized by a distribution $P(q,q_i,q_o)$, where q, q_i, and q_o are the numbers of undirected, in-directed, and out-directed connections of a vertex, respectively.

The exponents of the critical singularities for transitions of the emergence of various giant connected components in directed networks were calculated by Schwartz *et al.* (2002). Note that, although the in and out degrees of different vertices in these networks are uncorrelated, there may be arbitrary correlations between in and out degrees of the same vertex. The critical exponents, as well as the critical points, essentially depend on these in- and out-degree correlations.

F. Giant component in growing networks

The intrinsic large-scale inhomogeneity of nonequilibrium (e.g., growing) networks may produce a surprising critical phenomenon. Large-scale inhomogeneity means the difference between properties of vertices according to their age. This difference usually makes the "old" part of a growing network more "dense" than the "young" one.

Callaway *et al.* (2001) found an unexpected effect in the emergence of the giant connected component already in a simple model of the growing network. In their model, the network grows due to two parallel processes: (i) there is an inflow of new vertices with unit rate, and (ii) there is an inflow of edges with rate b, which interconnect randomly chosen vertex pairs. The rate b plays the role of the control parameter. As one might expect, the resulting degree distribution is simple—exponential. Inspection of this network when it is already infinite shows that it has a giant connected component for $b>b_c$, where b_c is some critical value. Remarkably, the emergence of the giant connected component in this net strongly resembles the Berezinskii-Kosterlitz-Thouless (BKT) phase transition in condensed matter (Berezinskii, 1970; Kosterlitz and Thouless, 1973). Near the critical point, the relative size of the giant connected component has the specific BKT singularity

$$S \propto \exp(-\text{const}/\sqrt{b-b_c}). \tag{37}$$

Note that in an equilibrium network with the same degree distribution, S would be proportional to the small deviation $b-b_c$. The singularity (37), with all derivatives vanishing at the critical point, implies an infinite-order phase transition.

Normally, the BKT transition occurs at the lower critical dimension of an interacting system, where critical fluctuations are strong, e.g., dimension 2 for the XY model. Most of the known models with this transition have a continuous symmetry of the order parameter, so the discovery of the BKT singularity in infinite-dimensional small worlds, that is, in the mean-field regime, was somewhat surprising. The mean size of a finite connected component to which a vertex belongs in this network was also found to be nontraditional. This characteristic (an analogy of susceptibility) has a finite jump at this transition and not a divergence generic for equilibrium networks and disordered lattices.

Dorogovtsev *et al.* (2001b) analytically studied a much wider class of growing networks with an arbitrary linear

preferential attachment (which may be scale-free or exponential) and arrived at similar results. In particular, they found that the constant and b_c in Eq. (37) depend on the rules of the growth. Looking for clues and parallels with the canonical BKT transition, they calculated the size distribution of connected components $\mathcal{P}_s(s)$ characterizing correlations. The resulting picture looks as follows.

- The distribution $\mathcal{P}_s(s)$ slowly (in a power-law fashion) decays in the whole phase without the giant connected component, and this distribution rapidly decreases in the phase with the giant connected component.

This picture is in stark contrast to the equilibrium networks, where

- the distribution $\mathcal{P}_s(s)$ slowly decays only at the emergence point of the giant connected component (if a network is non-scale-free; see Sec. III.B.3).

In this respect, the observed transition in growing networks strongly resembles the canonical BKT transitions, where the critical point separates a phase with rapidly decreasing correlations and a "critical phase" with correlations decaying in a power-law fashion. (Note, however, the inverted order of phases with a power-law decay and with a rapid drop in these transitions.)

This phase transition was later observed in other growing networks with exponential and scale-free degree distributions [only for some of these networks; see Lancaster (2002), Coulomb and Bauer (2003), Krapivsky and Derrida (2004), Bollobás and Riordan (2005), and Durrett (2006)]. Moreover, even ordinary "equilibrium" bond percolation considered on special networks has the same critical phenomenon. For example, (i) grow an infinite random recursive graph (at each time step, add a new vertex and attach it to m randomly chosen vertices of the graph), and (ii) consider the bond percolation problem on this infinite network. We emphasize that the attachment must be only random here. It is easy to see that the resulting network may be equivalently prepared by using a stochastic growth process that leads to the BKT-like transition. Similar effects were observed on the Ising and Potts models placed on growing networks; see Sec. VI.F.1. A more realistic model of a growing protein interaction network where a giant connected component emerges with the BKT-type singularity was described by Kim *et al.* (2002).

Various percolation problems on deterministic (growing) graphs may be solved exactly. Surprisingly, percolation properties of deterministic graphs are similar to those of their random analogs. For detailed discussion of these problems, see Dorogovtsev *et al.* (2002a), Dorogovtsev (2003), and Rozenfeld and ben-Avraham (2007).

G. Percolation on small-world networks

We consider a small-world network based on a d-dimensional hypercubic lattice ($N \cong L^d$) with random shortcuts added with probability ϕ per lattice edge. Note that in this network, in the infinite network limit, there are no finite loops including shortcuts. All finite loops are only of lattice edges. This fact allows one to apply the usual tree ansatz to this loopy network. In this way, Newman *et al.* (2002) obtained the statistics of connected components in the bond percolation problem for two-dimensional small-world networks. Their qualitative conclusions are also valid for bond and site percolation on one-dimensional (Newman and Watts, 1999a, 1999b; Moore and Newman, 2000a, 2000b) and arbitrary-dimensional small-world networks.

In the spirit of classical random graphs, at the percolation threshold point p_c there must be one end of a retained shortcut per connected component in the lattice substrate. In stricter terms, this condition is $2d\phi p_c = 1/\langle n_0\rangle(p_c)$, i.e., the mean density of the ends of shortcuts on the lattice substrate must be equal to the mean size $\langle n_0\rangle$ of a connected component (on a lattice) to which a vertex belongs. In the standard percolation problem on a lattice, $\langle n_0\rangle(p) \propto (p_{c0}-p)^{-\tilde{\gamma}}$, where p_{c0} and $\tilde{\gamma}$ are the percolation threshold and the "susceptibility" critical exponent in the standard percolation. So the percolation threshold is displaced by

$$p_{c0} - p_c \propto \phi^{1/\tilde{\gamma}} \tag{38}$$

if ϕ is small (Warren *et al.*, 2003). For example, for bond percolation on the two-dimensional small-world network, $p_{c0}=1/2$ and $\tilde{\gamma}=43/18=2.39\ldots$. The mean size of a connected component to which a random vertex belongs is also easily calculated,

$$\langle n\rangle = \langle n_0\rangle/(1 - 2d\phi p\langle n_0\rangle) \propto (p_c - p)^{-1}, \tag{39}$$

so that its critical exponent equals 1, as in classical random graphs. The other percolation exponents also coincide with their values for classical graphs. In general, this claim is equally valid for other cooperative models on small-world networks in a close environment of a critical point.

Ozana (2001) described the entire crossover from the lattice regime to the small-world one and finite-size effects by using scaling functions with dimensionless combinations of the three characteristic lengths: (i) L, (ii) the mean Euclidean distance between the neighboring shortcut ends $\xi_{sw} \equiv 1/(2d\phi p)^{1/d}$, and (iii) the usual correlation length ξ_l for percolation on the lattice. For an arbitrary physical quantity, $X(L) = L^x f(\xi_{sw}/L, \xi_l/L)$, where x and $f(,)$ are the scaling exponent and function. In the case of $L \to \infty$, this gives $X = \xi_{sw}^y \xi_l^z g(\xi_{sw}/\xi_l)$, where y, z, and $g(\,)$ are other scaling exponents and function. This scaling is equally applicable to many other cooperative models on small-world networks.

H. k-clique percolation

A possible generalization of percolation was put forward by Derényi *et al.* (2005). They considered percolation on the complete set of k-cliques of a network. The k-clique is a fully connected subgraph of k vertices. Two

k-cliques are adjacent if they share $k-1$ vertices. For example, the smallest nontrivial clique, the 3-clique, is a triangle, so that two triangles must have a common edge to allow the "3-percolation."

In fact, Derényi *et al.* (2005) described the emergence of the giant connected component in the set of the k-cliques of a classical random graph—the Gilbert model. The k-clique graph has vertices (k cliques) and edges—connections between adjacent k-cliques. The total number of k-cliques equals approximately $N^k p^{k(k-1)/2}/k!$. The degree distribution of this graph is Poissonian, and the mean degree is $\langle q\rangle \cong Nkp^{k-1}$, which may be much less than the mean degree in the Gilbert model, Np.

Since the sparse classical random graphs have few ($k \geqslant 3$)-cliques, this kind of percolation obviously implies a dense network with a divergent mean degree. Applying the Molloy-Reed criterion to the k-clique graph gives the emergence point of the k-clique giant connected component

$$p_c(k)N = \frac{1}{k-1} N^{(k-2)/(k-1)} \quad \text{as } N \to \infty \tag{40}$$

[for more details, see Palla *et al.* (2007)].

The emergence of the giant connected component in the k-clique graph looks quite standard so that its relative size is proportional to the deviation $[p-p_c(k)]$ near the critical point. On the other hand, the relative size S_k of the ($k \geqslant 3$)-clique giant connected component in the original graph (namely, the relative number of vertices in this component) evolves with p in a quite different manner. This component emerges abruptly, and for any p above the threshold $p_c(k)$ it contains almost all vertices of the network: $S_k[p<p_c(k)]=0$ and $S_k[p>p_c(k)]=1$.

IV. CONDENSATION TRANSITION

Numerous models of complex networks show the following phenomenon. A finite fraction of typical structural elements in a network (motifs)—edges, triangles, etc.—turn out to be aggregated into an ultracompact subgraph with diameters much smaller than the diameter of this network. In this section, we discuss various types of condensation.

A. Condensation of edges in equilibrium networks

1. Networks with multiple connections

We start with rather simple equilibrium uncorrelated networks, where multiple connections, loops of length one, and other arbitrary configurations are allowed. There exist a number of more or less equivalent models of these networks (Burda *et al.*, 2001; Bauer and Bernard, 2002; Berg and Lässig, 2002; Dorogovtsev *et al.*, 2003b; Farkas *et al.*, 2004). In many respects, these networks are equivalent to an equilibrium non-network system (balls statistically distributed among boxes) so that they can be easily treated. On the other hand, the balls-in-boxes model has a condensation phase transition (Bialas *et al.*, 1997; Burda *et al.* 2002).

We can arrive at uncorrelated networks with complex degree distribution in various ways. Here we mention two equivalent approaches to networks with a fixed number N of vertices.

(i) (i) Similar to the balls-in-boxes model, one can define the statistical weights of the random ensemble members in the following factorized form: $\Pi_{i=1}^{N} p(q_i)$ (Burda *et al.*, 2001) where the one-vertex probability $p(q)$ is the same for all vertices (or boxes) and depends on the degree of a vertex. If the number of edges L is fixed, these weights additionally take into account the following constraint: $\Sigma_i q_i = 2L$. With various $p(q)$ (and the mean degree $\langle q\rangle = 2L/N$) we can obtain various complex degree distributions.

(ii) (ii) A more "physical," equivalent approach is as follows. A network is treated as an evolving statistical ensemble, where edges permanently change their positions between vertices (Dorogovtsev *et al.*, 2003b). After relaxation, this ensemble approaches a final state—an equilibrium random network. If the rate of relinking factors into the product of simple, one-vertex-degree preference functions $f(q)$, the resulting network is uncorrelated. For example, one may choose a random edge and move it to vertices i and j selected with probability proportional to the product $f(q_i)f(q_j)$. The form of the preference function and $\langle q\rangle$ determines the distribution of connections in this network.

It turns out that in these equilibrium networks scale-free degree distributions can be obtained only if $f(q)$ is a linear function. Furthermore, the value of the mean degree plays a crucial role. If, say, $f(q) \cong q+1-\gamma$ as $q \to \infty$, then three distinct regimes are possible. (i) When the mean degree is lower than some critical value q_c [which is determined by the form of $f(q)$], the degree distribution $P(q)$ is an exponentially decreasing function. (ii) If $\langle q\rangle = q_c$, then $P(q) \sim q^{-\gamma}$ is scale-free. (iii) If $\langle q\rangle > q_c$, then one vertex attracts a finite fraction of all connections, in sum, $L_{\text{ex}} = N(\langle q\rangle - q_c)/2$ edges, but the other vertices are described by the same degree distribution as at the critical point. In other words, at $\langle q\rangle > q_c$, a finite fraction of edges are condensed on a single vertex. One can show that it is exactly one vertex that attracts these edges and not two or three or several. Notice the large number of one-loop structures and multiple connections attached to this vertex. We emphasize that a scale-free degree distribution without condensation occurs only at one point—at the critical mean degree. This is in contrast to networks growing under the mechanism of the preferential attachment, where linear preference functions generate scale-free architectures for a wide range of mean degrees.

One can arrive at the condensation of edges in a quite different way. Following the work of Bianconi and Barabási (2001), who applied this idea to growing networks, let few vertices, or even a single vertex, be more attractive than others. Let, for example, the preference function for this vertex be $gf(q)$, where $f(q)$ is the preference function for the other vertices, and $g>1$ is a constant characterizing the relative "strength" or "fitness" of this vertex. It turns out that when g exceeds some critical value g_c, a condensation of edges on this strong vertex occurs (Dorogovtsev and Mendes, 2003).

2. Networks without multiple connections

If multiple connections and one-loop structures are forbidden, the structure of the condensate changes crucially. This problem was analytically solved by Dorogovtsev, Mendes, Povolotsky, *et al.* (2005). The essential difference from the previous case is only in the structure of the condensate. It turns out that in these networks, at $\langle q\rangle > q_c$, a finite fraction of edges, involved in the condensation, link together a relatively small, highly interconnected core of N_h vertices, $N_h(N) \ll N$. This core, however, is not fully interconnected, i.e., it is not a clique. (i) If the degree distribution $P(q)$ of this network decreases more slowly than any stretched exponential dependence, e.g., the network is scale-free, then $N_h \sim N^{1/2}$. (ii) In the case of a stretched exponential $P(q) \sim \exp(-\text{const} \times q^{\alpha})$, $0<\alpha<1$, the core consists of

$$N_h \sim N^{(2-\alpha)/(3-\alpha)} \tag{41}$$

vertices, that is, the exponent of $N_h(N)$ is in the range $(1/2, 2/3)$. The connections inside the core are distributed according to the Poisson law, and the mean degree $\sim N/N_h$ varies in the range from $\sim N/N^{1/2} \sim N^{1/2}$ to $\sim N/N^{2/3} \sim N^{1/3}$.

In the framework of traditional statistical mechanics, one can also construct networks with various correlations (Berg and Lässig, 2002), directed networks (Angel *et al.*, 2006), and many others. Derényi *et al.* (2004), Farkas *et al.* (2004), and Palla *et al.* (2004) constructed a variety of network ensembles, with statistical weights of members proportional to $\Pi_i \exp[-E(q_i)]$, to where $E(q)$ is a given one-vertex degree function—"energy," as they called it. In particular, in the case $E(q) = -\text{const} \times q \ln q$, they numerically found an additional, first-order phase transition. They studied a variation of the maximum vertex degree $q_{\max}$ in a network. As $\langle q\rangle$ reaches q_c, a condensation transition takes place, and $q_{\max}$ approaches the value $\sim N\langle q\rangle$, i.e., a finite fraction of all edges. Remarkably, at some essentially higher mean degree, q_{c2}, $q_{\max}$ sharply (with hysteresis) drops to $\sim N^{1/2}$. That is, the network demonstrates a first-order phase transition from the condensation ("star") phase to the fully connected graph regime.

B. Condensation of triangles in equilibrium nets

The condensation of triangles in network models was observed in the work of Strauss (1986). Strauss proposed the exponential model, where statistical weights of graphs are

$$W(g) = \exp\left[-\sum_n \beta_n E_n(g)\right]. \tag{42}$$

Here $E_n(g)$ is a set of some quantities of a graph g, a member of this statistical ensemble, and β_n is a set of some positive constants. Note that many current studies of equilibrium networks are based on the exponential model. Strauss included the quantity $E_3(g)$, that is, the number of triangles in the graph g taken with the minus sign, in the exponential. This term leads to the presence of a large number of triangles in the network. On the other hand, they turn out to be inhomogeneously distributed over the network. By simulating this (small) network, Strauss discovered that all triangles merge together forming a clique (fully connected subgraph) in the network—the condensation of triangles.

Burda *et al.* (2004a, 2004b) analytically described and explained this nontrivial phenomenon. We now discuss the idea and results of their theory. The number of edges L and the number of triangles T in a network are expressed in terms of its adjacency matrix $\hat{A}$, namely, $L = \mathrm{Tr}(\hat{A}^2)/2!$ and $T = \mathrm{Tr}(\hat{A}^3)/3!$. The partition function of the Erdős-Rényi graph is simply $Z_0 = \Sigma_{\hat{A}} \delta(\mathrm{Tr}(\hat{A}^2) - 2L)$, where the sum is over all possible adjacency matrices. Following Strauss, the simplest generalization of the Erdős-Rényi ensemble, favoring triangles, has the following partition function:

$$Z = \sum_{\hat{A}} \delta(\mathrm{Tr}(\hat{A}^2) - 2L) e^{G\,\mathrm{Tr}(\hat{A}^3)/3!} = Z_0 \langle e^{G\,\mathrm{Tr}(\hat{A}^3)/3!}\rangle_0, \tag{43}$$

where the constant G quantifies the tendency to have many triangles and $\langle\cdots\rangle_0$ denotes the averaging over the Erdős-Rényi ensemble. Equation (43) shows the form of the partition function for the canonical ensemble, i.e., with fixed L. In the grand canonical formulation, it looks more invariant: $Z_{\mathrm{gc}} = \Sigma_{\hat{A}} \exp[-C\,\mathrm{Tr}(\hat{A}^2)/2! + G\,\mathrm{Tr}(\hat{A}^3)/3!]$ (here we do not discuss the constant C). In fact, based on this form, Strauss (1986) argued that with L/N finite and fixed, there exists a configuration where all edges belong to a fully connected subgraph and $\mathrm{Tr}(\hat{A}^3) \sim N^{3/2} \gg N$. Therefore, as $N \to \infty$, for any positive interaction constant G, the probability of realization of such a configuration should go to 1, which is the stable state of this theory.

The situation, however, is more delicate. Burda *et al.* showed that apart from this stable condensation state, the network has a metastable, homogeneous one. These states are separated by a barrier, whose height approaches infinity as $N \to \infty$. In large networks (with sufficiently small G), it is practically impossible to approach

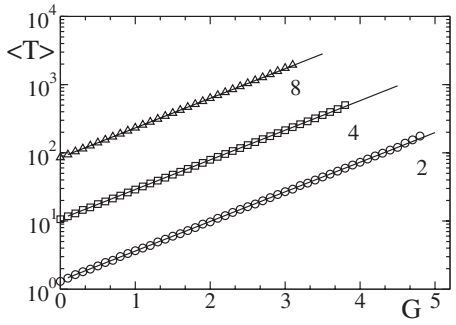

FIG. 13. Mean number of triangles $\langle T\rangle$ as a function of the parameter G in the metastable state of the network of $N=2^{14}$ vertices for three values of the mean degree $\langle q\rangle=2,4,8$. The dots are results of a simulation, and the lines are theoretical curves $\langle T\rangle=(\langle q\rangle^3/6)\exp(G)\lesssim N$. The rightmost dot in each set corresponds to the threshold value $G_t(\langle q\rangle)$ above which the network quickly approaches the condensation state with $\langle T\rangle \sim N^{3/2}$. From Burda *et al.*, 2004a.

the condensation state if we start evolution (relaxation) from a homogeneous configuration. (Recall that Strauss numerically studied very small networks.)

Assuming small G, Burda *et al.* used the second equality in Eq. (43) to make a perturbative analysis of the problem. They showed that in the perturbative phase the mean number of triangles is $\langle T\rangle=(\langle q\rangle^3/6)\exp(G)$, where $\langle q\rangle$ is the mean degree of the network; see Fig. 13. In this regime, the number of triangles may be large, $\langle T\rangle\lesssim N$. Above the threshold $G_t(\langle q\rangle,N)\approx a\ln N+b$, where the coefficients a and b depend only on $\langle q\rangle$, the system easily jumps over the barrier and quickly approaches the condensation state.

Burda *et al.* (2004b) generalized this theory to networks with complex degree distributions using the partition function $Z=\Sigma_{\hat{A}}\delta(\mathrm{Tr}(\hat{A}^2)-2L)e^{G\,\mathrm{Tr}(\hat{A}^3)}\Pi_i^N p(q_i)$, where q_i is the degree of vertex i and the weight $p(q)$ is given. In an even more general approach, $\mathrm{Tr}(\hat{A}^3)$ in the exponential should be replaced by a more general perturbation $S(\hat{A})$. Note that a different perturbation theory for the exponential model was developed by Park and Newman (2004a, 2004b).

C. Condensation of edges in growing networks

Bianconi and Barabási (2001) discovered the condensation phase transition in networks, growing under the mechanism of preferential attachment. In their inhomogeneous network, the preference function of vertices had a random factor (fitness) $g_i f(q_i)$ distributed according to a given function $p(g)$. They indicated a class of sufficiently long-tailed distributions $p(g)$, for which an infinitely small fraction of vertices (maximally fitted ones) attracts a finite fraction of edges. In fact, this condensation may be obtained even with a single, more fitted vertex (j): $g_{i\neq j}=1$, $g_j=g>1$ (Dorogovtsev and Mendes, 2001). In this case, the condensation on this vertex occurs in large networks of size $t\gg j$ if g exceeds some critical value g_c.

Suppose that the network is a recursive graph, and the preference function $f(q)$ is linear. Then $g_c=\gamma_0-1$, where γ_0 is the exponent of the degree distribution of this network with all equal vertices ($g=1$). Note that if the degree distribution is exponential ($\gamma_0\to\infty$), $g_C\to\infty$, and the condensation is impossible. If $g<g_c$, the degree distribution of the network is the same as in the pure network. On the other hand, the phase with the condensate $g>g_c$ has the following characteristics. (i) A finite fraction of edges $d\propto(g-g_c)$ is attached to the fittest vertex. (ii) The degree distribution exponent increases: $\gamma=1+g>\gamma_0$. (iii) In the entire condensation phase, relaxation to the final state (with the fraction d of edges in the condensate) is slow, of a power-law kind: $d_j(t)-d\sim t^{-(g-g_c)/g}$. Here $d_j(t)$ is a condensed fraction of edges at time t.

Bianconi and Barabási called this phenomenon the Bose-Einstein condensation based on evident parallels (in fact, this term was also applied to condensation in equilibrium networks, the balls-in-boxes model, and zero-range processes). We emphasize the completely classical nature of this condensation.

V. CRITICAL EFFECTS IN DISEASE SPREADING

The epidemic spreading in various complex networks was extensively studied in recent years, and it is impossible to review in detail and even cite numerous works on this issue. In this section, we explain only basic facts about the spread of diseases in networks, discuss relations to other phenomena in complex networks, and describe several recent results. The reader may refer to Pastor-Satorras and Vespignani (2003, 2004) for a comprehensive introduction to this topic.

A. The SIS, SIR, SI, and SIRS models

Four basic models of epidemics are widely used: the SIS, SIR, SI, and SIRS models; see Nâsell (2002). S denotes susceptible, I infective, and R recovered (or removed). In the network context, vertices are individuals which are in one of these three (S,I,R) or two (S,I) states, and infections spread from vertex to vertex through edges. Note that an ill vertex can infect only its nearest neighbors: S→I.

The SIS model describes infections without immunity, where recovered individuals are susceptible. In the SIR model, recovered individuals are immune forever, and do not infect. In the SI model, recovery is absent. In the SIRS model, the immunity is temporary. The SIS, SIR, and SI models are particular cases of the more general SIRS model. We touch upon only the first three models.

Here we consider a heuristic approach of Pastor-Satorras and Vespignani (2001, 2003). This (a kind of mean-field) theory describes fairly well the epidemic spreading in complex networks. For a stricter approach, see Newman (2002a), Kenah and Robins (2007), and references therein.

Let a network have only degree-degree correlations, and so it is defined by the conditional probability $P(q'|q)$; see Sec. III.C. Consider the evolution of the probabilities $i_q(t)$, $s_q(t)$, and $r_q(t)$ that a vertex of degree q is in the I, S, and R states, respectively. For example, $i_q(t)$= (number of infected vertices degree q) /$NP(q)$. As is natural, $i_q(t)+s_q(t)+r_q(t)=1$. Let λ be the infection rate. In other words, a susceptible vertex becomes infected with the probability λ (per unit time) if at least one of the nearest neighbors is infected. Remarkably, λ is the only parameter in the SIS and SIR models—other parameters can be easily set to 1 by rescaling. Here we list evolution equations for the SIS, SIR, and SI models. For derivations, see Boguñá *et al.* (2003b). However, the structure of these equations is so clear that one can easily explain them to himself or herself, exploiting obvious similarities with percolation.

The SIS model. In this model, infected vertices become susceptible with unit rate, $r_q(t)=0$, $s_q(t)=1-i_q(t)$. The equation is

$$\frac{di_q(t)}{dt} = -i_q(t) + \lambda q[1-i_q(t)]\sum_{q'} P(q'|q) i_{q'}(t). \tag{44}$$

The SIR model. In this model, infected vertices become recovered with unit rate. Two equations describe this system:

$$\frac{dr_q(t)}{dt} = i_q(t),$$

$$\frac{di_q(t)}{dt} = -i_q(t) + \lambda q[1-i_q(t)]\sum_{q'} \frac{q'-1}{q'} P(q'|q) i_{q'}(t). \tag{45}$$

Note the factor $(q'-1)/q'$ in the sum. This ratio is due to the fact that an infected vertex in this model cannot infect back its infector, and so one of the q' edges is effectively blocked.

The SI model. Here infected vertices are infected forever, $s_q(t)=1-i_q(t)$, and the dynamics is described by

$$\frac{di_q(t)}{dt} = \lambda q[1-i_q(t)]\sum_{q'} \frac{q'-1}{q'} P(q'|q) i_{q'}(t) \tag{46}$$

[compare with Eq. (45)]. This simplest model has no epidemic threshold. Moreover, in this model, λ may be set to 1 without loss of generality.

If a network is uncorrelated, substitute $P(q'|q) = q'P(q')/\langle q\rangle$ into these equations. It is convenient to introduce $\Theta=\Sigma_{q'}(q'-1)P(q')i_{q'}\langle q\rangle$ (for the SIR model) or $\Theta=\Sigma_{q'}q'P(q')i_{q'}\langle q\rangle$ (for the SIS model) and then solve a simple equation for this degree-independent quantity. We stress that the majority of results on epidemics in complex networks were obtained using only Eqs. (44)–(46). Note that one can also analyze these models assuming a degree-dependent infection rate λ (Giuraniuc *et al.*, 2006).

B. Epidemic thresholds and prevalence

The epidemic threshold λ_c is a basic notion in epidemiology. The fractions of infected and recovered (or removed) vertices in the final state are defined as $i(\infty) = \Sigma_q P(q) i_q(t\to\infty)$ and $r(\infty)=\Sigma_q P(q) r_q(t\to\infty)$, respectively. Below the epidemic threshold, $i(\infty)=r(\infty)=0$. In epidemiology, the fraction $i(t)$ of infected vertices in a network is called prevalence. On the other hand, above the epidemic thresholds, (i) in the SIS model, $i(\infty,\lambda > \lambda_c^{\mathrm{SIS}})$ is finite, and (ii) in the SIR model, $i(\infty,\lambda>\lambda_c^{\mathrm{SIR}}) =0$ and $r(\infty,\lambda>\lambda_c^{\mathrm{SIR}})$ is finite.

Linearization of Eqs. (44)–(46) readily provides the epidemic thresholds. The simplest SI model on any network has no epidemic threshold—all vertices are infected in the final state, $i_q(t\to\infty)=1$. Here we only discuss results for uncorrelated networks Pastor-Satorras and Vespignani (2001, 2003); for correlated networks, see Boguñá *et al.* (2003b). One can easily check that the SIS and SIR models have the following epidemic thresholds:

$$\lambda_c^{\mathrm{SIS}} = \langle q\rangle/\langle q^2\rangle, \quad \lambda_c^{\mathrm{SIR}} = \langle q\rangle/(\langle q^2\rangle - \langle q\rangle). \tag{47}$$

Notice the coincidence of λ_c^{SIR} with the percolation threshold p_c in these networks, Eq. (17). (Recall that for bond and site percolation problems, p_c is the same.) This coincidence is not occasional—strictly speaking, the SIR model is equivalent to dynamic percolation (Grassberger, 1983). In simpler terms, the SIR model, with respect to its final state, is practically equivalent to the bond percolation problem [see Hastings (2006) for a discussion of some difference; see also discussions in Kenah and Robins (2007) and Miller (2007)]. Equation (47) shows that general conclusions for percolation on complex networks are also valid for the SIS and SIR models. In particular, (i) the estimates and conclusions for p_c from Secs. III.B.2–III.B.4 are valid for the SIS and SIR models (replace p_c by λ_c^{SIS} or λ_c^{SIR}), and the finite-size relations also work; and (ii) the estimates and conclusions for the size S of the giant connected component from these sections are also valid for $i(\infty)$ in the SIS model and for $r(\infty)$ in the SIR model, i.e., for prevalence.

In particular, Pastor-Satorras and Vespignani (2001) discovered that in uncorrelated networks with diverging $\langle q^2\rangle$ the epidemic thresholds approach zero value, but a finite epidemic threshold is restored if a network is finite (May and Lloyd, 2001; Pastor-Satorras and Vespignani, 2002a; Boguñá *et al.*, 2004). Similar to percolation, the same condition is valid for networks with degree-degree correlations (Boguñá *et al.*, 2003a; Moreno and Vázquez, 2003).

The statistics of outbreaks near an epidemic threshold in the SIR model is similar to that for finite connected components near the point of emergence of a giant component. In particular, at an (SIR) epidemic threshold in a network with a rapidly decreasing degree distribution, the maximum outbreak scales as $N^{2/3}$ and the mean outbreak scales as $N^{1/3}$ (Ben-Naim and Krapivsky, 2004). (In

the SIS model, the corresponding quantities behave as N and $N^{1/2}$.) These authors also estimated the duration of epidemic outbreaks. At a SIR epidemic threshold in these networks, the maximum duration of an outbreak scales as $N^{1/3}$, the average duration scales as ln N, and the typical duration is of the order of 1.

Interestingly, some of the results on the disease spreading on complex networks were obtained before those for percolation; see Pastor-Satorras and Vespignani (2001). For example, they found that in the SIS and SIR models on the uncorrelated scale-free network with degree distribution exponent $\gamma=3$ the final prevalence is proportional to $\exp[-g(\langle q\rangle)/\lambda]$. Here $g(\langle q\rangle)$ depends only on the mean degree. That is, all derivatives of the prevalence over λ equal zero at this specific point (recall the corresponding result for percolation). Furthermore, Boguñá and Pastor-Satorras (2002) carried out numerical simulations of the SIS model on the growing network of Callaway *et al.* (2001) and observed prevalence proportional to $\exp(-\text{const}/\sqrt{\lambda-\lambda_c})$, i.e., the Berezinskii-Kosterlitz-Thouless singularity.

Disease spreading was also studied in many other networks. For example, for small-world networks, see Moore and Newman (2000a), Newman (2002a), Newman *et al.* (2002), and references therein. For epidemics in networks with high clustering, see Newman (2003b), Petermann and De Los Rios (2004), and Serrano and Boguna (2006a). A popular topic is various immunization strategies; see Dezsõ and Barabási (2002), Pastor-Satorras and Vespignani (2002b, 2003), Cohen *et al.* (2003b), Gallos Liljeros, Argyrakis, *et al.* (2007), and many other works.

Note that the excitation of a system of coupled neurons in response to external stimuli, in principle, may be considered similarly to the disease spreading. Excitable networks with complex architectures were studied by Kinouchi and Copelli (2006), Copelli and Campos (2007), and Wu, Xu, and Wang (2007).

C. Evolution of epidemics

Equations (44)–(46) describe the dynamics of epidemics. We discuss this dynamics above an epidemic threshold, where epidemic outbreaks are giant, that is, they involve a finite fraction of vertices in a network (Moreno *et al.*, 2002; Barthelemy *et al.*, 2004, 2005; Vázquez, 2006a, 2006b). The demonstrative SI model is easy to analyze. A characteristic time scale of the epidemic outbreak can be obtained in the following way (Barthelemy *et al.*, 2004, 2005). Let the initial condition be uniform, $i_q(t=0)=i_0$. Then in the range of short times, the prevalence $i(t)=\Sigma_q P(q)i_q(t)$ rises according to the law

$$\frac{i(t)-i_0}{i_0}=\frac{\langle q\rangle^2-\langle q\rangle}{\langle q^2\rangle-\langle q\rangle}(e^{t/\tau}-1) \tag{48}$$

with the time scale

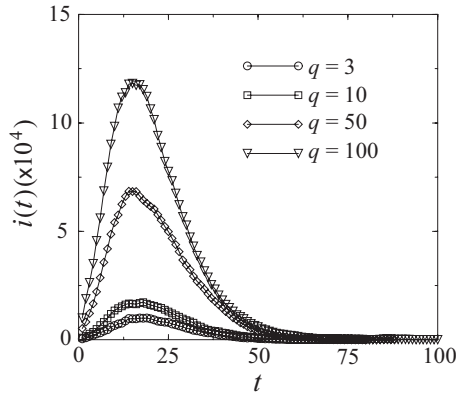

FIG. 14. Evolution of the average fraction of infected vertices in the SIR model on the Barabási-Albert network of 10^6 vertices for various initial conditions. At $t=0$, randomly chosen vertices of a given degree q are infected. The spreading rate is $\lambda=0.09$, which is above the epidemic threshold of this finite network. From Moreno *et al.*, 2002.

$$\tau=\langle q\rangle/\lambda(\langle q^2\rangle-\langle q\rangle). \tag{49}$$

Thus τ decreases with increasing $\langle q^2\rangle$. As is natural, the law (48) is violated at long times, when $i(t)\sim 1$. Expressions for τ in the SIS and SIR models are qualitatively similar to Eq. (49).

Notice some difference between the SIR and SIS (or SI) models. In the SIS and SI models, the fraction of infected vertices $i(t)$ grows monotonously with time until it approaches the final stationary state. Conversely, in the SIR model, $i(t)$ shows a peak (outbreak) at $t\sim\tau$ and approaches zero value as $t\to\infty$. As a result of heterogeneity of a complex network, the epidemic outbreaks depend strongly on initial conditions, actually on a first infected individual. Figure 14 shows how the average fraction of infected vertices evolves in the SIR model placed on the Barabási-Albert network if the first infected individual has exactly q neighbors (Moreno *et al.*, 2002). The spreading rate is supposed to be above the epidemic threshold. If q is large, then the outbreak is massive with high probability. On the other hand, if q is small, then as a rule the infection disappears after a small outbreak, and the probability of a giant outbreak is low.

When $\langle q^2\rangle$ diverges ($\gamma\leqslant 3$), Eqs. (48) and (49) are not applicable. Vázquez (2006a) considered disease spreading in this situation on a scale-free growing (or causal) tree. Actually he studied a variation of the SI model, with an average generation time $T_G\sim 1/\lambda$. In this model, he analytically found

$$di(t)/dt\propto t^{\ell_{\max}-1}e^{-t/T_G}, \tag{50}$$

where $\ell_{\max}(N)$ is the diameter of the network (the maximum intervertex distance). He compared this dependence with numerical simulations of the SI model on a generated network and a real-world one (the Internet at the autonomous system level). He concluded that Eq. (50) provides a reasonable fitting to these results even in rather small networks.

VI. THE ISING MODEL ON NETWORKS

The Ising model, named after the physicist Ernst Ising, is an extremely simplified mathematical model describing the spontaneous emergence of order. Despite its simplicity, this model is valuable for verification of general theories and assumptions, such as scaling and universality hypotheses in the theory of critical phenomena. It is important that many real systems can be approximated by the Ising model. The Hamiltonian of the model is

$$\mathcal{H} = -\sum_{i<j} J_{ij} a_{ij} S_i S_j - \sum_i H_i S_i, \tag{51}$$

where the indices i and j numerate vertices on a network, $i,j=1,2,\ldots,N$. a_{ij} is an element of the adjacency matrix: $a_{ij}=1$ or 0 if vertices i and j are connected or disconnected, respectively. Network topology is encoded in the adjacency matrix. In general, couplings J_{ij} and local fields H_i can be random parameters.

What kind of a critical behavior might one expect if we put the Ising model on the top of a complex network? Is it the standard mean-field-like behavior? A naive answer is yes because a complex network is an infinite-dimensional system. Indeed, it is generally accepted that the critical behavior of the ferromagnetic Ising model on a d-dimensional lattice at $d>4$ is described by the simple mean-field theory, which assumes that an average effective magnetic field $H+Jz_1M$ acts on spins, where M is an average magnetic moment and $z_1=\langle q\rangle$ is the mean number of the nearest neighbors. An equation

$$M = \tanh(\beta H + \beta J z_1 M) \tag{52}$$

determines M. This theory predicts a second-order ferromagnetic phase transition at the critical temperature $T_{\mathrm{MF}}=Jz_1$ in zero field with the standard critical behavior: $M\sim\tau^{\beta}$, $\chi=dM/dH\sim|\tau|^{-\tilde{\gamma}}$, where $\tau\equiv T_{\mathrm{MF}}-T$, $\beta=1/2$, and $\tilde{\gamma}=1$. First investigations of the ferromagnetic Ising model on the Watts-Strogatz networks revealed the second-order phase transition (Barrat and Weigt, 2000; Gitterman, 2000; Herrero, 2002; Hong, Kim, and Choi, 2002). This result agreed qualitatively with the simple mean-field theory.

Numerical simulations of the ferromagnetic Ising model on a growing Barabási-Albert scale-free network (Aleksiejuk *et al.*, 2002) demonstrated that the critical temperature T_c increases logarithmically with increasing N: $T_c(N)\sim\ln N$. Therefore, in the thermodynamic limit, the system is ordered at any finite T. The simple mean-field theory fails to explain this behavior. Analytical investigations (Dorogovtsev *et al.*, 2002b; Leone *et al.*, 2002) based on a microscopic theory revealed that the critical behavior of the ferromagnetic Ising model on complex networks is richer and extremely far from that expected from the standard mean-field theory. They showed that the simple mean-field theory does not take into account the strong heterogeneity of networks.

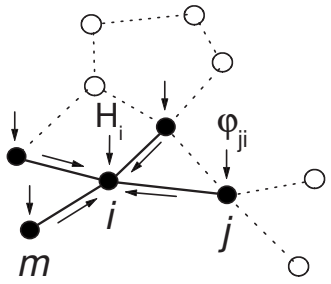

FIG. 15. A cluster on a graph. Within the Bethe-Peierls approach, we choose a cluster consisting of spin i and its nearest neighbors (closed circles). Cavity fields $\phi_{j\setminus i}$ (vertical arrows) take into account interactions with remaining spins (dotted lines and open circles). H_i is a local field. Arrows along edges show fields created by neighboring spins at vertex i.

Here we look first at exact and approximate analytical methods [for a comprehensive description of these methods, see Dorogovtsev *et al.* (2007)] and then consider critical properties of ferromagnetic, antiferromagnetic, and spin-glass Ising models on complex networks.

A. Main methods for treelike networks

1. Bethe approach

The Bethe-Peierls approximation is one of the most powerful methods for studying cooperative phenomena (Domb, 1960). It was proposed by Bethe (1935) and then applied by Peierls (1936) to the Ising model. This approximation gives a basis for developing a remarkably accurate mean-field theory. What is important is that it can be successfully used to study a finite system with a given quenched disorder. The list of current applications of the Bethe-Peierls approximation includes solid-state physics and information and computer sciences (Pearl, 1988), for example, image restoration (Tanaka, 2002), artificial vision (Freeman *et al.*, 2000), decoding of error-correcting codes (McEliece *et al.*, 1998), combinatorial optimization problems (Mézard and Zecchina, 2002), medical diagnosis (Kappen, 2002), and social models.

Consider the Ising model Eq. (51) on an arbitrary complex network. In order to calculate the magnetic moment of a spin S_i, we must know the total magnetic field $H_i^{(t)}$ which acts on this spin. This gives $M_i=\langle S_i\rangle=\tanh(\beta H_i^{(t)})$, where $\beta=1/T$. $H_i^{(t)}$ includes both a local field H_i and fields created by nearest-neighboring spins. The spins interact with their neighbors, who in turn interact with their neighbors, and so on. As a result, in order to calculate $H_i^{(t)}$, we have to account for all spins in the system. Bethe and Peierls proposed to take into account only interactions of a spin with its nearest neighbors. Interactions of these neighbors with remaining spins on a network were included in "mean fields." This simple idea reduces the problem of N interacting spins to a problem of a finite cluster.

Consider a cluster consisting of a central spin S_i and its nearest neighbors S_j; see Fig. 15. The energy of this cluster is

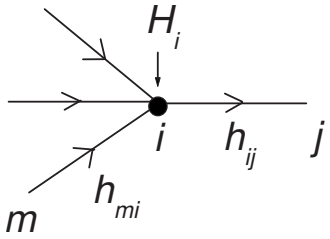

FIG. 16. Diagrammatic representation of Eq. (57). An outgoing message h_{ij} from vertex i to vertex j is determined by the local field H_i and incoming messages to i excluding the message from j.

$$H_{\rm cl} = -\sum_{j\in N(i)} J_{ij}S_iS_j - H_iS_i - \sum_{j\in N(i)} \phi_{j\backslash i}S_j, \tag{53}$$

where $N(i)$ represents all vertices neighboring vertex i. Interactions between spins $j\in N(i)$ are neglected. They will be approximately taken into account by the fields $\phi_{j\backslash i}$. These fields are called cavity fields within the cavity method (Mézard and Parisi, 2001). The cavity fields must be determined in a self-consistent way.

It is easy to calculate the magnetic moments of spins in the cluster. The magnetic field $H_i^{(t)}$ acting on i is

$$H_i^{(t)} = H_i + \sum_{j\in N(i)} h_{ji}, \tag{54}$$

where h_{ji} is an additional field created by a spin S_j at vertex i (see Fig. 15),

$$\tanh \beta h_{ji} \equiv \tanh \beta J_{ij} \tanh \beta \phi_{j\backslash i}. \tag{55}$$

In turn, the field $H_j^{(t)}$ acting on spin j is

$$H_j^{(t)} = \phi_{j\backslash i} + h_{ij}, \tag{56}$$

where the additional field h_{ij} is created by the central spin i at vertex j. This field is related to the additional fields in Eq. (55) as follows:

$$\tanh \beta h_{ij} = \tanh \beta J_{ij} \tanh\left[\beta\left(H_i + \sum_{m\in N(i)\backslash j} h_{mi}\right)\right], \tag{57}$$

where $N(i)\backslash j$ represents all vertices neighboring vertex i, except j. In the framework of the belief-propagation algorithm (Sec. VI.A.2), the additional fields h_{ji} are called *messages*. Using this term, we can interpret Eq. (57) as follows (see Fig. 16). An outgoing message sent by spin i to neighbor j is determined by incoming messages that spin i receives from other neighbors $m\in N(i)$, except j. Note that if vertex i is a dead end, then from Eq. (57) we obtain that the message h_{ij} from i to the only neighbor j is determined by a local field H_i,

$$\tanh \beta h_{ij} = \tanh \beta J_{ij} \tanh(\beta H_i). \tag{58}$$

We can choose a cluster in which S_j is the central spin. The field $H_j^{(t)}$ is given by the same Eq. (54). Comparing Eq. (54), where j replaces i, with Eq. (56), we obtain

$$\varphi_{i\backslash j} = H_i + \sum_{m\in N(i)\backslash j} h_{mi}. \tag{59}$$

Equations (54)–(59) establish relations between the fields $\{h_{ij}\}$ and $\{\phi_{i\backslash j}\}$. All we need is to solve Eq. (57) and find messages $\{h_{ij}\}$ in a graph. Apart from the local magnetic moments, the Bethe-Peierls approximation allows one to find a spin correlation function and the free energy. These formulas can be found in Dorogovtsev *et al.* (2007).

The Bethe-Peierls approach is exact for a treelike graph and the fully connected graph. It leads to the same equations as the cavity method and the exact recursion method; see Sec. VI.B. This approach is approximate for graphs with loops due to spin correlations induced by loops. However, even in this case, it usually leads to remarkably accurate results. The approach can be improved using the Kikuchi cluster variation method (Kikuchi, 1951; Domb, 1960; Yedidia *et al.*, 2001). How large are loop corrections to the Bethe-Peierls approximation? There is no clear answer to this question. Several methods have been proposed for calculating loop corrections (Yedidia *et al.*, 2001; Montanari and Rizzo, 2005; Chertkov and Chernyak, 2006a, 2006b; Parisi and Slanina, 2006; Rizzo *et al.*, 2007); however, this problem is still unsolved.

a. Regular Bethe lattice

The Bethe-Peierls approach gives an exact solution of the ferromagnetic Ising model in a uniform magnetic field on a regular Bethe lattice with a coordination number q (Baxter, 1982). In this case, all vertices and edges on the lattice are equivalent; therefore, $M_i = M$ and $h_{ij} = h$. From Eqs. (54) and (57), we obtain

$$M = \tanh(\beta H + \beta q h), \tag{60}$$

$$\tanh \beta h = \tanh \beta J \tanh(\beta H + \beta B h). \tag{61}$$

The parameter $B \equiv q-1$ on the right-hand side is the branching parameter.

At $H=0$, the model undergoes the standard second-order phase transition at a critical point in which $B \tanh \beta J = 1$, which gives the critical temperature

$$T_{\rm BP} = 2J/\ln[(B+1)/(B-1)]. \tag{62}$$

In the limit $q \gg 1$, the critical temperature $T_{\rm MF}$ tends to $T_{\rm BP}$, i.e., the simple mean-field approach Eq. (52) becomes exact in this limit. At the critical temperature $T = T_{\rm BP}$, the magnetic moment M is a nonanalytic function of H: $M(H) \sim H^{1/3}$.

b. Fully connected graph

The Bethe-Peierls approximation is exact for the fully connected graph. Consider the spin-glass Ising model with random interactions $|J_{ij}| \propto N^{-1/2}$ on the graph (the Sherrington-Kirkpatrick model). The factor $N^{-1/2}$ gives a finite critical temperature. To leading order in N, Eqs. (54) and (57) lead to a set of equations for magnetic moments M_i,

$$M_i = \tanh\left(\beta H + \beta \sum_j J_{ij} M_j - \beta^2 \sum_j J_{ij}^2 M_i (1 - M_j^2)\right). \tag{63}$$

These are the TAP (Thouless-Anderson-Palmer) equations (Thouless *et al.*, 1977), which are exact in the thermodynamic limit.

2. Belief-propagation algorithm

The belief-propagation algorithm is an effective numerical method for solving inference problems on sparse graphs. It was originally proposed by Pearl (1988) for treelike graphs. Among its numerous applications are computer vision problems, decoding of high performance turbo codes, and many others; see Frey (1998) and McEliece *et al.* (1998). Empirically it was found that it works surprisingly well even for graphs with loops. Yedidia *et al.* (2001) discovered that the belief-propagation algorithm coincides with the minimization of the Bethe free energy. This discovery renewed interest in the Bethe-Peierls approximation and related methods (Pretti and Pelizzola, 2003; Hartmann and Weigt, 2005; Mooij and Kappen, 2005). Recent progress in the survey propagation algorithm, which was proposed to solve some difficult combinatorial optimization problems, is a good example of interference between computer science and statistical physics (Mézard and Zecchina, 2002; Mézard *et al.*, 2002; Braunstein and Zecchina, 2004).

In this section, we give a physical interpretation of the belief-propagation algorithm applied to the Ising and other physical models on a complex network.

We start with the Ising model on a graph. Consider a spin i. Choose one of its nearest neighbors, say, a spin $j \in N(i)$. We define a parameter $\mu_{ji}(S_i)$ as the probability to find spin i in a state S_i under the following conditions: (i) spin i interacts only with spin j while other neighboring spins are removed and (ii) a local magnetic field H_i is zero. We normalize $\mu_{ji}(S_i)$ as follows: $\Sigma_{S_i=\pm 1}\mu_{ji}(S_i)=1$. For example, if $\mu_{ji}(+1)=1$ and $\mu_{ji}(-1)=0$, then the spin j permits the spin state $S_i=+1$ and forbids the spin state $S_i=-1$. Similarly, we define probabilities $\mu_{ni}(S_i)$ for other neighboring spins $n \in N(i)$. We assume that the probabilities $\mu_{ji}(S_i)$ for all $j \in N(i)$ are statistically independent. Strictly speaking, this assumption holds true only in a treelike graph. For a graph with loops, this approach is approximate. In the belief-propagation algorithm, the probabilities $\mu_{ji}(S_i)$ are traditionally called messages (do not mix with the messages in the Bethe-Peierls approach).

Search for an equilibrium state using an iteration algorithm. We start from an initial set of nonequilibrium normalized probabilities $\{\mu_{ji}^{(0)}(S_i)\}$. Choose two neighboring vertices i and j. Using the initial probabilities, we can calculate a probability to find a spin j in a state S_j under the condition that the state S_i is fixed. This probability is proportional to the product of independent probabilities that determine the state S_j. First, we have the product of all incoming messages $\mu_{nj}^{(0)}(S_j)$ from nearest-neighboring spins n of j, except i, because its state is fixed. This is $\Pi_{n\in N(j)\setminus i}\mu_{nj}^{(0)}(S_j)$. Second, we have a probabilistic factor $\exp(\beta H_j S_j)$ due to a local field H_j. Third, we have a probabilistic factor $\exp(\beta J_{ij} S_i S_j)$ due to the interaction between i and j. Summing the total product of these factors over two possible states $S_j=\pm 1$, we obtain a new probability,

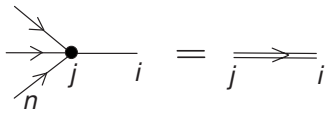

FIG. 17. Diagrammatic representation of the belief-propagation update rule. Arrows show incoming messages to a vertex j. A factor $\exp(\beta H_j S_j)$ is shown as the closed circle. A solid line between j and i shows a factor $\exp(\beta J_{ij} S_i S_j)$. The double line is a new (outgoing) message from j to i.

$$A \sum_{S_j=\pm 1} e^{\beta H_j S_j + \beta J_{ij} S_i S_j} \prod_{n\in N(j)\setminus i} \mu_{nj}^{(0)}(S_j) = \mu_{ji}^{\text{new}}(S_i), \tag{64}$$

where A is a normalization constant. This equation is the standard update rule of the belief-propagation algorithm. Its diagrammatic representation is shown in Fig. 17. We assume that the update procedure converges to a fixed point $\mu_{ji}^{\text{new}}(S_i) \to \mu_{ji}(S_i)$. Sufficient conditions for convergence of the belief-propagation algorithm to a unique fixed point have been derived by Ihler *et al.* (2005) and Mooij and Kappen (2005). This fixed point determines an equilibrium state of the Ising model on a given graph. Indeed, we can write $\mu_{ji}(S_i)$ in a general form as

$$\mu_{ji}(S_i) = \exp(\beta h_{ji} S_i)/(2\cosh \beta h_{ji}), \tag{65}$$

where h_{ji} is some parameter. Inserting Eq. (65) into Eq. (64), we obtain that the fixed-point equation is exactly the recursion equation (57) in the Bethe-Peierls approach. This demonstrates a close relationship between the belief-propagation algorithm and the Bethe-Peierls approximation. Calculations of local magnetic moments and the Bethe free energy have been described by Dorogovtsev *et al.* (2007).

One can apply the belief-propagation algorithm to a practically arbitrary physical model with discrete (Potts states) or continuous (many component vectors) local parameters x_i. Introduce local energies $E_i(x_i)$ and pairwise interaction energies $E_{ij}(x_i, x_j)$. A generalized fixed-point equation is

$$A \sum_{x_j} e^{-\beta E_j(x_j) - \beta E_{ij}(x_i, x_j)} \prod_{n\in N(j)\setminus i} \mu_{nj}(x_j) = \mu_{ji}(x_i), \tag{66}$$

where A is a normalization constant. If x_i is a continuous variable, then we integrate over x_j instead of summing. In particular, one can show that for the Potts model, this equation leads to an exact recursion equation (Dorogovtsev *et al.*, 2007).

3. Annealed network approach

In this subsection, we describe an improved mean-field theory that accounts for heterogeneity of a complex network. Despite its simplicity, this approximation gives surprisingly good results in the critical region.

The main idea of the annealed network approach is to replace a model on a complex network by a model on a weighted, fully connected graph. Consider the Ising model Eq. (51) on a graph with the adjacency matrix a_{ij}. We replace a_{ij} by the probability that vertices i and j with degrees q_i and q_j are connected. For the configuration model, this probability is $q_i\, q_j/z_1N$, where $z_1=\langle q\rangle$. We obtain the Ising model on the fully connected graph,

$$\mathcal{H}_{\rm an} = -\frac{1}{z_1 N}\sum_{i<j} J_{ij} q_i q_j S_i S_j - \sum_i H_i S_i, \tag{67}$$

where q_i plays the role of a "fitness" of vertex i. The resulting fully connected graph with these inhomogeneous fitnesses approximates the original complex network. Assuming that couplings J_{ij} are finite and using the exact equation (63), we find magnetic moments,

$$M_i = \tanh\left(\beta H_i + \frac{\beta q_i}{z_1 N}\sum_{j=1}^{N} J_{ij} q_j M_j\right). \tag{68}$$

Note that this set of equations is exact for the model (67) in the limit $N\to\infty$. For the ferromagnetic Ising model with $J_{ij}=J$ in zero field, i.e., $H_i=0$ for all i, the magnetic moment M_i is given by

$$M_i = \tanh(\beta J q_i M_w), \tag{69}$$

where we introduced a weighted magnetic moment $M_w \equiv (z_1N)^{-1}\Sigma_j q_j M_j$, which is a solution of the equation

$$M_w = \frac{1}{z_1}\sum_q P(q) q \tanh(\beta J q M_w). \tag{70}$$

Equations (69) and (70) were first derived by Bianconi (2002) for the Barabási-Albert network. They give an approximate mean-field solution of the ferromagnetic Ising model on an uncorrelated random complex network.

The effective model (67) undergoes a continuous phase transition at a critical temperature $T_c/J=z_2/z_1+1$, which approaches the exact critical temperature, Eq. (81), at $z_2/z_1\gg 1$. The annealed network approach gives correct critical behavior of the ferromagnetic Ising model. It shows that at T near T_c the magnetic moment $M_i\propto q_i M_w$ for degree q_i not too large in agreement with the microscopic results in Sec. VI.C.2. However, this approach gives wrong results for a cooperative model on an original network with $z_2/z_1\to 1$, i.e., near the emergence point of the giant connected component. The approach predicts a nonzero T_c contrary to the exact one, which tends to 0. At $T=0$, the annealed network approximation gives the average magnetic moment $M=1$. The exact calculations in Sec. VI.C.2 give $M<1$ due to the existence of finite clusters with zero magnetic moment.

B. The Ising model on a regular tree

The Ising model (51) on a regular tree can be solved using the exact recursion method developed for Bethe lattices and Cayley trees (Baxter, 1982). Recall that by definition a Cayley tree is a finite tree while a Bethe lattice is infinite (see Sec. II.B). We show that, even in the thermodynamic limit, thermodynamic properties of the ferromagnetic Ising model on a regular Cayley tree differ from those for a regular Bethe lattice.

1. Recursion method

Consider the ferromagnetic Ising model on a regular Cayley tree; see Fig. 1 in Sec. II.B. Any vertex can be considered as a root of the tree. This enables us to write a magnetic moment M_i of spin i and the partition function Z as follows:

$$M_i = \frac{1}{Z}\sum_{S_i=\pm 1} S_i e^{\beta H_i S_i}\prod_{j\in N(i)} g_{ji}(S_i), \tag{71}$$

$$Z = \sum_{S_i=\pm 1} e^{\beta H_i S_i}\prod_{j\in N(i)} g_{ji}(S_i). \tag{72}$$

Here $g_{ji}(S_i)$ is a partition function of subtrees growing from vertex j, under the condition that the spin state S_i is fixed,

$$g_{ji}(S_i) = \sum_{\{S_n=\pm 1\}} \exp[\beta J_{ij} S_i S_j - \beta \mathcal{H}_{j\backslash i}(\{S_n\})]. \tag{73}$$

Here $\mathcal{H}_{j\backslash i}(\{S_n\})$ is the interaction energy of spins, including spin j, on the subtrees except the edge (ij). The advantage of a regular tree is that we can calculate the parameters $g_{ji}(S_i)$ at a given vertex i using the following recursion relation:

$$g_{ji}(S_i) = \sum_{S_j=\pm 1} \exp(\beta J_{ij} S_i S_j + \beta H_j S_j)\prod_{m\in N(j)\backslash i} g_{mj}(S_j). \tag{74}$$

Note that this equation is equivalent to Eq. (64) at the fixed point within the belief-propagation algorithm. In order to show this, we introduce a parameter

$$h_{ji} \equiv (T/2)\ln[g_{ji}(+1)/g_{ji}(-1)] \tag{75}$$

and obtain $M_i=\tanh[(\beta H_i+\beta\Sigma_j h_{ji})]$. According to the Bethe-Peierls approach in Sec. VI.A.1, the parameter h_{ji} has the meaning of the additional field (message) created by vertex j at nearest-neighboring vertex i. These fields satisfy the recursion equation (57). In turn, Eq. (58) determines messages that go out of boundary spins of a given tree. Starting from the boundary spins and using Eq. (57), we can calculate one by one all fields h_{ij} on the Cayley tree and then find thermodynamic parameters of the Ising model.

2. Spin correlations

Using the recursion method, one can calculate the spin correlation function $\langle S_i S_j\rangle$ for two spins that are at a distance ℓ_{ij} from each other. We consider the general

case in which couplings J_{ij} on a Cayley tree are arbitrary parameters. In zero field, $\langle S_i S_j \rangle$ is equal to a product of parameters $\tanh \beta J_{ij}$ along the shortest path connecting i to j,

$$\langle S_i S_j \rangle = \prod_{m=0}^{\ell_{ij}-1} \tanh \beta J_{m,m+1}. \tag{76}$$

Here the index m numerates vertices on the shortest path, $m=0,1,\ldots,\ell_{ij}$, where $m=0$ corresponds to vertex i and $m=\ell_{ij}$ corresponds to vertex j (Mukamel, 1974; Falk 1975; Harris, 1975). This function coincides with a correlation function of an Ising spin chain (Bedeaux *et al.*, 1970), and spin correlations on a treelike graph have a one-dimensional character.

An even-spin correlation function $\langle S_1 S_2, \ldots, S_{2n} \rangle$ can also be calculated and presented as a product of pairwise correlation functions (Falk, 1975; Harris, 1975). Odd-spin correlation functions are zero in zero field.

3. Magnetic properties

The free energy of the ferromagnetic Ising model with $J_{ij}=J>0$ in zero magnetic field, $H=0$, on a regular Cayley tree was calculated by Eggarter (1974),

$$F = -TL \ln(2 \cosh \beta J), \tag{77}$$

where L is the number of edges. Moreover, this is the exact free energy of an arbitrary tree with L edges. F is an analytic function of T. Hence there is no phase transition even in the limit $N \to \infty$ in contrast to a regular Bethe lattice. The magnetization is zero at all temperatures except $T=0$. Muller-Hartmann and Zittartz (1974) revealed that the ferromagnetic Ising model on a regular Cayley tree with a branching parameter $B=q-1 \geqslant 2$ exhibits a new type of phase transition that is seen only in the magnetic field dependence of the free energy. The free energy becomes a nonanalytic function of magnetic field $H>0$ at temperatures below the critical temperature T_{BP} given by Eq. (62),

$$F(T,H) = F(T,H=0) + \sum_{l=1}^{\infty} a_n(T) H^{2l} + A(T) H^{\kappa} + O(H^{\kappa+1}), \tag{78}$$

where $a_n(T)$ and $A(T)$ are temperature-dependent coefficients. The exponent κ depends on T: $\kappa = \ln B / \ln(Bt)$, where $t \equiv \tanh \beta J$. The exponent increases smoothly from 1 to ∞ as temperature varies from 0 to T_{BP}; see Fig. 18. $F(T,H)$ is a continuous function of H at $T=T_{\mathrm{BP}}$. All derivatives of F with respect to H are finite. Therefore, the phase transition is of the infinite order in contrast to the second-order phase transition on a regular Bethe lattice; see Sec. VI.A.1. As T decreases below T_{BP}, the singularity in F is enhanced. The leading nonanalytic part of F has a form $H^{2l}|\ln H|$ at critical temperatures T_l given by $tB^{1-1/2l}=1$, which leads to $T_1 < T_2 < \cdots < T_\infty = T_{\mathrm{BP}}$. The zero-field susceptibility $\chi(T)$ diverges as $(1-t^2B)^{-1}$ at $T=T_1$. Note that this divergence does not mean the appearance of spontaneous magnetization. Magnetic properties of the Ising model on a regular Cayley tree were studied by von Heimburg and Thomas (1974), Matsuda (1974), Falk (1975), Melin *et al.* (1996), and Stosic *et al.* (1998).

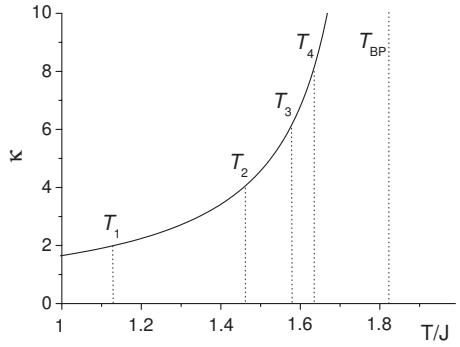

FIG. 18. Exponent κ vs T for the ferromagnetic Ising model on the regular Cayley tree with degree $q=3$. The critical temperatures T_l are shown by dotted lines.

Insight into the origin of the critical points T_1 and T_{BP} may be gained by considering local magnetic properties of the Cayley tree. Apply a small local magnetic field ΔH_i on a vertex i. Due to ferromagnetic coupling between spins, this field induces a magnetic moment $\Delta \mathcal{M}(i) = \beta V(i) \Delta H_i$ in a region around i, where $V(i)$ is a so-called correlation volume that determines a size of likely ferromagnetic correlations around i (see Sec. VI.C.4). An exact calculation of $V(i)$ shows that the correlation volume of the central spin diverges at $T=T_{\mathrm{BP}}$ in the infinite size limit $N \to \infty$. The central spin has long-ranged ferromagnetic correlations with almost all spins except for spins at a finite distance from the boundary. The correlation volume of a boundary spin diverges at a lower temperature $T=T_1<T_{\mathrm{BP}}$ simultaneously with the zero-field susceptibility $\chi(T) = N^{-1} \Sigma_i \beta V(i)$. Therefore, long-ranged spin correlations only cover the whole system at $T<T_1$.

A specific structure of the Cayley tree leads to the existence of numerous metastable states (Melin *et al.*, 1996), which do not exist on a Bethe lattice. These states have a domain structure (see Fig. 19) and are stable with respect to single-spin flips. In order to reverse all spins in a large domain, it is necessary to overcome an energy barrier that is proportional to the logarithm of the domain size. Therefore, a state with large domains will relax slowly to the ground state.

C. The ferromagnetic Ising model on uncorrelated networks

Here we show how strong the influence of network topology is on the critical behavior of the ferromagnetic Ising model. We show that when increased, network heterogeneity changes the critical behavior (the ferromagnetic phase transition becomes less sharp) and simultaneously increases the critical temperature. We also discuss spin correlations and finite-size effects.

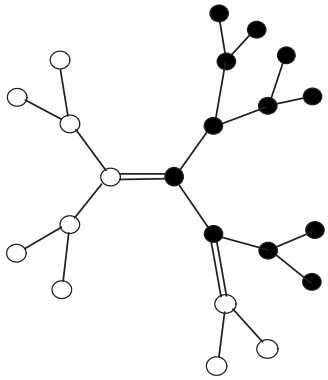

FIG. 19. Domains of flipped spins in the ferromagnetic Ising model on a regular Cayley tree. Filled and open circles represent spins up and down. Double lines shows "frustrated" edges connecting antiparallel spins.

1. Derivation of thermodynamic quantities

The microscopic theory of the ferromagnetic Ising model on uncorrelated random networks was developed using the exact recursion method (Dorogovtsev *et al.*, 2002b), which is equivalent to the Bethe-Peierls approximation, and the replica trick (Leone *et al.*, 2002).

Consider the Ising model with couplings $J_{ij}=J>0$ in uniform magnetic field $H_i=H$ within the Bethe-Peierls approach; see Sec. VI.A.1. A thermodynamic state of this model is completely described by additional fields (messages) created by spins. In a complex network, due to intrinsic heterogeneity, the fields are random parameters. We introduce a distribution function $\Psi(h)$ of messages h_{ij}: $\Psi(h)=(1/Nz_1)\Sigma_{i,j}\delta(h-h_{ij})$, where Nz_1 is the normalization constant. If we assume the self-averageness, then, in the limit $N\to\infty$, the average over a graph is equivalent to the average over a statistical network ensemble.

A self-consistent equation for $\Psi(h)$ follows from the recursion equation (57) (see also Fig. 16 in Sec. VI.A.1),

$$\Psi(h)=\sum_q \frac{P(q)q}{z_1}\int \delta\Bigg(h-T\tanh^{-1}\Bigg[\tanh\beta J \times\tanh\Bigg(\beta H+\beta\sum_{m=1}^{q-1}h_m\Bigg)\Bigg]\Bigg)\prod_{m=1}^{q-1}\Psi(h_m)dh_m. \tag{79}$$

First, this equation assumes that all incoming messages $\{h_m\}$ are statistically independent. This assumption is valid for an uncorrelated random network. Second, an outgoing message h is sent along a chosen edge by a vertex of degree q with the probability $P(q)q/z_1$. If we know $\Psi(h)$, we can find the free energy and other thermodynamic parameters [see Dorogovtsev *et al.* (2007)]. For example, the average magnetic moment is

$$M=\sum_q P(q)\int \tanh\Bigg(\beta H+\beta\sum_{m=1}^{q}h_m\Bigg)\prod_{m=1}^{q}\Psi(h_m)dh_m. \tag{80}$$

2. Phase transition

In the paramagnetic phase at zero field $H=0$, Eq. (79) has a trivial solution: $\Psi(h)=\delta(h)$, i.e., all messages are zero. A nontrivial solution (which describes a ferromagnetically ordered state) appears below a critical temperature T_c,

$$T_c=2J\Big/\ln\Big(\frac{z_2+z_1}{z_2-z_1}\Big). \tag{81}$$

This is the exact result for an uncorrelated random network (Dorogovtsev *et al.*, 2002b; Leone *et al.*, 2002).

The critical temperature T_c can be found from a "naive" estimate. As noted in Sec. VI.A.1, the critical temperature $T_{\rm BP}$, Eq. (62), is determined by the branching parameter rather than the mean degree. In a complex network, the branching parameter fluctuates from edge to edge. The average branching parameter B may differ remarkably from the mean degree z_1. For the configuration model, inserting the average branching parameter $B=z_2/z_1$ into Eq. (62), we obtain Eq. (81). If the parameter z_2 tends to z_1, then $T_c\to 0$. This is not surprising, because at the percolation threshold we have $z_2=z_1$, and the giant connected component disappears.

A general analytical solution of Eq. (79) for the distribution function $\Psi(h)$ is unknown. A correct critical behavior of the Ising model at T near T_c can be found using an effective-medium approximation,

$$\sum_{m=1}^{q-1}h_m\approx(q-1)\bar{h}+O(q^{1/2}), \tag{82}$$

where $\bar{h}\equiv\int h\Psi(h)dh$ is the average field, which can be found self-consistently (Dorogovtsev *et al.*, 2002b). This approximation takes into account the most "dangerous" highly connected spins. The ansatz (82) is equivalent to $\Psi(h)\sim\delta(h-\bar{h})$ (Leone *et al.*, 2002). At lower temperatures, a finite width of $\Psi(h)$ becomes important.

The ferromagnetic Ising model on uncorrelated random networks demonstrates three classes of universal critical behavior:

(i) The standard mean-field critical behavior in networks with a finite fourth moment $\langle q^4\rangle$ (scale-free networks with the degree distribution exponent $\gamma>5$).

(ii) A critical behavior with nonuniversal critical exponents depending on a degree distribution in networks with divergent $\langle q^4\rangle$, but a finite second moment $\langle q^2\rangle$ (scale-free networks with $3<\gamma\leqslant 5$).

(iii) An infinite-order phase transition in networks with a divergent second moment $\langle q^2\rangle$, but a finite mean degree $\langle q\rangle$ (scale-free networks with $2<\gamma\leqslant 3$).

The corresponding critical exponents ($M\sim\tau^{\beta}$, $\delta C\sim\tau^{-\alpha}$, $\chi\sim\tau^{-\tilde{\gamma}}$) are reported in Table I. Evolution of the critical behavior with increasing heterogeneity is shown schematically in Fig. 20. Notice that the Ising model on a regular random network demonstrates the standard

TABLE I. Critical behavior of the magnetization M, the specific heat δC, and the susceptibility χ in the Ising model on networks with a degree distribution $P(q) \sim q^{-\gamma}$ for various values of exponent γ. $\tau \equiv 1 - T/T_c$.

	M	$\delta C(T<T_c)$	χ
$\gamma>5$	$\tau^{1/2}$	Jump at T_c	τ^{-1}
$\gamma=5$	$\tau^{1/2}/(\ln \tau^{-1})^{1/2}$	$1/\ln \tau^{-1}$	
$3<\gamma<5$	$\tau^{1/(\gamma-3)}$	$\tau^{(5-\gamma)/(\gamma-3)}$	
$\gamma=3$	$e^{-2T/\langle q\rangle}$	$T^2 e^{-4T/\langle q\rangle}$	T^{-1}
$2<\gamma<3$	$T^{-1/(3-\gamma)}$	$T^{-(\gamma-1)/(3-\gamma)}$	

mean-field critical behavior in the infinite size limit (Scalettar, 1991). The corresponding exact solution is given in Sec. VI.A.1.a.

The conventional scaling relation between the critical exponents takes place at $\gamma>3$,

$$\alpha + 2\beta + \tilde{\gamma} = 2. \tag{83}$$

Interestingly, the magnetic susceptibility χ has universal critical behavior with $\tilde{\gamma}=1$ when $\langle q^2\rangle<\infty$, i.e., at $\gamma>3$. This agrees with the scaling relation $\tilde{\gamma}/\nu = 2-\eta$ if we insert the standard mean-field exponents: $\nu=\frac{1}{2}$ and the Fisher exponent $\eta=0$; see Sec. IX.B. When $2<\gamma\leqslant 3$, the susceptibility χ has a paramagnetic temperature dependence, $\chi \propto 1/T$, at temperatures $T \gtrsim J$ despite the system being in the ordered state.

At $T<T_c$, the ferromagnetic state is strongly heterogeneous because the magnetic moment M_i fluctuates from vertex to vertex. The ansatz (82) enables us to find an approximate distribution function of M_i,

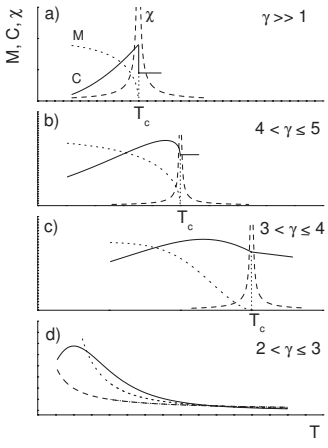

FIG. 20. Schematic representation of the critical behavior of the magnetization M (dotted lines), the magnetic susceptibility χ (dashed lines), and the specific heat C (solid lines) for the ferromagnetic Ising model on uncorrelated random networks with a degree distribution $P(q) \sim q^{-\gamma}$. (a) $\gamma \gg 1$, the standard mean-field critical behavior. A jump of C disappears when $\gamma \to 5$. (b) $4<\gamma\leqslant 5$, the ferromagnetic phase transition is of second order. (c) $3<\gamma\leqslant 4$, the transition becomes of higher order. (d) $2<\gamma\leqslant 3$, the transition is of infinite order, and $T_c \to \infty$ as $N \to \infty$.

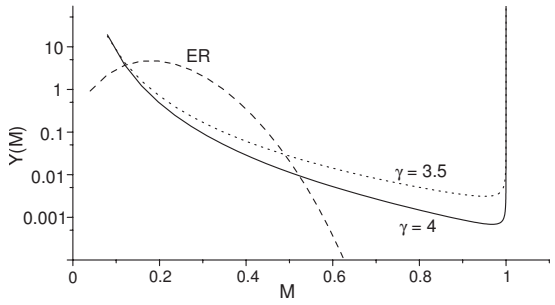

FIG. 21. Distribution function $Y(M)$ of magnetic moments M in the ferromagnetic Ising model on the Erdős-Rényi graph with mean degree $z_1=5$ (dashed line) and scale-free graphs with $\gamma=4$ and 3.5 (solid and dotted lines) at T close to T_c, $\beta\bar{h}=0.04$.

$$Y(M) \equiv \frac{1}{N}\sum_{i=1}^{N} \delta(M - M_i) \approx \frac{P[q(M)]}{\beta\bar{h}(1-M^2)}, \tag{84}$$

where the function $q(M)$ is a solution of an equation $M(q)=\tanh(\beta\bar{h}q)$. Near T_c, low-degree vertices have a small magnetic moment, $M(q) \sim q|T_c - T|^{1/2} \ll 1$, while hubs with degree $q > T/\bar{h} \gg 1$ have $M(q) \sim 1$. The function $Y(M)$ is shown in Fig. 21. Note that the distribution of magnetic moments in scale-free networks is more inhomogeneous than in the Erdős-Rényi graphs. In the former case, $Y(M)$ diverges at $M \to 1$. A local magnetic moment depends on its neighborhood. In particular, a magnetic moment of a spin neighboring a hub may differ from a moment of a spin surrounded by low-degree vertices (Giuraniuc *et al.*, 2006).

At $T=H=0$, the exact distribution function $\Psi(h)$ converges to a function with two delta peaks,

$$\Psi(h) = x\delta(h) + (1-x)\delta(h-J), \tag{85}$$

where the parameter x is determined by an equation describing percolation in networks; see Sec. III.B.1. Equation (85) tells us that in the ground state, spins, which belong to a finite cluster, have zero magnetic moment while spins in a giant connected component have magnetic moment 1. The average magnetic moment is $M=1-\Sigma_q P(q)x^q$. This is exactly the size of the giant connected component of the network.

3. Finite-size effects

When $2<\gamma\leqslant 3$, a dependence of T_c on the size N is determined by the finite-size cutoff $q_{\rm cut}(N)$ of the degree distribution in Sec. II.E.4. We obtain

$$T_c(N) \approx \begin{cases} \dfrac{z_1 \ln N}{4} & \text{at } \gamma = 3 \quad (86) \\ \dfrac{(\gamma-2)^2 z_1 q_{\rm cut}^{3-\gamma}(N)}{(3-\gamma)(\gamma-1)} & \text{at } 2<\gamma<3 \quad (87) \end{cases}$$

(Bianconi, 2002; Dorogovtsev *et al.*, 2002b; Leone *et al.*, 2002). These estimates agree with the numerical simulations of Aleksiejuk *et al.* (2002) and Herrero (2004). No-

tice that Herrero used the cutoff $q_{\rm cut}(N) \sim N^{1/\gamma}$, which leads to $T_c \sim N^z$ with the exponent $z=(3-\gamma)/\gamma$.

4. Ferromagnetic correlations

Consider spin correlations in the ferromagnetic Ising model in the paramagnetic state. Recall that the correlation length ξ of spin correlations in a finite-dimensional lattice diverges at T_c. In contrast, in an uncorrelated random complex network, the correlation length ξ is finite at any T. Indeed, according to Eq. (76), the correlation function $C(\ell)=\langle S_i S_j \rangle$ decays exponentially with distance $\ell \equiv \ell_{ij}$: $C(\ell)=e^{-\ell/\xi}$, where the coherence length $\xi \equiv 1/|\ln \tanh \beta J| \neq 0$ at $T \neq 0$. Moreover, spin correlations have a one-dimensional character despite the fact that a complex network is an infinite-dimensional system. Strictly speaking, this is valid at distances $\ell < \bar{\ell}(N) \sim \ln N$ when a network is treelike.

In complex networks, the so called correlation volume rather than ξ plays a fundamental role; see also Sec. III.B.3. We define a correlation volume $V(i)$ around a spin i as follows:

$$V(i) \equiv \sum_{j=1}^{N} a_{ij} \langle S_i S_j \rangle. \tag{88}$$

The volume determines the size of likely ferromagnetic fluctuations around the spin. In the paramagnetic phase, $V(i)$ is expressed through local network characteristics: $V(i)=\Sigma_{\ell=0}^{\infty} z_\ell(i) t^\ell$, where $t \equiv \tanh \beta J$, $z_\ell(i)$ is the number of vertices that are at a distance ℓ from vertex i, and $z_0(i) \equiv 1$. The average correlation volume $\bar{V}$ is related with the total magnetic susceptibility,

$$\bar{V} \equiv \frac{1}{N} \sum_{i=1}^{N} V(i) = \sum_{\ell=0}^{\infty} z_\ell t^\ell = T\chi, \tag{89}$$

where z_ℓ is the average number of ℓth nearest neighbors of a vertex on a given network: $z_\ell = N^{-1} \Sigma_i z_\ell(i)$. The average correlation volume $\bar{V}$ diverges as $\ln N$ in the critical point of a continuous phase transition. The divergence condition of the series in Eq. (89) leads to the equation $B \tanh \beta_c J = 1$, where $B \equiv \lim_{\ell \to \infty} \lim_{N \to \infty} [z_\ell]^{1/\ell}$ is the average branching parameter of the network. This criterion for the critical point is valid for any treelike network (Lyons, 1989), including networks with degree-degree correlations, growing networks, etc. $B=1$ corresponds to the emergence point of the giant connected component. At $B<1$, a network consists of finite clusters, the correlation volume is finite at all T, and there is no phase transition.

Using Eq. (89), we can calculate χ in the paramagnetic phase. In the configuration model of uncorrelated random networks, we have $z_\ell = z_1 (z_2/z_1)^{\ell-1}$. This gives

$$T\chi = \bar{V} = 1 + z_1 t/(1 - z_2 t/z_1). \tag{90}$$

So χ diverges as $|T-T_c|^{-1}$.

Equation (76) for the correlation function $\langle S_i S_j \rangle$ is not valid for scale-free networks with $2<\gamma<3$ due to numerous loops. Dorogovtsev, Goltsev, and Mendes (2005) found that in these networks the pair correlation function $\langle S_i S_j \rangle$ between the second and more distant neighbors vanishes in the limit $N \to \infty$. Only pair correlations between nearest neighbors are observable.

5. Degree-dependent interactions

Giuraniuc *et al.* (2005, 2006) studied analytically and numerically a ferromagnetic Ising model on a scale-free complex network with a topology-dependent coupling: $J_{ij}=J z_1^{2\mu} (q_i q_j)^{-\mu}$, where a constant $J>0$, μ is a tunable parameter, and q_i and q_j are degrees of neighboring vertices i and j. They demonstrated that the critical behavior of the model on a scale-free network with degree distribution exponent γ is equivalent to the critical behavior of the ferromagnetic Ising model with a constant coupling J on a scale-free network with renormalized degree distribution exponent $\gamma'=(\gamma-\mu)/(1-\mu)$. Therefore, the critical exponents can be obtained, replacing γ by γ' in Table I. Varying μ in the range $[2-\gamma, 1]$ allows us to explore the whole range of the universality classes represented in Table I. For example, the ferromagnetic Ising model with $J_{ij}=J$ on a scale-free network with $\gamma=3$ undergoes an infinite-order phase transition while the model with degree-dependent coupling for $\mu=1/2$ undergoes a second-order phase transition with the critical behavior corresponding to $\gamma'=5$.

D. The Ising model on small-world networks

The phase transition in the ferromagnetic Ising model on small-world networks resembles that in the percolation problem for these nets; see Sec. III.G. This system was studied by Barrat and Weigt (2000), Gitterman (2000), Pękalski (2001), and many others. Here we discuss small-world networks based on one-dimensional lattices, with a fraction p of shortcuts. We estimate the critical temperature $T_c(p)$ assuming for simplicity only nearest-neighbor interactions in the one-dimensional lattice. One may see that if p is small, this network has a locally treelike structure. At small p, the mean branching parameter in this graph is $B=1+cp+O(p^2)$, where c is some model-dependent constant. Substituting B into Eq. (62), we arrive at

$$T_c(p) \sim J/|\ln p|, \tag{91}$$

where J is the ferromagnetic coupling. Barrat and Weigt (2000) arrived at this result using the replica trick. Exact calculations of Lopes *et al.* (2004) confirmed this formula.

Far from the critical temperature, the thermodynamic quantities of this system are close to those of the d-dimensional substrate lattice. However, in the vicinity of the critical temperature, the ordinary mean-field picture is valid. Two circumstances naturally explain these traditional mean-field features. (i) In the range of small p, the small-world networks effectively have a locally treelike structure (short loops due to the lattice are not

essential). (ii) The small-world networks have rapidly decreasing degree distributions. As explained, this architecture leads to the traditional mean-field picture of critical phenomena. The region of temperatures around $T_c(p)$, where this mean-field picture is realized, is narrowed as p decreases. Lopes *et al.* (2004) obtained the specific heat as a function of temperature and p and showed that its jump at the critical point approaches zero as $p \to 0$. Roy and Bhattacharjee (2006) demonstrated numerically that the Ising model on the Watts-Strogatz network is self-averaging in the limit $N \to \infty$, i.e., the average over this ensemble is equivalent to the average over a single Watts-Strogatz network. With increasing network size N, the distributions of the magnetization, the specific heat, and the critical temperature of the Ising model in the ensemble of different realizations of the Watts-Strogatz network approach the δ function. The size dependence of these parameters agrees with the finite scaling theory in Sec. IX.B.

Hastings (2003) investigated the Ising model on the d-dimensional small world. He found that for any d the shift of the critical temperature is $T_c(p) - T_c(p=0) \sim p^{1/\tilde{\gamma}}$, where $\tilde{\gamma}$ is the susceptibility exponent at $p=0$, $\chi(T, p=0) \sim |T - T_c(0)|^{-\tilde{\gamma}}$. Compare this shift with the similar shift of the percolation threshold in the same network; see Sec. III.G. Simulations of Herrero (2002) and Zhang and Novotny (2006) confirmed this prediction.

In their simulations, Jeong *et al.* (2003) studied the Ising model with specific interactions placed on the ordinary one-dimensional small-world network. In their system, the ferromagnetic interaction between two neighboring spins, say, spins i and j, is $|i-j|^{-\alpha}$. $|i-j|$ is a distance measured along the chain. Surprisingly, a phase transition was revealed only at $\alpha=0$; no long-range order for $\alpha>0$ was observed at any nonzero temperature. Chatterjee and Sen (2006) performed numerical simulations of the ferromagnetic Ising model placed on a one-dimensional small-world network, where vertices, say, i and j, are connected by a shortcut with probability $\sim |i-j|^{-\alpha}$ (Kleinberg's network; see Sec. II.I). They observed a phase transition at least at $\alpha<1$. In both these studies, the small sizes of simulated networks made it difficult to arrive at reliable conclusions. On the other hand, these two systems were not studied analytically.

E. Spin-glass transition on networks

Despite years of effort the understanding of spin glasses is still incomplete. The nature of the spin-glass state is well understood for the infinite-range Sherrington-Kirkpatrick model (Binder and Young, 1986; Mézard *et al.*, 1987) The basic property of the spin-glass model is that a large number of pure thermodynamic states with nonzero local magnetic moments M_i spontaneously emerge below a critical temperature. This corresponds to replica-symmetry breaking.

Investigations of a spin-glass Ising model on treelike networks began soon after the discovery of spin glasses. Viana and Bray (1985) proposed the so-called dilute Ising spin-glass model, which is equivalent to the Ising model on the Erdős- Rényi graph [for a review of early investigations see Mézard and Parisi (2001)]. Most studies considered a spin glass on random regular and Erdős-Rényi networks. A spin glass on a complex network only recently drew attention.

Here we first review recent studies of the spin-glass Ising model on complex networks. Then we consider a pure antiferromagnetic Ising model, which becomes a spin glass when placed on a complex network, and we discuss the relationships of this model with famous NP-complete problems (MAX-CUT and vertex cover).

1. The Ising spin glass

The spin-glass state arises due to frustrations. Frustrations in the Sherrington-Kirkpatrick model and a spin-glass model on a finite-dimensional lattice are due to numerous finite loops. Uncorrelated random networks have a treelike structure in the thermodynamic limit. How do frustrations appear in this case? It turns out that frustrations in these networks are due to numerous long loops of typical length $O(\ln N)$; see Sec. II.G.

Early investigations of a spin glass on a Bethe lattice assumed that there is only one pure thermodynamic state, and the replica symmetry is unbroken. This assumption led to unphysical results such as, for example, a negative specific heat. Much evidence has been accumulated indicating that a spin-glass state may exist in the spin-glass Ising model on a Bethe lattice (Mézard and Parisi, 2001), meaning that this model has many pure thermodynamic states at low temperatures. In order to obtain a complete description of a spin-glass state, it is necessary to solve the recursion equation (57), which is exact in the thermodynamic limit, and find the distribution function $\Psi_\alpha(h)$ of the messages for every pure state α. It is a difficult mathematical problem that is equivalent to searching for a solution with replica-symmetry breaking. In order to find an approximate solution, a one-step replica-symmetry breaking approximation was developed (Mézard and Parisi, 2001; Pagnani *et al.*, 2003; Castellani *et al.*, 2005) This approximation assumes that a space of pure states has a simple cluster structure (a set of clusters). Numerical simulations of the spin-glass Ising model on a random regular network demonstrated that this approximation gives better results than the replica-symmetric solution. A similar result was obtained for the Watts-Strogatz network (Nikoletopoulos *et al.*, 2004). Unfortunately, the space of pure states is probably more complex, and a solution with a complete replica-symmetry breaking is necessary.

The exact critical temperature of the spin-glass transition T_{SG} on a treelike complex network can be found without the replica trick. The criterion of this transition is the divergence of the spin-glass susceptibility,

$$\chi_{SG} = \frac{1}{N}\sum_{i=1}^{N}\sum_{j=1}^{N}\langle S_i S_j\rangle^2. \quad (92)$$

Using Eq. (76) for the correlation function $\langle S_i S_j\rangle$, we find that χ_{SG} diverges at a critical temperature T_{SG} determined by

$$B\int \tanh^2(\beta_{SG} J_{ij}) P(J_{ij}) dJ_{ij} = 1, \quad (93)$$

where B is the average branching parameter.

If the distribution function $P(J_{ij})$ is asymmetric, and the mean coupling $\bar{J} = \int J_{ij} P(J_{ij}) dJ_{ij}$ is larger than a critical value, then a ferromagnetic phase transition occurs at a critical temperature T_c higher than T_{SG}. The criterion of the ferromagnetic phase transition is the divergence of the magnetic susceptibility χ,

$$B\int \tanh(\beta_c J_{ij}) P(J_{ij}) dJ_{ij} = 1. \quad (94)$$

At a multicritical point, we have $T_c = T_{SG}$. Equations (93) and (94) generalize the results obtained by the replica trick and other methods for different uncorrelated random networks (Viana and Bray, 1985; Thouless, 1986; Baillie *et al.*, 1995; Kim *et al.*, 2005; Mooij and Kappen, 2005; Ostilli, 2006a, 2006b).

It is well known that, in the Sherrington-Kirkpatrick model, ferromagnetism and spin glass coexist at low temperatures if $\bar{J}$ exceeds a critical value. This is a *mixed* state. Castellani *et al.* (2005) studied the spin-glass Ising model on a random regular graph with degree q and a random coupling J_{ij}, which takes values $\pm J$ with probabilities $(1\pm\rho)/2$. They found that at $T=0$, the system is in the mixed state if $\rho_F < \rho \le \rho_c(q)$. In particular, $\rho_c(q=3) = 5/6$, and $\rho_c(q) \sim \ln q/\sqrt{q}$ at $q \gg 1$. At $\rho < \rho_F$, the ground state is a nonmagnetic spin-glass state. Liers *et al.* (2003) numerically studied the spin-glass model with a Gaussian coupling J_{ij}. No mixed state was observed in contrast to Castellani *et al.* (2005).

Kim *et al.* (2005) studied the Ising spin-glass model with $J_{ij} = \pm J$ on an uncorrelated scale-free network using the replica-symmetric perturbation approach of Viana and Bray (1985). It turned out that for the degree exponent $3 < \gamma < 4$ the critical behavior of the spin-glass order parameter at T near T_{SG} differs from the critical behavior of the Sherrington-Kirkpatrick model. For the paramagnetic-ferromagnetic phase transition, a deviation from the standard critical behavior takes place at $\gamma < 5$ similarly to the ferromagnetic Ising model in Sec. VI.C.2. At $2 < \gamma < 3$, critical temperatures of the ferromagnetic and spin-glass phase transitions approach infinity in the thermodynamic limit. These transitions become of infinite order.

2. The antiferromagnetic Ising model and MAX-CUT problem

The antiferromagnetic (AF) Ising model becomes nontrivial on a complex network. As shown, the model is a spin glass. We also discuss here a mapping of the ground-state problem onto the MAX-CUT problem.

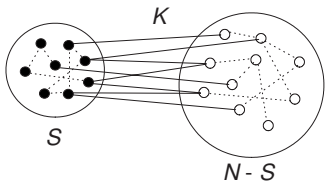

FIG. 22. Partition of vertices in a graph into two sets consisting of S and $N-S$ vertices, and K edges (solid lines) in the cut. Dotted lines show edges inside the sets.

Consider the pure AF model on a graph,

$$E = \frac{J}{2}\sum_{i,j} a_{ij} S_i S_j, \quad (95)$$

where $J > 0$. The search for the ground state is equivalent to coloring a graph in two colors (colors correspond to spin states $S = \pm 1$) in such a way that no two adjacent vertices have the same color. First consider a bipartite network, which is a network without odd loops. It is obvious that this network is 2-colorable. The ground-state energy of the AF model on a bipartite graph is $E_0 = -JL$, where L is the total number of edges in the graph. An uncorrelated complex network with a giant connected component cannot be colored with two colors due to numerous odd loops. So the ground-state energy E_0 of the AF model on a random graph is higher than $-JL$ due to frustrations produced by odd loops.

The ground-state problem can be mapped to the MAX-CUT problem, which belongs to the class of NP-complete optimization problems. Divide vertices of a graph (of N vertices and L edges) into two sets in such a way that the number K of edges that connect these sets is maximum; see Fig. 22. If we define spins at vertices in one set as spins up and spins in the other set as spins down, then the maximum cut gives a minimum energy E_0 of the AF model. Indeed, K edges between two sets connect antiparallel spins and give a negative contribution $-JK$ into E_0. The remaining $L-K$ edges connect parallel spins and give a positive contribution $J(L-K)$. The ground-state energy $E_0 = J(L-2K)$ is minimum when K is maximum.

The maximum cut of the Erdős-Rényi graph with high probability is

$$K_c \equiv \max K = L/2 + AN\sqrt{z_1} + o(N) \quad (96)$$

for mean degree $z_1 \gg 1$ (Kalapala and Moore, 2002; Coppersmith *et al.*, 2004). Here A is a constant with lower and upper bounds $0.26 < A < \sqrt{\ln 2}/2 \approx 0.42$. Recall that $L = z_1 N/2$. For the estimation of K_c, see Dorogovtsev *et al.* (2007). Thus the ground-state energy is

$$E_0/N = -2JA\sqrt{z_1}. \quad (97)$$

The fraction of "frustrated" edges, i.e., edges that connect "unsatisfied" parallel spins, is $(L-K_c)/L = 1/2 - 2A/\sqrt{z_1}$. Thus almost half of the edges are frustrated.

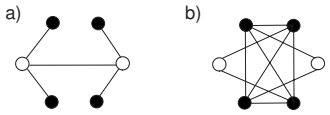

FIG. 23. Vertex cover of a graph. (a) Open circles form a minimum vertex cover of the graph. Every edge has at least one end point that belongs to the vertex cover. The closed circles form the maximum independent set of the graph. (b) The complement of the same graph (we add the missing edges and remove the already existing edges). Closed circles form the maximum clique.

This result is valid not only for classical random graphs but also for arbitrary uncorrelated random networks.

Interestingly, the lower bound of the ground-state energy Eq. (97) is quite similar to the lower bound for the ground-state energy of the random energy model by Derrida (1981). This model approximates to spin glass in any dimensions. Replacing the mean degree z_1 in Eq. (97) by degree of a D-dimensional cubic lattice, $2D$, we obtain the ground-state energy of Derrida's model: $E_0/N=-J\sqrt{2D\ln 2}$.[1]

Despite the seeming simplicity, the pure AF model on complex networks is not well studied. We assume that this model is the usual spin glass. Spin-glass behavior was observed in numerical simulations of the model on the Barabási-Albert network (Bartolozzi *et al.*, 2006).

In order to measure the bipartivity of real-world networks (professional collaborations, on-line interactions, and so on), Holme *et al.* (2003) proposed to put the antiferromagnetic Ising model on the top of a network and calculate a fraction of edges between spins with opposite signs in the ground state. The larger this fraction is, the closer the network is to bipartite. This procedure is equivalent to finding the maximum cut of the graph. It allows one to reveal the bipartite nature of seemingly one-partite networks. Note that only their one-mode projections are usually studied, while most of the real-world networks are actually multipartite.

3. Antiferromagnet in a magnetic field, the hard-core gas model, and vertex covers

Here we discuss relations between an antiferromagnetic Ising model, the hard-core gas model, and the vertex cover problem on classical random graphs. On complex networks, these problems are poorly studied.

a. The vertex cover problem

This problem is one of the basic NP-complete optimization problems. A vertex cover of a graph is a set of vertices with the property that every edge of the graph has at least one end point that belongs to this set. In general, there are many different vertex covers. We look for a vertex cover of a minimum size; see Fig. 23. Weigt and Hartmann (2000) proposed a vivid picture for this problem: "Imagine you are director of an open-air museum situated in a large park with numerous paths. You want to put guards on crossroads to observe every path, but in order to economize cost you have to use as few guards as possible."

Find the size of a minimum vertex cover of the Erdős-Rényi graph of N vertices, $L=z_1N/2$ edges, and mean degree z_1. We denote the number of vertices in a vertex cover as $N_{\rm vc}=xN$. The parameter x can be interpreted as the probability that a randomly chosen vertex is covered, i.e., it belongs to the vertex cover. An edge can be between every pair of vertices with the same probability. So the probability that a randomly chosen edge connects two vertices that do not belong to the vertex cover is $(1-x)^2$. With the conjugate probability $1-(1-x)^2=2x(1-x)$, an edge has at least one covered end point. There are $\binom{N}{N_{\rm vc}}$ ways to choose $N_{\rm vc}$ vertices from N vertices. Only a small fraction of the partitions, $[2x(1-x)]^L$, are vertex covers. Thus the number of possible vertex covers is

$$\mathfrak{N}_{\rm vc}(x)=\binom{N}{N_{\rm vc}}[2x(1-x)]^L\equiv e^{N\Xi(x)}. \tag{98}$$

The threshold fraction x_c is determined by the condition $\Xi(x_c)=0$. The condition gives $x_c(z_1)\approx 1-2\ln z_1/z_1+O(\ln\ln z_1)$ at $z_1\gg 1$. The exact asymptotics was found by Frieze (1990). At $x<x_c$, with high probability there is no vertex cover of size $xN<x_cN$, while at $x>x_c$ there are exponentially many different covers of size $xN>x_cN$. The appearance of many vertex covers looks like a phase transition at the threshold parameter $x=x_c$.

The exact threshold $x_c(z_1)$ and the number of minimum vertex covers were calculated for the Erdős-Rényi graph using a hard-core model (see below) and the replica method (Weigt and Hartmann, 2000; Weigt and Zhou, 2006) The replica-symmetric solution gives an exact result in the interval $1<z_1\leqslant e$,

$$x_c(z_1)=1-[2W(z_1)+W(z_1)^2]/2z_1, \tag{99}$$

where $W(x)$ is the Lambert function defined by $W\exp(W)=x$. The same result was derived by Bauer and Golinelli (2001a, 2001b) using the leaf algorithm. Note that the giant connected component of the Erdős-Rényi graph disappears at $z_1<1$. The presence of the replica symmetry indicates that, in the interval $1<z_1\leqslant e$, one can interchange a finite number of covered and uncovered vertices in order to receive another minimum vertex cover. Many nontrivial minimum vertex covers appear at mean degrees $z_1>e$. The replica symmetry is broken and Eq. (99) is not valid. For this case, the threshold $x_c(z_1)$ and the degeneracy of the minimum vertex cover were calculated using the one-step replica-symmetry breaking by Weigt and Hartmann (2000, 2001) and Zhou (2003). The typical running time of an algorithm for finding a vertex cover at $z_1\leqslant e$ is polynomial while the time grows exponentially with the graph size at $z_1>e$ (Barthel and Hartmann, 2004).

[1]We are grateful to M. Ostilli for attracting our attention to this fact.

The vertex cover problem on correlated scale-free networks was studied by Vázquez and Weigt (2003). It turned out that an increase of likewise degree-degree correlations (assortative mixing) increases the computational complexity of this problem in comparison with an uncorrelated scale-free network having the same degree distribution. If the assortative correlations exceed a critical threshold, then many nontrivial vertex covers appear.

Interestingly, the minimum vertex cover problem is equivalent to another NP-hard optimization problem—the maximum clique problem. Recall that a clique is a subset of vertices in a given graph such that each pair of vertices in the subset is linked. In order to establish the equivalence of these two optimization problems, it is necessary to introduce the notion of the *complement* or *inverse* of a graph. The complement of a graph G is a graph $\bar{G}$ with the same vertices such that two vertices in $\bar{G}$ are connected if and only if they are not linked in G. In order to find the complement of a graph, we must add the missing edges, and remove the already existing edges. One can prove that vertices, which do not belong to the maximum clique in $\bar{G}$, form the minimum vertex cover in G; see Fig. 23.

A generalization of the vertex cover problem to hypergraphs can be found in Mézard and Tarzia (2007).

b. The hard-core gas model

Treat uncovered vertices as particles, so that we assign a variable $\nu=1$ for uncovered and $\nu=0$ for covered vertices. Hence there are $\Sigma_i \nu_i = N - N_{\rm vc}$ particles on the graph. We also introduce a repulsion between particles such that only one particle can occupy a vertex (the exclusion principle). A repulsion energy between two nearest-neighboring particles is $J>0$. Then we arrive at the so-called hard-core gas model with the energy

$$E = \frac{J}{2}\sum_{i,j} a_{ij}\nu_i\nu_j, \tag{100}$$

where a_{ij} are the adjacency matrix elements. If the number of particles is not fixed, and there is a mass exchange with a thermodynamic bath, then we add a chemical potential $\mu>0$. This results in the Hamiltonian of the hard-core gas model: $\mathcal{H} = E - \mu\Sigma_{i=1}^{N}\nu_i$.

One may see that searching for the ground state is exactly equivalent to the minimum vertex cover problem. In the ground state, particles occupy uncovered vertices. Their number is equal to $(1-x_c)N$, where x_c is the fraction of vertices in the minimum vertex cover. The ground-state energy is $E_0=0$ because configurations in which two particles occupy two nearest-neighboring vertices are energetically unfavorable. In other words, particles occupy the maximum subset of vertices in a given graph such that no two vertices are adjacent. In graph theory, this subset is called the maximum independent set; see Fig. 23. Unoccupied vertices form the minimum vertex cover of the graph. Thus finding the minimum vertex cover (or, equivalently, the maximum independent set) of a graph is equivalent to finding the maximum clique of the complement of this graph.

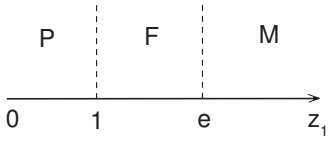

FIG. 24. Phase diagram of the antiferromagnetic Ising model Eq. (101) at $T=0$. P, F, and M denote paramagnetic, ferromagnetic, and mixed (spin-glass) phases, respectively. At mean degree $z_1>e$, in the mixed phase, ferromagnetism and spin-glass order coexist.

c. Antiferromagnet in a random field

Consider the following antiferromagnetic Ising model:

$$E = \frac{J}{2}\sum_{i,j} a_{ij}S_iS_j - \sum_{i=1}^{N} S_iH_i + JL \tag{101}$$

(Zhou, 2003, 2005). Here $J>0$ and $H_i=-Jq_i$ is a degree-dependent local field, where q_i is the degree of vertex i. L is the number of edges in a graph. The negative local fields force spins to be in the state -1; however, the antiferromagnetic interactions compete with these fields.

Consider a spin S_i surrounded by q_i nearest neighbors j in the state $S_j=-1$. The energy of this spin is

$$\left(J\sum_{j\in N(i)} S_j - H_i\right)S_i = 0 \times S_i = 0 \tag{102}$$

in any state $S_i=\pm 1$. Therefore, this spin is effectively free. Positions of "free" spins on a graph are not quenched. If one of the neighboring spins flips up, then the state $S_i=-1$ becomes energetically favorable.

Apply a small uniform magnetic field μ, $0<\mu\ll J$. At $T=0$, all free spins are aligned along μ, i.e., they are in the state $+1$. One can prove that the spins $S=+1$ occupy vertices that belong to the maximum independent set, while the spins $S=-1$ occupy the minimum vertex cover of a given graph. For this, make the transformation $S_i = 2\nu_i - 1$, where $\nu_i=0,1$ for spin states ∓ 1, respectively. Then the antiferromagnetic model Eq. (101) is reduced to the hard-core gas model where the external field μ corresponds to the chemical potential of the particles. All pure ground states have the same energy $E_0=0$ and the same average magnetic moment $M=1-2x_c$, but correspond to different nontrivial minimum vertex covers.

The exact mapping of the antiferromagnetic model Eq. (101) onto the vertex cover problem leads to the zero-temperature phase diagram shown in Fig. 24. This model is in a paramagnetic state at small degree $0<z_1<1$ because the network is below the percolation threshold and consists of finite clusters. Above the percolation threshold, at $1<z_1<e$, the ground state is ferromagnetic with an average magnetic moment $M=1-2x_c(z_1)$, where $x_c(z_1)$ is given by Eq. (99). The replica symmetry is unbroken at $z_1<e$. Many pure states appear spontaneously and the replica symmetry is broken at $z_1>e$. In this case,

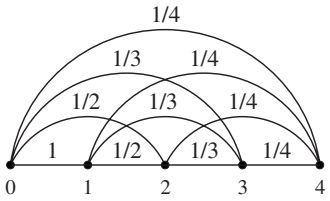

FIG. 25. Deterministic fully connected graph (Costin *et al.*, 1990), which is equivalent to the asymmetric annealed network. The values of the Ising coupling are shown on the edges.

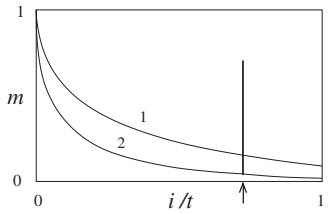

FIG. 26. Magnetization profile for the ferromagnetic Ising model on the graph shown in Fig. 25. i labels vertices starting from the "oldest" one, and t is the network size. Curve 1 is valid both for $T<T_c$ with an arbitrary homogeneous applied field H and for $T>T_c$, $H\neq 0$. Curve 2 describes the profile when an external field is applied to a single spin, while $T>T_c$. The arrow indicates the point of application of the local magnetic field. The mean magnetic moment of this vertex is distinct from others.

this model is in a mixed phase in which ferromagnetism and spin-glass order coexist, $H_i > -H+(q-2n)J$.

F. The Ising model on growing networks

In this section, we assume that a spin system on a growing network approaches equilibrium much faster than the network changes, and the adiabatic approximation works. We discuss the following circle of problems: a network is grown to an infinite size and then the Ising model is placed on it.

1. Deterministic graphs with BKT-like transitions

As is natural, the use of deterministic graphs facilitates the analysis of any problem. Surprisingly, very often results obtained in this way appear to be qualitatively similar to conclusions for models on random networks. Various graphs similar to those shown in Fig. 4 allow one to effectively apply the real-space renormalization-group technique. For example, Andrade and Herrmann (2005) studied the Ising model on the graph shown in Fig. 4(c) (the Apollonian network) and observed features typical for the Ising model on a random scale-free network with exponent $\gamma<3$.

More interestingly, the Ising model on some deterministic graphs shows the BKT-like singularities, which were already discovered in the 1990s by Costin *et al.* (1990) and Costin and Costin (1991). In a network context, their model was studied by Bauer *et al.* (2005). This network substrate is an asymmetric annealed network, which is actually an annealed version of the random recursive graph. Vertices are labeled $i=0,1,2,\ldots,t$, as in a growing network. Each vertex, say, vertex i, has a single connection of unit strength to "older" vertices. One end of this edge is solidly fixed at vertex i, while the second end frequently hops at random among vertices $0,1,\ldots,i-1$, which means the specific asymmetric annealing. The resulting network is equivalent to the fully connected graph with a specific large-scale inhomogeneity of the coupling; see Fig. 25.

The ferromagnetic Ising model on this network is described by the Hamiltonian

$$\mathcal{H} = -\sum_{0\leqslant i<j\leqslant t} \frac{s_i s_j}{j} - \sum_{i=0}^{t} H_i s_i, \tag{103}$$

where H_i are local magnetic fields. The mean-field theory, exact for this Hamiltonian, indicates the presence of a phase transition in this system. Figure 26 shows an inhomogeneous distribution of the magnetization $m(i)$ over the network. Only in the normal phase, without field, does $m(i)=0$. Otherwise, the oldest spin turns out to be strictly directed, $m(i=0)=1$, and the profile is nonanalytic: $m(i)\cong 1-\text{const}\times(i/t)^{2/T}$. Earlier, Coulomb and Bauer (2003) observed a resembling effect studying a giant connected component in random growing networks. The full magnetization $M(T)$ demonstrates the BKT-type behavior near the phase transition,

$$M(T) \propto \exp\left(-\frac{\pi}{2}\sqrt{\frac{T_c}{T_c-T}}\right). \tag{104}$$

Note that the BKT singularity, Eq. (104), and the specific nonanalyticity of $m(i)$ at $i=0$ are closely related.

The distribution of the linear response $\Sigma_i \partial m(i)/\partial H_j|_{H=0}$ to a local magnetic field, also called the distribution of correlation volumes, in this model is similar to the size distribution of connected components in growing networks with the BKT-like transition. The distribution has a power-law decay in the whole normal phase. Exactly the same decay has the distribution of correlations $\partial m(i)/\partial H_j|_{H=0}$ in this phase (Khajeh *et al.*, 2007).

We may generalize the inhomogeneity of the interaction in the Hamiltonian to a power law, $\propto j^{-\alpha}$, with an arbitrary exponent. (For brevity, we omit the normalization—the sum of the coupling strengths must grow proportionally to the size of the network.) One may show that in this model, the BKT singularity exists only when $\alpha=1$. For $\alpha>1$, phase ordering is absent at any nonzero temperature as in the one-dimensional Ising model, and for $0<\alpha<1$, there is a quite ordinary second-order transition.

Compare this picture with the well-studied ferromagnetic Ising model for a spin chain with regular long-range interactions $\propto|i-j|^{-\alpha}$ [see Luijten and Blöte (1997)]. In this model, (i) for $\alpha>2$, $T_c=0$, similar to the one-dimensional Ising model; (ii) at $\alpha=2$, there is a transition resembling the BKT one; and (iii) for $1<\alpha<2$, there is a transition at finite T_c. One may see that in both

models, there exist boundary values of exponent α, where BKT-kind phenomena take place. In simple terms, these special values of α play the role of lower critical dimensions. (Recall that the BKT transitions in solid-state physics occur only at a lower critical dimension.) These associations show that the BKT singularities in these networks are less unexpected than one may think at first glance.

Khajeh *et al.* (2007) solved the q-state Potts model on this network and, for all $q \geqslant 1$, arrived at results similar to the Ising model, i.e., $q=2$. Recall that $q=1$ corresponds to the bond percolation model, and that the traditional mean-field theory on lattices gives a first-order phase transition if $q>2$. Thus, both the first- and second-order phase transitions transformed into the BKT-like one on this network.

Hinczewski and Berker (2006) found another deterministic graph, on which the Ising model shows the BKT-like transition, so that this singularity is widespread in evolving networks with large-scale inhomogeneity.

2. The Ising model on growing random networks

There is still no analytical solution of the Ising model on growing random networks. Aleksiejuk *et al.* (2002) and numerous others simulated the Ising model on the specific Barabási-Albert network, where degree-degree correlations are virtually absent. The resulting picture is similar to the Ising model on an uncorrelated scale-free network with degree distribution exponent $\gamma=3$. In general, the growth results in a wide spectrum of structural correlations, which may dramatically change the phase transition.

Based on known results for the percolation (the one-state Potts model), see Sec. III.F, we expect the following picture for the Ising model on recursive growing graphs. If each new vertex has a single connection, the recursive graph is a tree, and ferromagnetic ordering takes place only at zero temperature. Now let a number of connections of new vertices be greater than 1, so that these networks are not trees. (i) If new vertices are attached to randomly chosen ones, there will be the Berezinskii-Kosterlitz-Thouless critical singularity. (ii) If the growth mechanism is preferential attachment, then the critical feature is less exotic, and more similar to that for uncorrelated networks.

VII. THE POTTS MODEL ON NETWORKS

The Potts model is related to a number of outstanding problems in statistical and mathematical physics (Baxter, 1982; Wu, 1982). The bond percolation and the Ising model are only particular cases of the p-state Potts model. The bond percolation is equivalent to the one-state Potts model [Kasteleyn and Fortuin (1969); Fortuin and Kasteleyn (1972); see also Lee *et al.* (2004c)]. The Ising model is exactly the two-state Potts model. Here we first look at critical properties of the Potts model and then consider its applications for coloring a random graph and extracting communities.

A. Solution for uncorrelated networks

The energy of the Potts model with p states is

$$E = -\frac{1}{2}\sum_{i,j} J_{ij} a_{ij} \delta_{\alpha_i,\alpha_j} - H\sum_i \delta_{\alpha_i,1}, \tag{105}$$

where $\delta_{\alpha,\beta}=0,1$ if $\alpha \neq \beta$ and $\alpha=\beta$, respectively. Each vertex i can be in any of p states: $\alpha_i=1,2,\ldots,p$. The magnetic field $H>0$ distinguishes the state $\alpha=1$. The α component of the magnetic moment of vertex i is defined as follows:

$$M_i^{(\alpha)} = (p\langle \delta_{\alpha_i,\alpha}\rangle - 1)/(p-1). \tag{106}$$

In the paramagnetic phase at zero magnetic field, $M_i^{(\alpha)}=0$ for all α. In an ordered state, $M_i^{(\alpha)} \neq 0$.

Exact equations for magnetic moments of the Potts model on a treelike complex network were derived by Dorogovtsev *et al.* (2004) using the recursion method, which as demonstrated is equivalent to the Bethe-Peierls approximation and the belief-propagation algorithm. It was shown that the ferromagnetic Potts model with uniform couplings ($J_{ij}=J>0$) on the configuration model has the critical temperature

$$T_P = J \Big/ \ln\left(\frac{B+p-1}{B-1}\right), \tag{107}$$

where $B=z_2/z_1$ is the average branching parameter. Interestingly, T_P has different meanings for $p=1,2$ and $p \geqslant 3$. In the case $p=1$, the critical temperature T_P determines the percolation threshold. When $p=2$, T_P is equal to the exact critical temperature Eq. (81) of the ferromagnetic phase transition in the Ising model (it is only necessary to rescale $J \to 2J$). For $p \geqslant 3$, T_P gives the lower temperature boundary of the hysteresis phenomenon at the first-order phase transition.

B. A first-order transition

In the standard mean-field theory, the ferromagnetic Potts model with $J_{ij}=J>0$ undergoes a first-order phase transition for all $p \geqslant 3$ (Wu, 1982). In order to study critical properties of the Potts model on a complex network, we need to find effective fields (messages) acting on Potts spins [see Dorogovtsev *et al.* (2007)], which is difficult to do analytically. An approximate solution based on the ansatz (82) was obtained by Dorogovtsev *et al.* (2004). It turned out that in uncorrelated random networks with a finite second moment $\langle q^2 \rangle$ (which corresponds to scale-free networks with $\gamma>3$), a first-order phase transition occurs at a critical temperature T_c for $p \geqslant 3$. In the region $T_P<T<T_c$, two metastable thermodynamic states with magnetic moments $M=0$ and $M \neq 0$ coexist. This leads to hysteresis phenomena that are typical for a first-order phase transition. At $T<T_P$, only the ordered state with $M \neq 0$ is stable. When γ tends to 3 from above, T_c increases while the jump of the magnetic moment at the first-order phase transition tends to zero. The influence of the network heterogeneity becomes

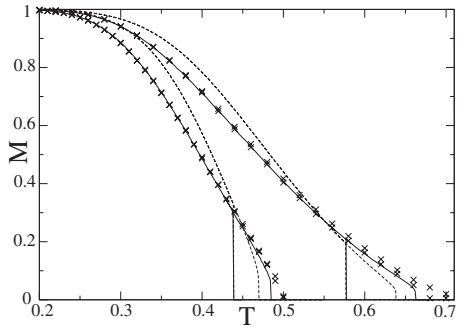

FIG. 27. Magnetic moment M vs T for the ferromagnetic Potts model on an uncorrelated scale-free network with average degree $z_1=10$. Leftmost curves, $\gamma=4$; rightmost curves, $\gamma=3.5$. Numerical simulations and exact numerical solution (Ehrhardt and Marsili, 2005) are shown by crosses and solid lines. Dotted lines, an approximate solution (Dorogovtsev *et al.*, 2004). Vertical lines, the lower-temperature boundary T_P of the hysteresis region. From Ehrhardt and Marsili, 2005.

dramatic when $2<\gamma\leqslant 3$ and the second moment $\langle q^2\rangle$ diverges: instead of a first-order phase transition, the p-state Potts model with $p\geqslant 3$ undergoes an infinite-order phase transition at the critical temperature $T_c(N)/J\approx z_2/(z_1 p)\gg 1$, similarly to the Ising model in Sec. VI.C.2. In the limit $N\to\infty$, the Potts model is ordered at any finite T.

Ehrhardt and Marsili (2005) used a population dynamics algorithm to find the effective fields for uncorrelated scale-free networks. The exact numerical calculations and numerical simulations of the Potts model confirmed that a first-order phase transition occurs at $p\geqslant 3$ when $\gamma>3$. Results obtained by Ehrhardt and Marsili (2005) are represented in Fig. 27, where they are compared with the approximate solution. The approximate solution gives poor results for vertices with small degree. For graphs with a large minimum degree (say, $q_0=10$), the approximate solution agrees well with the exact calculations and numerical simulations.

A simple mean-field approach to the Potts model on uncorrelated scale-free networks was used by Iglói and Turban (2002). Its conclusions deviate essentially from the exact results. Karsai *et al.* (2007) studied the ferromagnetic large-p state Potts model on evolving networks and described finite-size scaling in these systems.

C. Coloring a graph

Coloring random graphs is a remarkable problem in combinatorics (Garey and Johnson, 1979) and statistical physics (Wu, 1982). Given a graph, we want to know if this graph can be colored with p colors in such a way that no two neighboring vertices have the same color. A famous theorem states that four colors are sufficient to color a planar graph, such as a political map (Appel and Haken, 1977a, 1977b). Coloring a graph is not only beautiful mathematics but also has important applications. Good examples are scheduling of registers in the central processing unit of computers, frequency assignment in mobile radios, and pattern matching. Coloring a graph is a NP-complete problem. The time needed to properly color a graph grows exponentially with graph size.

How many colors do we need to color a graph? Intuitively it is clear that any graph can be colored if we have a large enough number of colors p. The minimum needed number of colors is called the chromatic number of the graph. The chromatic number is determined by the graph structure. It is also interesting to find the number of ways one can color a graph.

The coloring problem was extensively investigated for classical random graphs. There exists a critical degree c_p above which the graph becomes uncolorable by p colors with high probability. This transition is the so-called p-COL–UNCOL transition. Only graphs with average degree $z_1\equiv\langle q\rangle<c_p$ may be colored with p colors. For larger z_1, we need more colors. In order to estimate the threshold degree c_p for the Erdős-Rényi graph, one can use the so-called first-moment method (annealed computation, in other words). Suppose that p colors are assigned randomly to vertices. This means that a vertex may have any color with equal probability $1/p$. The probability that two ends of a randomly chosen edge have different colors is $1-1/p$. We can color N vertices of the graph in p^N different ways. However, only a small fraction $(1-1/p)^L$ of these configurations have the property that all $L=z_1N/2$ edges connect vertices of different colors. Hence the number of p-colorable configurations is

$$\mathfrak{N}(z_1)=p^N(1-1/p)^L\equiv\exp[N\Xi(p)]. \tag{108}$$

If $\Xi(p)\geqslant 0$, then with high probability there is at least one p-colorable configuration. At $p\gg 1$, this condition leads to the threshold average degree $c_p\sim 2p\ln p-\ln p$. The exact threshold $c_p\sim 2p\ln p-\ln p+o(1)$ was found by Luczak (1991); see also Achlioptas *et al.* (2005).

The coloring problem was reconsidered using methods of statistical mechanics of disordered systems, and a complex structure of the colorable phase was revealed (Mulet *et al.*, 2002; Braunstein, Mulet, Pagnani, *et al.*, 2003; Krząkała *et al.*, 2004; Mézard *et al.*, 2005). They found that the colorable phase itself contains several different phases. These studies used the equivalence of this problem to the problem of finding the ground state of the Potts model, Eq. (105), with p states (colors) and antiferromagnetic interactions $J_{ij}=-J<0$ in zero field. Within this approach, the graph is p-colorable if in the ground state the end points of all edges are in different Potts states. The corresponding ground-state energy is $E=0$. The degeneracy of this ground state means that there are several ways of coloring a graph. In the case of a p-uncolorable graph, the ground-state energy of the antiferromagnetic Potts model is positive due to a positive contribution from pairs of neighboring vertices having the same color. These studies showed that if the mean degree z_1 is sufficiently small, then it is easy to find a solution of the problem using usual computational algorithms. In these algorithms, colors of one or several

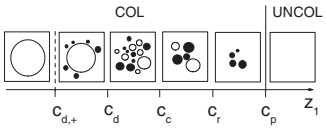

FIG. 28. Schematic phase diagram and structure of solutions for coloring Erdős-Rényi graphs in p-colors vs the average degree z_1. (i) $z_1<c_{d,+}$, solutions form one large connected cluster without frozen variables (open circle). (ii) $c_{d,+}<z_1<c_d$, in addition to a large cluster, small disjoint clusters with frozen variables (black circles) appear. They include, however, an exponentially small fraction of solutions. (iii) $c_d<z_1<c_c$, solutions are arranged in exponentially many clusters of different sizes with and without frozen variables. Exponentially many clusters without frozen variables dominate. (iv) $c_c<z_1<c_r$, there are a finite number of statistically dominating large clusters. These clusters do not contain frozen variables. (v) $c_r<z_1<c_p$, dominating clusters contain frozen variables. Above c_p, a graph is p-uncolorable. $c_{d,+}$ coincides with the 2-core point of emergence. c_d, c_c, and c_r correspond to so-called clustering, condensation, and rigidity (freezing) transitions, respectively. Adapted from Zdeborová and Krząkała, 2007.

randomly chosen vertices are changed one by one. For example, the Metropolis algorithm gives an exponentially fast relaxation from an arbitrary initial set of vertex colors to a correct solution (Svenson and Nordahl, 1999). On the other hand, for higher mean degrees (of course, still below c_p), these algorithms can approach a solution only in nonpolynomial times—computational hardness. The computational hardness is related to the presence of a hierarchy of numerous "metastable" states with a positive energy, which can dramatically slow down or even trap any simple numerical algorithm.

The mentioned works focused on the structure of the solution space for coloring a graph. (A solution here is a proper coloring of a graph.) This structure was found to qualitatively vary with the mean degree. In general, the space of solutions is organized as a set of disjoint clusters—pure states. Each of these clusters consists of solutions that can be approached from each other by changing colors of only $o(N)$ vertices. On the other hand, to transform a solution belonging to one cluster into a solution in another cluster, we have to change colors of $O(N)$ vertices, i.e., of a finite fraction of vertices. Clearly, if a network consists of only bare vertices ($z_1=0$), the space of solutions consists of a single cluster. However, above some threshold value of a mean degree, this space becomes highly clustered. The structure and statistics of these clusters at a given z_1 determine whether the coloring problem is computationally hard or not.

The statistics of clusters in a full range of mean degrees was obtained by Krząkała *et al.* (2007) and Zdeborová and Krząkała (2007). Their results indicate a chain of topologically different phases inside the colorable phase; see Fig. 28. An important notion in this kind of problems is *a frozen variable*. (A variable here is a vertex.) By definition, a frozen variable (vertex) has the same color in all solutions of a given cluster. Figure 28 demonstrates that clusters with frozen variables statistically dominate in the range $c_r<z_1<c_p$. Remarkably, the computational hardness was observed only in this region, although the replica-symmetry breaking was found in the essentially wider range $c_d<z_1<c_p$.

Coloring of the Watts-Strogatz small-world networks was studied numerically by Walsh (1999). He found that it is easy to color these networks at small and large densities of shortcuts p. However, it is hard to color them in the intermediate region of p.

D. Extracting communities

It is a matter of common experience that a complex system or a data set may consist of clusters, communities, or groups. A common property of a network having a community structure is that edges are arranged denser within a community and sparser between communities. If a system is small, we can reveal a community structure by eye. For a large network we need a special method (Newman, 2003a). Statistical physics can provide useful tools for this purpose. In particular, the Potts model has interesting applications that range from extracting species of flowers, collective listening habits, communities in a football league, and a search for groups of configurations in a protein-folding network.

Reichardt and Bornholdt (2004, 2006) proposed to map the communities of a network onto the magnetic domains forming the ground state of the p-state Potts model. In this approach, each vertex in the network is assigned a Potts state $\alpha=1,2,\ldots,p$. Vertices that are in the same Potts state α belong to the same community α. The authors used the following Hamiltonian:

$$\mathcal{H}=-\frac{1}{2}\sum_{i,j}a_{ij}\delta_{\alpha_i,\alpha_j}+\frac{\lambda}{2}\sum_{\alpha=1}^{p}n_s(n_s-1), \tag{109}$$

where a_{ij} are the elements of the adjacency matrix of the network and n_s is the number of vertices in the community α, i.e., $n_s=\Sigma_i\delta_{\alpha_i,\alpha}$. The number of possible states p is chosen large enough to take into account all possible communities. λ is a tunable parameter. The first sum in Eq. (109) is the energy of the ferromagnetic Potts model. It favors merging vertices into one community. The second repulsive term is minimal when the network is partitioned into as many communities as possible. In this approach, the communities arise as domains of aligned Potts spins in the ground state that can be found by Monte Carlo optimization.

At $\lambda=1$ the energy Eq. (109) is proportional to the modularity measure Q, namely, $\mathcal{H}=-QL$, where L is the total number of edges in the network. Thus the ground state of the model Eq. (109) corresponds to the maximum modularity Q. The modularity measure was introduced by Clauset *et al.* (2004) and Newman and Girvan (2004). For a given partition of a network into communities, the modularity is the difference between the fraction of edges within communities and the expected fraction of such edges under an appropriate *null model* of

the network (a random network model assuming the absence of a modular structure),

$$Q = \sum_{\alpha} \left(\frac{L_{\alpha}}{L} - \frac{L_{\alpha}^{\exp}}{L} \right) = \frac{1}{2L} \sum_{\alpha} \sum_{i,j} (a_{ij} - p_{ij}) \delta_{\alpha_i,\alpha_j}. \quad (110)$$

Here L_{α} and $L_{\alpha}^{\exp}$ are the numbers of edges within community α in the network and in its null model, respectively; p_{ij} is the probability that vertices i and j are connected in the null model. Reichardt and Bornholdt (2004, 2006) used the configuration model as the null model, i.e., $p_{ij}=q_i q_j/2L$, where q_i and q_j are degrees of vertices i and j, respectively. Tuning λ and p, one can find a partition of a given network into communities such that a density of edges inside communities is maximal when compared to one in a completely random network. If, however, the size distribution of communities is sufficiently broad, then it is not easy to find an optimal value of the parameter λ. Searching for small communities and the resolution limit of this method have been discussed by Kumpula *et al.* (2007). Interestingly, finding the partition of a complex network into communities, such that it maximizes the modularity measure, is a NP-complete problem (Brandes *et al.*, 2006).

Reichardt and Bornholdt (2004, 2006) applied the Potts model Eq. (109) to study a community structure of real-world networks, such as a U.S. college football network and a large protein-folding network.

Guimerà *et al.* (2004) proposed another approach to the problem of extracting communities based on a specific relation between the modularity measure Q and the ground-state energy of a Potts model with multiple interactions.

VIII. THE *XY* MODEL ON NETWORKS

The XY model describes interacting planar rotators. The energy of the XY model on a graph is

$$\mathcal{H} = -\frac{J}{2} \sum_{i,j} a_{ij} \cos(\theta_i - \theta_j), \quad (111)$$

where a_{ij} are the elements of the adjacency matrix of the graph, θ_i is the phase of a rotator at vertex i, and J is the coupling strength. Unlike the Ising and Potts models with discrete spins, the XY model belongs to the class of models with continuous symmetry.

A one-dimensional XY model has no phase transition. On a two-dimensional regular lattice, this model ($J>0$) undergoes the unusual Berezinskii-Kosterlitz-Thouless phase transition. On a d-dimensional lattice at $d>4$ and the fully connected graph (Antoni and Ruffo, 1995), the ferromagnetic phase transition in the XY model is of second order with the standard mean-field critical exponents.

A. The *XY* model on small-world networks

There were a few studies of the XY model on complex networks. Kim *et al.* (2001) carried out Monte Carlo simulations of the ferromagnetic XY model on the Watts-Strogatz small-world network generated from a ring of N vertices. They measured the order parameter $r=|N^{-1}\Sigma_j \exp(i\theta_j)|$. Using the standard finite-size scaling analysis, they showed that the phase transition appears even at a tiny fraction of shortcuts, p. The transition is of second order with the standard mean-field critical exponent $\beta=\frac{1}{2}$ (similar to the phase transition in the Ising model in Sec. VI.D). The phase diagram of the XY model is shown in Fig. 29. There is no phase transition at $p=0$ because the system is one dimensional. Surprisingly, the dependence of the critical temperature T_c on p was well fitted by a function $T_c(p)/J=0.41 \ln p+2.89$ in contrast to $T_c(p)/J \propto 1/|\ln p|$ for the Ising model. The dynamical Monte Carlo simulations of Medvedyeva *et al.* (2003) confirmed the mean-field nature of the phase transition.

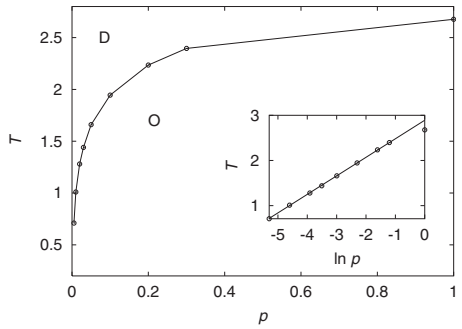

FIG. 29. p-T phase diagram of the ferromagnetic XY model on the Watts-Strogatz network. p is the fraction of shortcuts. D and O denote the disordered and ordered phases, respectively. The inset shows that the critical temperature is well approximated by a function $0.41 \ln p+2.89$. From Kim *et al.*, 2001.

B. The *XY* model on uncorrelated networks

An exact solution of the XY model on treelike networks, in principle, can be obtained in the framework of the belief propagation algorithm; see Eq. (66). Another analytical approach based on the replica theory and the cavity method was developed by Coolen *et al.* (2005) and Skantzos *et al.* (2005); see also Skantzos and Hatchett (2007) for the dynamics of a related model. We study here the XY model, using the annealed network approximation from Sec. VI.A.3. In this way, for the configuration model, we obtain the XY model with a degree-dependent coupling on the fully connected graph,

$$\mathcal{H}_{\mathrm{MF}} = -\frac{J}{Nz_1} \sum_{i<j} q_i q_j \cos(\theta_i - \theta_j). \quad (112)$$

This model is solved exactly using a weighted complex order parameter, $\tilde{r}e^{i\psi}=\Sigma_{j=1}^{N} q_j e^{i\theta_j}/Nz_1$. The phase ψ determines the direction along which rotators are spontaneously aligned. $\tilde{r}$ is a solution of an equation,

$$\tilde{r} = \frac{1}{z_1}\sum_q P(q) q \frac{I_1(\tilde{r}q\beta J)}{I_0(\tilde{r}q\beta J)}, \tag{113}$$

where $I_0(x)$ and $I_1(x)$ are the modified Bessel functions. An analysis of Eq. (113) shows that the ferromagnetic XY model has the same critical behavior as the ferromagnetic Ising model. The critical temperature of the continuous phase transition is $T_c = J\langle q^2\rangle/2z_1$. The critical temperature is finite in a complex network with a finite second moment $\langle q^2\rangle$, and diverges if $\langle q^2\rangle \to \infty$. In the latter case, the XY model is in the ordered state at any finite T. The annealed network approximation predicts that the XY model on the Watts-Strogatz small-world network has the standard mean-field critical behavior. This agrees with the simulations by Kim *et al.* (2001) and Medvedyeva *et al.* (2003).

IX. PHENOMENOLOGY OF CRITICAL PHENOMENA IN NETWORKS

Why do critical phenomena in networks differ so much from those in usual substrates and what is their common origin? Why do all investigated models demonstrate universal behavior when $\langle q^2\rangle$ diverges? In order to answer these questions and analyze results of simulations and experiments from a general point of view, we need a general theory that is not restricted by specific properties of any model.

In the phenomenological approach, the origin of interactions and the nature of interacting objects are irrelevant. In this section, we consider a phenomenological theory of cooperative phenomena in networks proposed by Goltsev *et al.* (2003). This theory is based on concepts of the Landau theory of continuous phase transitions and leads to the conclusion that the universal critical behavior in networks is determined by two factors: (i) the structure of a network and (ii) the symmetry of a given model.

A. Generalized Landau theory

Consider a system of interacting objects. Interactions or links between these objects form a net. We assume that some kind of order can emerge. This ordered phase may be characterized by some quantitative characteristic x while it will vanish in a disordered phase above a critical point. We also assume that the thermodynamic potential Φ of the system is not only a function of the order parameter x but also depends on the degree distribution,

$$\Phi(x,H) = -Hx + \sum_q^{\infty} P(q)\phi(x,qx). \tag{114}$$

Here H is a field conjugated with x. Equation (114) is not obvious *a priori*. The function $\phi(x,qx)$ can be considered as a contribution of vertices with q connections. There are arguments in favor of this assumption. Consider the interaction of an arbitrary vertex with q neighboring vertices. In the framework of a mean-field approach, q neighbors with a spontaneous "moment" x produce an effective field qx acting on this vertex.

We impose only general restrictions on $\phi(x,y)$:

(i) $\phi(x,y)$ is a smooth function of x and y and can be represented as a series in powers of both x and y. Coefficients of this series are functions of temperature T and field H or another pair of relevant control parameters.

(ii) $\Phi(x,H)$ is finite for any finite average degree $\langle q\rangle$.

A network topology affects analytical properties of Φ. If the distribution function $P(q)$ has a divergent moment $\langle q^p\rangle$, then we have

$$\Phi(x,H) = -Hx + \sum_{n=2}^{p-1} f_n x^n + x^p s(x), \tag{115}$$

where $s(x)$ is a nonanalytic function. The specific form of $s(x)$ is determined by the asymptotic behavior of $P(q)$ at $q \gg 1$. It is the nonanalytic term that can lead to a deviation from the standard mean-field behavior.

Following Landau, we assume that near the critical temperature the coefficient f_2 can be written as $a(T - T_c)$, where a is chosen to be positive for the stability of the disordered phase. The stability of the ordered phase demands that either $f_3 > 0$ or, if $f_3 = 0$, then $f_4 > 0$. The order parameter x is determined by the condition that $\Phi(x,H)$ is minimum: $d\Phi(x,H)/dx = 0$.

If the degree distribution exponent γ is noninteger, then the leading nonanalytic term in $\Phi(x)$ is $x^{\gamma-1}$. If γ is integer, then the leading nonanalytic term is $x^{\gamma-1}|\ln x|$. Interestingly, this nonanalyticity resembles that of the free energy for the ferromagnetic Ising model in a magnetic field on a Cayley tree; see Sec. VI.B.

We now take into account a symmetry of the system. When $\Phi(x,H) = \Phi(-x,-H)$ and the coefficient f_4 is positive, we arrive at the critical behavior that describes the ferromagnetic Ising model on equilibrium uncorrelated random networks in Sec. VI.C.2. In a network with $\langle q^4\rangle < \infty$, a singular term in Φ is irrelevant, and we have the usual x^4 Landau theory, which leads to the standard mean-field phase transition. The singular term $x^{\gamma-1}$ becomes relevant for $2 < \gamma \leqslant 5$ (this term is $x^4|\ln x|$ at $\gamma = 5$). Critical exponents are given in Table I. At the critical point $T = T_c$, the order parameter x is a nonanalytic function of H: $x \propto H^{1/\delta}$, where $\delta(\gamma > 5) = 3$ and $\delta(3 < \gamma < 5) = \gamma - 2$.

If the symmetry of the system permits odd powers of x in Φ and f_3 is positive, then the phenomenological approach gives a critical behavior that was found for percolation on uncorrelated random networks in Sec. III.B.2. Note that when $\gamma > 4$, a singular term $x^{\gamma-1}$ is irrelevant. The term becomes relevant for $2 < \gamma \leqslant 4$ (this term is $x^3|\ln x|$ at $\gamma = 4$).

At $2 < \gamma \leqslant 3$, the thermodynamic potential has a universal form, independent of the symmetry,

$$\Phi(x,H) = -Hx + Cx^2 - Ds(x), \tag{116}$$

where $s(x)=x^2|\ln x|$ for $\gamma=3$ and $s(x)=x^{\gamma-1}$ for $2<\gamma<3$. We can choose $C\propto T^2$ and $D\propto T$; then the phenomenological theory gives the correct temperature behavior of the ferromagnetic Ising model.

When $f_3<0$ (or $f_4<0$ if $f_3=0$), the phenomenological theory predicts a first-order phase transition for a finite $\langle q^2\rangle$. This corresponds to the ferromagnetic Potts model with $p\geqslant 3$ states; see Sec. VII.

The phenomenological approach agrees with the microscopic theory and numerical simulations of the ferromagnetic Ising, Potts, *XY*, spin-glass, Kuramoto, and the random-field Ising models, percolation, and epidemic spreading on various uncorrelated random networks. These models have also been studied on complex networks with different clustering coefficients, degree correlations, etc. It seems that these characteristics are not relevant, or at least not essentially relevant, to critical behavior. When the tree ansatz for complex networks gives exact results, the phenomenology leads to the same conclusions. In these situations, the critical fluctuations are Gaussian. We suggest that the critical fluctuations are Gaussian in all networks with the small-world effect, as is natural for infinite-dimensional objects.

B. Finite-size scaling

Based on the phenomenological theory, one can find scaling exponents for finite-size scaling phenomena in complex networks. Let $\Phi(m,\tau,H,N)$ be a thermodynamic potential per vertex, where τ is the deviation from a critical point. According to the standard scaling hypothesis (in its finite-size scaling form), in the critical region

$$N\Phi(m,\tau,H,N) = f_\phi(mN^x,\tau N^y,HN^z), \tag{117}$$

where $f_\phi(a,b,c)$ is a scaling function. Note that there is exactly N on the left-hand side of this relation and not an arbitrary power of N. Formally substituting $\Phi(m,\tau,H)=A\tau m^2+Bm^{\Delta(\gamma)}-Hm$, one can find exponents x, y, and z. As explained, Δ may be (i) $\min(4,\gamma-1)$, as in the Ising model, or (ii) $\min(3,\gamma-1)$, as in percolation. This naive substitution, however, does not allow one to obtain a proper scaling function, which must be analytical, as is natural. The derivation of the scaling function demands more rigorous calculations.

As a result, for the two classes of theories listed above, we arrive at the following scaling forms of the order parameter:

$$m(\tau,H,N) = \begin{cases} N^{-1/4} f(N^{1/2}\tau, N^{3/4}H) & \text{for } \gamma \geqslant 5, \quad (118) \\ N^{-1/3} f(N^{1/3}\tau, N^{2/3}H) & \text{for } \gamma \geqslant 4, \quad (119) \end{cases}$$

and for smaller $3<\gamma<5$ (i) or $3<\gamma<4$ (ii), m scales as

$$m(\tau,H,N) = N^{-1/(\gamma-1)} f(N^{(\gamma-3)/(\gamma-1)}\tau, N^{(\gamma-2)/(\gamma-1)}H). \tag{120}$$

Hong, Ha, and Park (2007) obtained these scaling relations (without field) using other arguments and confirmed them simulating the Ising model on the static and configuration models of uncorrelated networks. Their idea may be formally reduced to the following steps. Recall a relevant standard scaling relation from the physics of critical phenomena in lattices. The standard form is usually written for dimension d lower than the upper critical dimension d_u. Rewrite this scaling relation for $d>d_u$: substitute d_u for d and use the mean-field values of the critical exponents, which should be obtained as follows. For networks, in this relation, formally substitute $\nu=\frac{1}{2}$ for the correlation length exponent and $\eta=0$ for the Fisher exponent, using the susceptibility exponent $\tilde{\gamma}=\nu(2-\eta)=1$, exponent $\beta=\beta(\gamma)$ (see Sec. IX.A), and

$$d_u(\gamma) = 2\Delta(\gamma)/[\Delta(\gamma)-2] \tag{121}$$

(Hong, Ha, and Park, 2007). This procedure allows one to derive various scaling relations. We have used it in Sec. III.B.3.

Finite-size scaling of this kind works in a wide class of models and processes on networks. Hong, Ha, and Park (2007) also applied these ideas to the contact process on networks. Earlier, Kim *et al.* (2001) and Medvedyeva *et al.* (2003) studied the finite-size scaling by simulating the *XY* model on the Watts-Strogatz network. In their work they investigated the dynamic finite-size scaling. In the framework of our phenomenology, we can reproduce their results and generalize them to scale-free networks. Assume the relaxational dynamics of the order parameter: $\partial m/\partial t=-\partial\Phi(m)/\partial m$. In dynamical models, the scaling hypothesis also implies the scaling time variable $t_{\rm scal}=tN^{-s}$, which means that the relaxation time diverges as N^s at the critical point. For brevity, we find only the form of this scaling variable, which actually resolves the problem. In terms of scaling variables, the dynamic equation for the order parameter must not contain N. With this condition, passing to the scaling variables mN^x and tN^{-s} in the dynamic equation, we get $s=y$, which means time scales with N exactly in the same way as $1/\tau$. For the indicated two classes of theories, (i) and (ii), the time scaling variable is of the following form:

$$\begin{aligned} &\text{in theory (i), for } \gamma \geqslant 5, \quad t_{\rm scal} = tN^{-1/2}, \\ &\text{in theory (ii), for } \gamma \geqslant 4, \quad t_{\rm scal} = tN^{-1/3}, \end{aligned} \tag{122}$$

and

$$\begin{aligned} &\text{in theory (i), for } 3<\gamma<5, \\ &\qquad\qquad \text{and in theory (ii), for } 3<\gamma<4, \\ &t_{\rm scal} = tN^{-(\gamma-3)/(\gamma-1)}. \end{aligned} \tag{123}$$

Finally, we recommend that the reader see Gallos, Song, Havlin, *et al.* (2007) for the finite-size scaling in scale-free networks with fractal properties. For description of these networks, see Song *et al.* (2005, 2006, 2007) and Goh *et al.* (2006).

X. SYNCHRONIZATION ON NETWORKS

The emergence of synchronization in a system of coupled individual oscillators is an intriguing phenomenon. Nature gives many well-known examples: synchronously flashing fireflies, crickets that chirp in unison, two pendulum clocks mounted on the same wall synchronizing their oscillations, synchronous neural activity, and many others. Different dynamical models were proposed to describe collective synchronization; see Strogatz (2000, 2003), Pikovsky *et al.* (2001), Acebrón *et al.* (2005), and Boccaletti *et al.* (2006).

Extensive investigations were aimed at searching for network architectures that optimize synchronization. First (mostly numerical) studies of various dynamical models have revealed that the ability to synchronize can be improved in small-world networks (Gade and Hu, 2000; Lago-Fernandez *et al.*, 2000; Jost and Joy, 2001; Barahona and Pecora, 2002; Hong, Choi, and Kim, 2002; Wang and Chen, 2002). On the other hand, an opposite effect was observed in synchronization dynamics of pulse-coupled oscillators (Guardiola *et al.*, 2000), where homogeneous systems synchronize better.

We consider here the effect of the network topology on the synchronization in the Kuramoto model and a network of coupled dynamical systems. These two models represent two different types of synchronization phenomena. One can find the discussion of this effect for coupled map lattices in Gade and Hu (2000), Jost and Joy (2001), Atay *et al.* (2004), Lind *et al.* (2004), Grinstein and Linsker (2005), and Huang *et al.* (2006), for networks of Hodgkin-Huxley neurons in Lago-Fernández *et al.* (2000) and Kwon and Moon (2002); for pulse-coupled oscillators in Denker *et al.* (2004) and Timme *et al.* (2004); and for the Edwards-Wilkinson model in Kozma *et al.* (2004).

A. The Kuramoto model

The Kuramoto model is the classical paradigm for the spontaneous emergence of collective synchronization (Kuramoto, 1984; Strogatz, 2000; Acebrón *et al.*, 2005). The model describes collective dynamics of N coupled phase oscillators with phases $\theta_i(t)$, $i=1,2,\ldots,N$, running at natural frequencies ω_i,

$$\dot{\theta}_i = \omega_i + J\sum_{j=1}^{N} a_{ij}\sin(\theta_j - \theta_i), \tag{124}$$

where a_{ij} is the adjacency matrix of a network. J is the coupling strength. The frequencies ω_i are distributed according to a distribution function $g(\omega)$. It is assumed that $g(\omega)$ is unimodular and symmetric about its mean frequency Ω. It is convenient to use a rotating frame and redefine $\theta_i \to \theta_i - \Omega t$ for all i. In this frame, we can set the mean of $g(\omega)$ to be zero. The state of oscillator j can be characterized by a complex exponent $\exp(i\theta_j)$, which is represented by a vector of unit length in the complex plane; see Fig. 30.

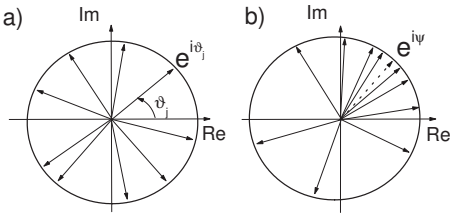

FIG. 30. Schematic view of phases in the Kuramoto model. (a) Incoherent phase. Unit length vectors representing individual states are randomly directed in the complex plane. (b) Coherent phase. The individual states condense around a direction ψ.

The Kuramoto model is solved exactly for the fully connected graph (all-to-all interaction), i.e., $a_{ij}=1$ for all $i \neq j$, with rescaling $J \to J/N$. When $J<J_c$, there is no collective synchronization between the rotations of individual oscillators. Nonetheless, some finite clusters of synchronized oscillators may exist. Collective synchronization between oscillators emerges spontaneously above a critical coupling J_c if $N \to \infty$. The global state of the model is characterized by the following average:

$$r(t)e^{i\psi(t)} = \frac{1}{N}\sum_{j=1}^{N} e^{i\theta_j}, \tag{125}$$

where $r(t)$ is the order parameter that measures the phase coherence and $\psi(t)$ is the average phase. Simulations show that if we start from any initial state, then at $J<J_c$ in the incoherent phase $r(t)$ decays to a tiny jitter of the order of $O(N^{-1/2})$. On the other hand, in the coherent phase ($J>J_c$), the parameter $r(t)$ decays to a finite value $r(t\to\infty)=r<1$. At J near J_c, the order parameter $r \propto |J-J_c|^{\beta}$ with $\beta=\frac{1}{2}$. In the original frame, $\psi(t)$ rotates uniformly at the mean frequency Ω. Substituting Eq. (125) into Eq. (124) gives

$$\dot{\theta}_i = \omega_i + Jr\sin(\psi - \theta_i). \tag{126}$$

The steady solution of this equation shows that at $J>J_c$ a finite fraction of synchronized oscillators emerges. These oscillators rotate coherently at frequency Ω in the original frame. In the rotating frame, their phases are locked according to $\sin\theta_i=\omega_i/Jr$ if $|\omega_i| \leqslant Jr$. Here we set $\psi=0$. Other oscillators, having individual frequencies $|\omega_i|>Jr$, are "drifting." Their phases are changed nonuniformly in time. The order parameter r satisfies the following self-consistent equation:

$$r = \int_{-Jr}^{Jr} \sqrt{1-\omega^2/J^2r^2}\, g(\omega)\, d\omega, \tag{127}$$

which gives the critical coupling $J_c=2/\pi g(0)$. Note that the order of the synchronization phase transition in the Kuramoto model depends on the distribution $g(\omega)$. In particular, it can be of first order if the natural frequencies are uniformly distributed (Tanaka *et al.*, 1997).

The Kuramoto model on finite networks and lattices shows synchronization if the coupling is sufficiently strong. Is it possible to observe collective synchronization in the Kuramoto model on an infinite regular lat-

tice? There is no synchronization in a one-dimensional system with a short-ranged coupling. According to Hong, Park, and Choi (2004, 2005), phase and frequency ordering is also absent in two-dimensional ($d=2$) lattices; frequency ordering is possible only in three-, four-, and higher-dimensional lattices, while phase ordering is possible only when $d>4$. The value of the upper critical dimension for the Kuramoto model is still under discussion (Acebrón *et al.*, 2005). Simulations in Hong, Chaté, Park, *et al.* (2007) indicate the mean-field behavior of the Kuramoto model at $d>4$.

B. Mean-field approach

The Kuramoto model was recently investigated numerically and analytically on complex networks of different architectures. Here we look first at analytical studies and then discuss simulations, though the model was first studied numerically by Hong, Choi, and Kim (2002).

Unfortunately, no exact results for the Kuramoto model on complex networks have been obtained yet. A finite mean degree and strong heterogeneity of a network make it difficult to find an analytical solution of the model. Ichinomiya (2004, 2005) and Lee (2005) developed a simple mean-field theory that is equivalent to the annealed network approximation in Sec. VI.A.3. Using this approximation, we arrive at the Kuramoto model with a degree-dependent coupling on the fully connected graph,

$$\dot{\theta}_i = \omega_i + \frac{Jq_i}{Nz_1}\sum_{j=1}^{N} q_j \sin(\theta_j - \theta_i). \tag{128}$$

This effective model can be solved exactly. Introducing a weighted order parameter

$$\tilde{r}(t)e^{i\tilde{\psi}(t)} = \frac{1}{Nz_1}\sum_{j=1}^{N} q_j e^{i\theta_j}, \tag{129}$$

one can write Eq. (128) as follows:

$$\dot{\theta}_i = \omega_i + J\tilde{r}q_i \sin(\tilde{\psi} - \theta_i). \tag{130}$$

The steady solution of this equation shows that in the coherent state oscillators with individual frequencies $|\omega_i| \leqslant J\tilde{r}q_i$ are synchronized. Their phases are locked and depend on vertex degree: $\sin\theta_i = \omega_i/J\tilde{r}q_i$, where we set $\tilde{\psi}=0$. This result shows that hubs with degree $q_i \gg 1$ synchronize more easy than oscillators with low degrees. The larger the degree q_i, the larger the probability that an individual frequency ω_i of an oscillator i falls into the range $[-J\tilde{r}q_i, J\tilde{r}q_i]$. Other oscillators are drifting. $\tilde{r}$ is a solution of the equation

$$\tilde{r} = \sum_q \frac{P(q)q}{z_1}\int_{-J\tilde{r}q}^{J\tilde{r}q}\sqrt{1-\frac{\omega^2}{(J\tilde{r}q)^2}}\,g(\omega)d\omega. \tag{131}$$

Spontaneous synchronization with $\tilde{r}>0$ emerges above the critical coupling,

$$J_c = 2z_1/\pi g(0)\langle q^2\rangle, \tag{132}$$

which depends strongly on the degree distribution. J_c is finite if the second moment $\langle q^2\rangle$ is finite. Note that at a fixed mean degree z_1, J_c decreases (i.e., the network synchronizes easily) with increasing $\langle q^2\rangle$—increasing heterogeneity. Similar to percolation, if the moment $\langle q^2\rangle$ diverges (i.e., $2<\gamma\leqslant 3$), the synchronization threshold J_c is absent, and the synchronization is robust against random failures. In finite networks, the critical coupling is finite, $J_c(N) \propto 1/q_{\rm cut}^{3-\gamma}(N)$, and determined by the size-dependent cutoff $q_{\rm cut}(N)$ in Sec. II.E.4.

Another important result, which follows from Eq. (131), is that the network topology strongly influences the critical behavior of the order parameter $\tilde{r}$. Lee (2005) found that the critical singularity of this parameter is described by the standard mean-field critical exponent $\beta=\frac{1}{2}$ if an uncorrelated network has a finite fourth moment $\langle q^4\rangle$, i.e., $\gamma>5$. If $3<\gamma<5$, then $\beta=1/(\gamma-3)$. Note that the order parameters r, Eq. (125), and $\tilde{r}$, Eq. (129), have the same critical behavior. Thus, with fixed z_1, the higher the heterogeneity of a network, the better its synchronizability and the smoother the phase transition. The critical behavior of the Kuramoto model is similar to the ferromagnetic Ising model in Sec. VI.C and confirms the phenomenological theory described in Sec. IX. A finite-size scaling analysis of the Kuramoto model in complex networks was carried out by Hong, Park, and Tang (2007). Within the mean-field theory, they found that the order parameter $\tilde{r}$ has finite-size scaling behavior,

$$\tilde{r} = N^{-\beta\bar{\nu}} f[(J-J_c)N^{1/\bar{\nu}}], \tag{133}$$

with the critical exponent β found above. Remarkably, the critical exponent $\bar{\nu}$ is different from that of the Ising model in Sec. IX.B, namely, $\bar{\nu}=\frac{5}{2}$ at $\gamma>5$, and $\bar{\nu}=(2\gamma-5)/(\gamma-3)$ at $4<\gamma<5$, and $\bar{\nu}=(\gamma-1)/(\gamma-3)$ at $3<\gamma<4$. Simulations of the Kuramoto model agree with these analytical results (Hong, Park, and Tang, 2007).

The mean-field theory of synchronization considered above is valid if the average degree z_1 is sufficiently large. In order to improve this approach, Restrepo *et al.* (2005) introduced a local order parameter at vertex n, $r_n e^{i\psi_n} = \Sigma_m a_{nm} e^{i\theta_m}$, and found it using intuitive arguments. In their approach, the critical coupling J_c is inversely proportional to the maximum eigenvalue $\lambda_{\max}$ of the adjacency matrix a_{ij}. However, in an uncorrelated random complex network, $\lambda_{\max}$ is determined by the cutoff $q_{\rm cut}(N)$ of the degree distribution, $\lambda_{\max} \approx q_{\rm cut}^{1/2}(N)$ (Chung *et al.*, 2003; Dorogovtsev *et al.*, 2003; Krivelevich and Sudakov, 2003). In scale-free networks ($\gamma<\infty$), the cutoff diverges in the limit $N\to\infty$. Therefore, this approach predicts $J_c=0$ in the thermodynamic limit even for a scale-free network with $\gamma>3$ in sharp contrast to the approach of Ichinomiya (2004) and Lee (2005).

Oh *et al.* (2007) studied the Kuramoto model with asymmetric degree-dependent coupling $Jq_i^{-\eta}a_{ij}$ instead of Ja_{ij} in Eq. (124) using the mean-field theory. They

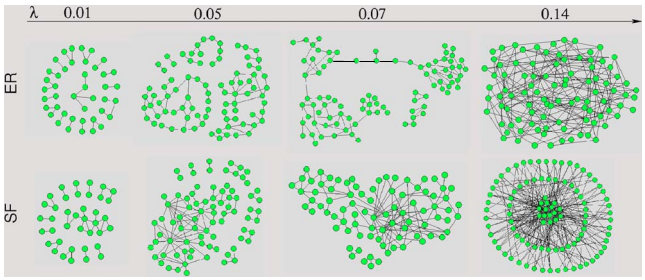

FIG. 31. (Color online) Synchronization patterns of Erdős-Rényi (ER) and scale-free (SF) networks for several values of coupling λ (or J in our notations). From Gómez-Gardeñes *et al.*, 2007a.

found that tuning the exponent η changes the critical behavior of collective synchronization. On scale-free networks, this model has a rich phase diagram in the plane (η,γ). In the case $\eta=1$, the critical coupling J_c is finite even in a scale-free network with $2<\gamma<3$ contrary to $J_c=0$ for the symmetric coupling, which corresponds to $\eta=0$. Note that the influence of the degree-dependent coupling is similar to the effect of degree-dependent interactions on the phase transition in the ferromagnetic Ising model; see Sec. VI.C.5.

C. Numerical study of the Kuramoto model

The Kuramoto model was investigated numerically on various networks. Hong, Choi, and Kim (2002) studied this model on the Watts-Strogatz network generated from a one-dimensional regular lattice. They observed that collective synchronization emerges even for a tiny fraction of shortcuts p, which cause the one-dimensional lattice to be a small world. The critical coupling J_c is well approximated as $J_c(p)\approx 2/\pi g(0)+ap^{-1}$, where a is a constant. As one might expect, the synchronization phase transition is of second order with the standard critical exponent $\beta=0.5$.

The evolution of synchronization in the Kuramoto model on the Erdős-Rényi and scale-free networks was recently studied by Gómez-Gardeñes *et al.* (2007a, 2007b). They solved numerically Eq. (124) for $N=1000$ coupled phase oscillators and demonstrated that (i) the synchronization on a scale-free network ($\gamma=3$) appears at a smaller critical coupling J_c than the one on the Erdős-Rényi network (with the same average degree as the scale-free network), and (ii) the synchronization phase transition on the Erdős-Rényi network is sharper than the transition on the scale-free network. This critical behavior agrees qualitatively with the mean-field theory. Gómez-Gardeñes *et al.* (2007a, 2007b) calculated a fraction of synchronized pairs of neighboring oscillators for several values of the coupling J and revealed an interesting difference in the synchronization patterns between the Erdős-Rényi and scale-free networks; see Fig. 31. In a scale-free network, a central core of synchronized oscillators formed by hubs grows with J by absorbing small synchronized clusters. In contrast, in the Erdős-Rényi network numerous small synchronized clusters homogeneously spread over the graph. As J approaches J_c, they progressively merge together and form larger clusters.

Moreno and Pacheco (2004) numerically studied the Kuramoto model the Barabási-Albert network of size $N=5\times10^4$. They found that the critical coupling is finite, though small. Surprisingly, the measured critical exponent was close to the standard mean-field value, $\beta\sim0.5$, contrary to an infinite-order phase transition and zero J_c predicted by the mean-field theory in the limit $N\to\infty$. The reason for this discrepancy is unclear.

A community (modular) structure of complex networks has a strong effect on synchronization. In such networks, oscillators inside a community are synchronized first because edges within a community are arranged denser than edges between communities. On the other hand, intercommunity edges stimulate the global synchronization. The role of network motifs for the synchronization in the Kuramoto model was first studied numerically by Moreno *et al.* (2004). Oh *et al.* (2005) solved numerically the dynamical equations (124) with the asymmetric degree-dependent coupling $Jq_i^{-1}a_{ij}$ for two real networks—the yeast protein interaction network and the Internet at the autonomous system level. These networks have different community structures. In the yeast protein network, communities are connected diversely, while in the Internet, communities are connected mainly to North America. It turned out that for a given coupling J, the global synchronization for the yeast network is stronger than that for the Internet. These numerical calculations showed that the distributions of phases of oscillators inside communities in the yeast network overlap each other. This corresponds to the mutual synchronization of the communities. In contrast, in the Internet, the phase distributions inside communities do not overlap; the communities are coupled weaker and synchronize independently. A modular structure produces a similar effect on synchronization of coupled-map networks (Huang *et al.*, 2006).

Arenas *et al.* (2006a, 2006b) showed that the evolution of a synchronization pattern reveals different topological scales at different time scales in a complex network with nested communities. Starting from random initial conditions, highly interconnected clusters of oscillators synchronize first. Then larger and larger communities do the same up to the global coherence. Clustering produces a similar effect. McGraw and Menzinger (2007) studied numerically the synchronization on the Barabási-Albert networks of size $N=1000$ with low and high clustering coefficients [networks with a high clustering coefficient were generated using the method proposed by Kim (2004)]. They found that in a clustered network the synchronization emerges at a lower coupling J than a network with the same degree distribution but with a lower clustering coefficient. However, in the latter network the global synchronization is stronger.

Timme (2006) simulated the Kuramoto model on directed networks and observed a topologically induced

transition from synchrony to disordered dynamics. This transition may be a general phenomenon for different types of dynamical models of synchronization on directed networks.

Synchronization of coupled oscillators in the Kuramoto model to an external periodic input, called a *pacemaker*, was studied for lattices, Cayley trees, and complex networks by Yamada (2002), Kori and Mikhailov (2004, 2006), and Radicchi and Meyer-Ortmanns (2006). This phenomenon is called *entrainment*. The pacemaker is assumed to be coupled with a finite number of vertices in a given network. Entrainment appears above a critical coupling strength J_{cr}. Kori and Mikhailov (2004) showed that J_{cr} increases exponentially with increasing the mean shortest path distance $\mathcal{L}$ from the pacemaker to all vertices in the network, i.e., $J_{cr} \sim e^{a\mathcal{L}}$. In a complex network, $\mathcal{L}$ is proportional to the mean intervertex distance $\bar{\ell}(N)$, which, in turn, is typically proportional to $\ln N$; see Sec. II.A. This leads to $J_{cr} \sim N^b$, where b is a positive exponent. It was shown that frequency locking to the pacemaker depends strongly on its frequency and the network architecture.

D. Coupled dynamical systems

Consider N identical dynamical systems. An individual system is described by a vector dynamical variable $\mathbf{x}_i(t)$, $i=1,\ldots,N$. The individual dynamics is governed by $\dot{\mathbf{x}}_i=\mathbf{F}(\mathbf{x}_i)$, where $\mathbf{F}$ is a vector function. These dynamical systems are coupled by edges and their dynamics can be described by

$$\dot{\mathbf{x}}_i = \mathbf{F}(\mathbf{x}_i) - J\sum_j L_{ij}\mathbf{H}(\mathbf{x}_j), \tag{134}$$

where J is the coupling strength and $\mathbf{H}(\mathbf{x}_j)$ is an output function that determines the effect of vertex j on the dynamics of vertex i. The network topology is encoded in the Laplacian matrix $L_{ij}=q_i\delta_{ij}-a_{ij}$, where a_{ij} is the adjacency matrix and q_i is the degree of vertex i. The Laplacian matrix is a zero-row-sum matrix, i.e., $\Sigma_j L_{ij}=0$ for all i. This property has the following consequence. Any solution of $\dot{\mathbf{s}}=\mathbf{F}(\mathbf{s})$ is also a solution of Eq. (134), $\mathbf{x}_i=\mathbf{s}(t)$, i.e., dynamical systems evolve coherently.

1. Stability criterion

We use the spectral properties of L in order to determine the stability of the fully synchronized state against small perturbations, $\mathbf{x}_i=\mathbf{s}(t)+\eta_i$. The Laplacian has nonnegative eigenvalues that can be ordered as $0=\lambda_1<\lambda_2 \leqslant \cdots \leqslant \lambda_N$. The zero eigenvalue corresponds to the uniform eigenfunction, $f_i^{(0)}=1$ for all i (the synchronized state). The remaining eigenfunctions $f_i^{(\lambda)}$ with $\lambda \geqslant \lambda_2$ are transverse to $f_i^{(0)}$. Representing a perturbation as a sum of the transversal modes, $\eta_i=\Sigma_{\lambda\geqslant\lambda_2}\eta_\lambda f_i^{(\lambda)}$, we find the master stability equation from Eq. (134),

$$\dot{\eta}_\lambda = [D\mathbf{F}(\mathbf{s}) - \alpha D\mathbf{H}(\mathbf{s})]\eta_\lambda, \tag{135}$$

where $\alpha=J\lambda$. $D\mathbf{F}$ and $D\mathbf{H}$ are the Jacobian matrices. If the largest Lyapunov exponent $\Lambda(\alpha)$ of this equation is negative, then the fully synchronized state is stable (Pecora and Carroll, 1998). $\Lambda(\alpha)$ is called the master stability function. This function is known for various oscillators such as Rössler, Lorenz, or double-scroll chaotic oscillators. Equation (135) is valid if the coupling matrix L_{ij} is diagonalizable. A generalization of the master stability equation for nondiagonalizable networks (i.e., for the case of a nonsymmetric coupling matrix) is given by Nishikawa and Motter (2006a, 2006b).

Thus we have the following criterion for the stability: the synchronized state is stable if and only if $\Lambda(J\lambda_n)<0$ for all $n=2,\ldots,N$. In this case, a small perturbation η_λ converges to zero exponentially as $t\to\infty$. The condition $\Lambda(J\lambda_1)=\Lambda(0)<0$ determines the dynamical stability of the solution $\mathbf{s}(t)$ to the individual dynamics.

Usually, the function $\Lambda(\alpha)$ is negative in a bound region $\alpha_1<\alpha<\alpha_2$. Therefore, a network is synchronizable if simultaneously $J\lambda_2>\alpha_1$ and $J\lambda_N<\alpha_2$. This is equivalent to the following condition:

$$\lambda_N/\lambda_2 < \alpha_2/\alpha_1 \tag{136}$$

(Barahona and Pecora, 2002). Note that λ_2 and λ_N are completely determined by the network topology, while α_1 and α_2 depend on the specific dynamical functions $\mathbf{F}$ and $\mathbf{H}$. The value of α_2/α typically ranges from 5 to 100 for various chaotic oscillators. The criterion Eq. (136) implies the existence of the interval $(\alpha_1/\lambda_2, \alpha_2/\lambda_N)$ of the coupling strength J where the synchronization is stable. The smaller the eigenratio λ_N/λ_2, the larger this interval and the better the synchronizability. If $J<\alpha_1/\lambda_2$, then modes with small eigenvalues $\lambda<\alpha_1/J$ break down synchronization. If $J>\alpha_2/\lambda_N$, then modes with large eigenvalues $\lambda>\alpha_2/J$ lead away from the synchronized state.

The spectrum of the Laplacian on the fully connected graph is simple: $\lambda_1=0$ and $\lambda_2=\cdots=\lambda_N=N$. The eigenratio λ_N/λ_2 is equal to 1, which corresponds to the highest possible synchronizability. In the d-dimensional cubic lattice of side length $l=N^{1/d}$, the minimum eigenvalue λ_2 of the Laplacian is small: $\lambda_2 \propto l^{-2}$. On the other hand, the largest eigenvalue λ_N is finite: $\lambda_N \sim d$. Therefore, the eigenratio λ_N/λ_2 diverges as $N\to\infty$, which means that complete synchronization is impossible in an infinite d-dimensional lattice (Wang and Chen, 2002; Hong, Kim, Choi, *et al.*, 2004). Only a finite lattice can be synchronized.

2. Numerical study

Synchronization of coupled dynamical systems on various complex networks has been extensively studied numerically. It turned out that the random addition of a small fraction of shortcuts p to a regular cubic lattice leads to a synchronizable network (Barahona and Pecora, 2002; Wang and Chen, 2002; Hong, Kim, Choi, *et al.*, 2004). For example, a ring of N vertices with short-

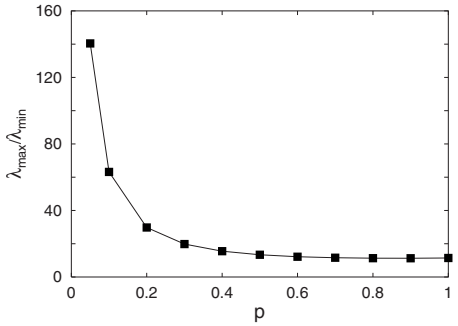

FIG. 32. Ratio λ_N/λ_2 vs the fraction of shortcuts p for the Watts-Strogatz network generated from a ring. Adapted from Hong *et al.*, 2004.

cuts is always synchronizable if N is sufficiently large. The shortcuts sharply decrease the ratio λ_N/λ_2 (see Fig. 32) until the network becomes synchronizable. The heuristic reason for this effect lies in the fact that adding shortcuts leads to the Watts-Strogatz network with the small-world effect. The average shortest path between two vertices chosen at random becomes small compared to the original regular lattice. In other words, the small-world effect improves the synchronizability of the Watts-Strogatz network compared with a regular lattice.

Synchronization is also enhanced in other complex networks. One can show that the minimum eigenratio λ_N/λ_2 is achieved for the Erdős-Rényi graph. In scale-free networks, the eigenratio λ_N/λ_2 increases with decreasing degree distribution exponent γ, and the synchronizability becomes worse. This effect was explained by the increase of heterogeneity (Nishikawa *et al.*, 2003; Motter *et al.*, 2005a, 2005b). A suppression of synchronization related to the increase of the load on vertices was found. Importantly, the eigenratio λ_N/λ_2 increases with N. Kim and Motter (2007) [see also Motter (2007)] found that the largest eigenvalue λ_N in an uncorrelated scale-free network is determined by the cutoff of the degree distribution: $\lambda_N=q_{\mathrm{cut}}+1$. The eigenvalue λ_2 is nearly size independent and ensemble averageable. (The last statement means that as $N\to\infty$ the ensemble distribution of λ_2 converges to a peaked distribution.) This leads to

$$\lambda_N/\lambda_2 \sim \min[N^{1/(\gamma-1)},N^{1/2}]; \tag{137}$$

see Sec. II.E.4. Therefore, it is difficult or even impossible to synchronize a large scale-free network with sufficiently small γ. These analytical results agree with numerical calculations of the Laplacian spectra for uncorrelated scale-free networks.

Another way to enhance synchronization is to use a network with asymmetric or weighted couplings. Motter *et al.* (2005a, 2005b, 2005c) considered an asymmetric degree-dependent coupling matrix $q_i^{-\eta}L_{ij}$ instead of L_{ij} in Eq. (134), where η is a tunable parameter. Their numerical and analytical calculations demonstrated that if $\eta=1$, then in a given network topology the synchronizability is maximum and does not depend on the network size. In this case, the eigenratio λ_N/λ_2 is insensitive to the form of the degree distribution. Interestingly, in a random network the eigenvalues λ_2 and λ_N of the normalized Laplacian matrix $q_i^{-1}L_{ij}$ achieve 1 as $\lambda_2=1-O(1/\sqrt{\langle q\rangle})$ and $\lambda_N=1+O(1/\sqrt{\langle q\rangle})$ in the limit of a large mean degree $\langle q\rangle\gg 1$ (Chung, 1997). Therefore in this limit the eigenratio λ_N/λ_2 is close to 1, and the system is close to the highest possible synchronizability.

Note that apart from synchronization, network spectra have numerous applications to structural properties of networks and processes in them. For results on Laplacian spectra of complex networks and their applications, see Chung (1997), Dorogovtsev *et al.* (2003), Kim and Motter (2007), Motter (2007), and references therein.

Chavez *et al.* (2005) found that further enhancement of synchronization in scale-free networks can be achieved by scaling the coupling strength to the load of each edge. Recall that the load l_{ij} of an edge ij is the number of shortest paths that go through this edge. They replaced the Laplacian L_{ij} with a zero-row-sum matrix with off-diagonal elements $-l_{ij}^{\alpha}/\Sigma_{j\epsilon N_i} l_{ij}^{\alpha}$, where α is a tunable parameter. This weighting procedure used global information of network pathways. Chavez *et al.* (2005) demonstrated that by varying the parameter α, one may efficiently get better synchronization. Similar improvement was obtained using a different, local weighting procedure based on the degrees of nearest neighbors (Motter *et al.*, 2005c). In networks with inhomogeneous couplings between oscillators, the intensity of a vertex is defined as the total strength of input couplings. Zhou *et al.* (2006) showed that the synchronizability in weighted random networks is enhanced as vertex intensities become more homogeneous.

The effect of degree correlations in a network on synchronization of coupled dynamical systems was revealed by Bernardo *et al.* (2007). They studied assortatively mixed scale-free networks. Their degree correlated networks were generated using the method proposed by Newman (2003d). They showed that disassortative mixing (connections between high-degree and low-degree vertices are more probable) enhances synchronization in both weighted and unweighted scale-free networks compared to uncorrelated networks. However, synchronization in a correlated network depends on the weighting procedure (Chavez *et al.*, 2006).

Above we showed that the fully connected graph gives optimal synchronization. However, this graph is "cost is no object" and uncommon in nature. Which other architectures maximize the synchronizability of coupled dynamical systems? Nishikawa and Motter (2006a, 2006b) came to the conclusion that the most optimal networks are directed and nondiagonalizable. Among the optimal networks, they found a subclass of hierarchical networks, with the following properties: (i) these networks embed an oriented spanning tree (i.e., there is a node from which all other vertices of the network can be reached by following directed links); (ii) there are no directed loops; and (iii) the total sum of input couplings at each vertex is the same for all verti-

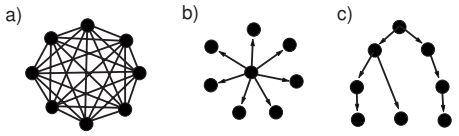

FIG. 33. Examples of graphs with optimal synchronizability: (a) a fully connected graph, (b) a directed star, and (c) a hierarchical directed random graph.

ces. Examples of optimal network topologies are shown in Fig. 33.

XI. SELF-ORGANIZED CRITICALITY PROBLEMS ON NETWORKS

In this section, we discuss avalanche processes in models defined on complex networks and related phenomena.

A. Sandpiles and avalanches

The sandpile dynamics on the Erdős-Rényi random graphs has been studied by Bonabeau (1995) and others, but no essential difference from high-dimensional lattices was found. Goh *et al.* (2003) and Lee *et al.* (2004a, 2004b) investigated a variation of the Bak-Tang-Wiesenfeld (BTW) model on scale-free uncorrelated networks and observed an effect of the network architecture on the self-organized criticality (SOC) phenomenon. We now discuss these results.

The model is defined as follows. For each vertex i, a threshold $a_i=q_i^{1-\eta}$ is defined, where $0\leqslant\eta\leqslant 1$, so that $a_i\leqslant q_i$. A number of grains at vertex i is denoted by h_i.

(i) A grain is added to a randomly chosen vertex i, and h_i increases by 1.

(ii) If the resulting $h_i<a_i$, go to (i). On the other hand, if $h_i\geqslant a_i$, then h_i is decreased by $\lceil a_i\rceil$, the smallest integer greater than or equal to a_i. That is, $h_i\to h_i-\lceil a_i\rceil$. These $\lceil a_i\rceil$ toppled grains jump to $\lceil a_i\rceil$ randomly chosen nearest neighbors of vertex i: $h_j\to h_j+1$.

(iii) If for these $\lceil a_i\rceil$ vertices the resulting $h_j<a_j$, then the "avalanche" process finishes. Otherwise, vertices with $h_j\geqslant a_j$ are updated in parallel (!), $h_j\to\lceil a_j\rceil$, their randomly chosen neighbors receive grains, and so on until the avalanche stops. Then repeat (i).

Note that the particular, "deterministic" case of $\eta=0$, where all nearest neighbors of an activated vertex receive grains (as in the BTW model), essentially differs from the case of $\eta>0$, where $\lceil a_i\rceil<q_i$.

As is usual in SOC problems, the statistics of avalanches was studied as follows: the size distribution $\mathcal{P}_s(s)\sim s^{-\tau}$ for the avalanches (the "size" here is the total number of toppling events in an avalanche) and the distribution $\mathcal{P}_t(t)\sim t^{-\delta}$ of their durations. [The distribution of the avalanche area (the number of vertices involved) is similar to $\mathcal{P}_s(s)$.] Taking into account the treelike structure of uncorrelated networks, one can see that (i) an avalanche in this model is a branching process, avalanches are trees; (ii) the duration of an avalanche t is the distance from its root to its most remote vertex; and (iii) the standard technique for branching processes is applicable to this problem.

The basic characteristic of the avalanche tree is the distribution of branching, $p(q)$. According to Goh *et al.* (2005) and Lee *et al.* (2004a, 2004b), $p(q)=p_1(q)p_2(q)$. The first factor is the probability that $q-1<a\leqslant q$, that is, q grains will fall from a vertex in the act of toppling. $p_2(q)$ is the probability that before the toppling, the vertex has exactly $q-1$ grains. The assumption that the distribution of h is homogeneous gives the estimate $p_2(q)\sim 1/q$. As for $p_1(q)$, one must take into account that (i) the degree distribution of an edge end is $qP(q)/\langle q\rangle$, (ii) $P(q)\sim q^{-\gamma}$, and (iii) $a=q^{1-\eta}$. As a result, $p_1(q)\sim q^{-(\gamma-1-\eta)/(1-\eta)}$. Thus, the distribution of branching is $p(q)\sim q^{-(\gamma-2\eta)/(1-\eta)}\equiv q^{-\gamma'}$. One can see that if $p_2(q)=1/q$, then $\Sigma_q qp(q)=1$.

Goh *et al.* (2003) and Lee *et al.* (2004a, 2004b) applied the standard technique to the branching process with this $p(q)$ distribution and arrived at power-law size and duration distributions, which indicate the presence of a SOC phenomenon for the assumed threshold $a=q^{1-\eta}$. They obtained exponents τ and δ. With these exponents, one can easily find the dynamic exponent $z=(\delta-1)/(\tau-1)$ (the standard SOC scaling relation), which in this case coincides with the fractal dimension of an avalanche. The results are as follows. There is a threshold value, $\gamma_c=3-\eta$, which separates two regimes:

$$\text{if } \gamma>3-\eta, \quad \text{then } \tau=\tfrac{3}{2}, \quad \delta=z=2, \tag{138}$$

$$\text{if } 2<\gamma<3-\eta, \quad \text{then } \tau=\frac{\gamma-2\eta}{\gamma-1-\eta},$$

$$\delta=z=\frac{\gamma-1-\eta}{\gamma-2}. \tag{139}$$

It is easy to understand these results for the fractal dimension of an avalanche, z. One may check that this z coincides exactly with the fractal dimension of equilibrium connected trees with the degree (or branching) distribution equal to $p(q)\sim q^{-\gamma'}$; see Sec. II.C.

For a numerical study of the BTW model on small-world networks, see de Arcangelis and Herrmann (2002). The BTW model is one of numerous SOC models. There were a few studies of other SOC models on complex networks. For example, for the Olami-Feder-Christensen model on various networks, see Caruso *et al.* (2006, 2007), and for a Manna-type sandpile model on small-world networks, see Lahtinen *et al.* (2005). The Bak-Sneppen model on networks has been studied by Kulkarni *et al.* (1999), Moreno and Vazquez (2002), Lee, Hong, and Lee (2005), and Masuda *et al.* (2005).

B. Cascading failures

Devastating power blackouts are in the list of most impressive large-scale accidents in artificial networks. In fact, a blackout is a result of an avalanche of overload failures in power grids. A simple though representative model of a cascade of overload failures was proposed by Motter and Lai (2002). The load of a vertex in this model is betweenness centrality—the number of the shortest paths between other vertices, passing through the vertex see Sec. II.A. Note that frequently the betweenness centrality is simply called load (Goh *et al.*, 2001).

For every vertex i in this model, a limiting load (capacity) is introduced,

$$c_i = (1 + \alpha)b_{0i}, \tag{140}$$

where b_{0i} is the load (betweenness centrality) of this vertex in the undamaged network. The constant $\alpha \geqslant 0$ is a tolerance parameter showing how much an initial load can be exceeded. A cascading failure in this model looks as follows.

(i) Delete a vertex. This leads to the redistribution of loads of the other vertices: $b_{0i} \to b'_{0i}$.

(ii) Delete all overloaded vertices, that is, the vertices with $b'_{0i} > c_i$.

(iii) Repeat this procedure until no overloaded vertices remain.

In their simulations of various networks, Motter and Lai measured the ratio $G = N_{\text{after}}/N$, where N and N_{after} are, respectively, the original number of vertices in a network and the size of its largest connected component after the cascading failure. (Assume that the original network coincides with its giant connected component.) Resulting $G(\alpha)$ depend on (i) the architecture of a network, (ii) the parameter α, and (iii) characteristics of the first failing vertex, e.g., on its degree.

In a random regular graph, for any $\alpha > 0$, G is 1, and only if $\alpha = 0$ will the network be completely destroyed, $G = 0$. On the other hand, in networks with heavy-tailed degree distributions, G depends strongly on the degree (load) of the first removed vertex. Motter and Lai used a scale-free network with $\gamma = 3$ in their simulation. We briefly discuss their results. $\alpha = 0$ gives $G = 0$ for any starting vertex in any network, while $\alpha \to \infty$ results in $G = 1$. The question is actually about the form of the monotonously growing curve $G(\alpha)$. When the first removed vertex is chosen at random, the cascade is large (G strongly differs from 1) only at small α, and $G(\alpha)$ rapidly grows from 0 to 1. If the first vertex is chosen from ones of the highest degrees, then G gently rises with α, and cascades may be giant even at rather large α.

Lee, Goh, Kahng, *et al.* (2005) numerically studied the statistics of the cascades in this model defined on a scale-free network with $2 < \gamma \leqslant 3$ and found that there is a critical point $\alpha_c \approx 0.15$. At $a < a_c$, there are giant avalanches, and at $\alpha > \alpha_c$, the avalanches are finite. They observed that at the critical point the size distribution of avalanches has a power-law form $\mathcal{P}(s) \sim s^{-\tau}$, where exponent $\tau \approx 2.1(1)$ in the range $2 < \gamma \leqslant 3$.

This model can be generalized as follows: α may be defined as a random variable; instead of betweenness centrality other characteristics may be used, etc. [see Motter (2004) or, for a model with overloaded links, Moreno *et al.* (2003) and Bakke *et al.* (2006)]. Note that there are other approaches to cascading failures. For example, Watts (2002) proposed a model where, in simple terms, cascading failures were treated as a kind of epidemic outbreak.

C. Congestion

Here we only touch upon basic models of jamming and congestion proposed by physicists. Ohira and Sawatari (1998) put forward a simple model of congestion. Originally it was defined on a lattice but it can be generalized to arbitrary network geometries.

The vertices in this model are of two types—hosts and routers. Hosts send packets at some rate λ to other (randomly chosen) hosts, so that every packet has its own target. Each packet passes through a chain of routers storing and forwarding packets. There is a restriction: the routers can forward not more than one packet per time step. The routers are supposed to have infinite buffer space, where a queue of packets is stored. The packet at the head of the queue is sent first. A router sends a packet to its neighboring router, which is the closest to the target. If there occur more than one such router, then one of them is selected by special rules. For example, one may choose the router with the smallest flow of packets through it.

In their simulations Ohira and Sawatari studied the average time a packet needs to reach its target versus the packet injection rate λ. It turned out that this time rises above some critical value λ_c, which indicates transition to the congestion phase. These observations suggest that it is a continuous transition, without a jump or hysteresis. The obvious reason for this jamming transition is the limited forwarding capabilities of routers—one packet per time step.

Solé and Valverde (2001) investigated this transition in the same model. They numerically studied the time-series dynamics of the number of packets at individual routers, and found a set of power laws at the critical point. In particular, they observed a $1/f$-type power spectrum of these series and a power-law distribution of queue lengths. [Similar critical effects were found in an analytically treatable model of traffic in networks with hierarchical branching; see Arenas *et al.* (2001).] They proposed the following idea. Since the traffic is most efficient at λ_c, the Internet self-organizes to operate at criticality. This results in various self-similar scaling phenomena in the Internet traffic.

These ideas became the subject of criticism from computer scientists (Willinger *et al.*, 2002). This criticism was from discoverers of the scaling properties for Internet

traffic (Leland *et al.*, 1994). They wrote, "self-similar scaling has been observed in networks with low, medium, or high loads, and any notion of a magical load scenario where the network has to run at critical rate λ_c to show self-similar traffic characteristics is inconsistent with the measurements." They listed alternative reasons for these self-similar phenomena. This criticism was, in fact, aimed at a wide circle of self-organized criticality models for various aspects of the real Internet, proposed by physicists. Willinger *et al.* stressed that these models "are only evocative; they are not explanatory." In their definition, an evocative model "can reproduce the phenomenon of interest but does not necessarily capture and incorporate the true underlying cause." On the other hand, an explanatory model "also captures the causal mechanisms (why and how, in addition to what)." Ask yourself, how many explanatory models of real networks were proposed?

Guimerà *et al.* (2002) developed an analytical approach in which search and congestion problems were interrelated. In their simple theory, the mean queue length at vertices of a network was related to a search cost in this network. The latter is the mean number of steps needed to find a target vertex. In this approach, minimizing the mean queue length is reduced to minimizing the search cost. This approach was used to find optimal network architectures with minimum congestion.

Echenique *et al.* (2005) introduced a model of network traffic with a protocol allowing one to prevent and relieve congestion. In their model, routers forward packets, taking into account the queue lengths at their neighbors. That is, a packet is sent to the neighboring router j, which has the minimum value

$$\delta_j \equiv h\ell_{jt} + (1-h)c_j. \tag{141}$$

Here ℓ_{jt} is the length of the shortest path from router j to the target of the packet, c_j is the queue length at the router, and the parameter h is in the range $0 \leqslant h \leqslant 1$. Echenique *et al.* performed numerical simulations using the map of a real Internet network, but their results should also be valid for other architectures. As an order parameter for congestion, they used the ratio ρ=(the number of packets that have not reached their targets during the observation)/(the total number of packets generated during this time period). It turned out that if the parameter h is smaller than 1, then the transition to the congestion phase occurs at an essentially higher rate λ_c. Furthermore, when $h<1$, the order parameter emerges with a jump as in a first-order phase transition, while at $h=1$ the transition resembles a usual second-order phase transition; see Fig. 34. Remarkably, the locations of these transitions, as well as the curves $\rho(\lambda)$, coincide at the studied values $h=0.95, 0.75, 0.5$. On the other hand, the congestion ρ at $h<1$ is much higher than at $h=1$ at the same $\lambda > \lambda_c$. The routing protocol of Echenique *et al.* was explored and generalized in a number of studies. For one possible generalization, see Liu *et al.* (2006) and Zhang *et al.* (2007).

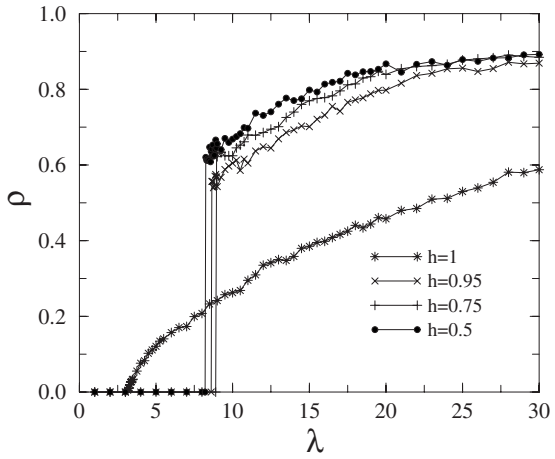

FIG. 34. Order parameter ρ vs the packet injection rate λ for various h using the model of Echenique *et al.* (2005). From Echenique *et al.*, 2005.

Another approach to network traffic, treating this process in terms of specific diffusion of packets, was developed by Tadić and Thurner (2004); Tadić *et al.* (2004, 2006); see also Wang *et al.* (2006). The theory of this kind of traffic was elaborated on by Fronczak and Fronczak (2007). Danila *et al.* (2006) studied routing based on local information. They considered "routing rules with different degrees of congestion awareness, ranging from random diffusion to rigid congestion-gradient driven flow." They found that the strictly congestion-gradient driven routing easily leads to jamming. Carmi, Cohen, and Dolev (2006) presented a physical solution to the problem of effective routing with minimal memory resources. Toroczkai and Bassler (2004) investigated the influence of network architectures on the congestion. Helbing *et al.* (2007) described the generation of oscillations in network flows. Rosvall *et al.* (2004) discussed how to use limited information to find the optimal routes in a network. For the problem of optimization of network flows, see also Gourley and Johnson (2006), and references therein.

XII. OTHER PROBLEMS AND APPLICATIONS

In this section, we review a number of critical effects and processes in networks, which have been omitted in the previous sections.

A. Contact and reaction-diffusion processes

1. Contact process

The contact process (Harris, 1974) is in a wide class of models exhibiting nonequilibrium phase transitions, for example, the SIS model of epidemics, which belong, to the directed percolation universality class (Grassberger and de la Torre, 1979); see Hinrichsen (2000). The contact process on a network is defined as follows. An initial population of particles occupies vertices in a network. Each vertex can be occupied by only one particle (or be empty). At each time step t, a particle on an arbitrary

chosen vertex either (i) disappears with a probability p or (ii) creates with the probability $1-p$ a new particle at an arbitrary chosen unoccupied neighboring vertex.

We introduce an average density $\rho_q(t)$ of particles at vertices with degree q. The time evolution of $\rho_q(t)$ is given by the mean-field rate equation,

$$\frac{d\rho_q(t)}{dt} = -p\rho_q(t) + (1-p)q[1-\rho_q(t)] \times \sum_{q'} \rho_{q'}(t)\frac{P(q'|q)}{q'}, \tag{142}$$

where $P(q'|q)$ is the conditional probability that a vertex of degree q is connected to a vertex of degree q' (Castellano and Pastor-Satorras, 2006a). The first and second terms in Eq. (142) describe the disappearance and emergence of particles, respectively, at vertices with degree q. The factor $1/q'$ shows that a new particle is created with the same probability at any (unoccupied) nearest-neighboring vertex of a vertex with degree q'. Recall that in uncorrelated networks, $P(q'|q) = q'P(q')/\langle q\rangle$.

Equation (142) shows that if the probability p is larger than a critical probability p_c, then any initial population of particles disappears at $t\to\infty$, because particles disappear faster than they are created. This is the so-called absorbing phase. When $p<p_c$, an initial population of particles achieves a state with a nonzero average density,

$$\rho = \sum_q P(q)\rho_q(t\to\infty) \propto \epsilon^{\beta}, \tag{143}$$

where $\epsilon=p_c-p$. This is the active phase. In the configuration model of uncorrelated random networks, the critical probability $p_c=\frac{1}{2}$ does not depend on the degree distribution while the critical exponent β does. In networks with a finite second moment $\langle q^2\rangle$, we have $\beta=1$. If $\langle q^2\rangle\to\infty$, then β depends on the asymptotic behavior of the degree distribution at $q\gg 1$. If the network is scale-free with $2<\gamma\leqslant 3$, the exponent β is $1/(\gamma-2)$. This critical behavior occurs in the infinite size limit, $N\to\infty$. In a finite network, ρ is small but finite at all $p>0$ and it is necessary to use finite-size scaling theory.

Ha *et al.* (2007) and Hong, Ha, and Park (2007) applied the mean-field finite-size scaling theory to the contact process on finite networks; see Sec. IX.B. They showed that near the critical point p_c the average density ρ behaves as $\rho(\epsilon,N)=N^{-\beta/\bar{\nu}}f(\epsilon N^{1/\bar{\nu}})$, where $f(x)$ is a scaling function; the critical exponent β is the same as above. The critical exponent $\bar{\nu}$ depends on degree distribution: $\bar{\nu}(\gamma>3)=2$ and $\bar{\nu}(2<\gamma\leqslant 3)=(\gamma-1)/(\gamma-2)$. They carried out Monte Carlo simulations of the contact process on the configuration model of uncorrelated scale-free networks with size up to $N=10^7$. These simulations agreed well with the predictions of the mean-field scaling theory, in contrast to earlier calculations of Castellano and Pastor-Satorras (2006a, 2007).

Based on the phenomenological theory of equilibrium critical phenomena in complex networks (Sec. IX.A), Hong, Ha, and Park (2007) proposed a phenomenological mean-field Langevin equation that describes the average density of particles in the contact process on uncorrelated scale-free networks near the critical point,

$$d\rho(t)/dt = \epsilon\rho - b\rho^2 - d\rho^{\gamma-1} + \sqrt{\rho}\eta(t), \tag{144}$$

where $\eta(t)$ is the Gaussian noise, and b and d are constants. Note that the contact process contains the so-called multiplicative noise $\sqrt{\rho}\eta(t)$, in contrast to an equilibrium process with a thermal Gaussian noise [see Hinrichsen (2000)]. Neglecting noise in Eq. (144), in the steady state one can obtain the critical behavior of ρ and finite-size scaling behavior for the relaxation rate; sec Sec. IX.B. As is natural, when a degree distribution is rapidly decreasing, this finite-size scaling coincides with scaling for the contact process on high-dimensional lattices (Lübeck and Janssen, 2005).

The time evolution of the average density $\rho(t)$ was studied by Castellano and Pastor-Satorras (2006a, 2007) and Hong, Ha, and Park (2007). When $p\neq p_c$, in an infinite network, an initial population of particles exponentially relaxes to a steady distribution. The relaxation time t_c is finite. At the critical point $p=p_c$ the characteristic time t_c diverges, and an initial distribution decays as $\rho(t)\sim t^{-\theta}$. The exponent $\theta=1$ for an uncorrelated complex network with a finite second moment $\langle q^2\rangle$, and $\theta=1/(\gamma-2)$ for a scale-free network with $2<\gamma<3$. In a finite network, $t_c(N)$ is finite even at the critical point. Castellano and Pastor-Satorras (2008) found that

$$t_c \sim (N\langle q\rangle^2/\langle q^2\rangle)^{1/2} \tag{145}$$

in an uncorrelated network with $\langle q^2\rangle<\infty$. Note that when exponent $\gamma>3$, the phenomenological approach based on Eq. (144) also leads to $t_c\propto N^{1/2}$. The size dependence of t_c in the range $2<\gamma<3$, where $\langle q^2\rangle$ depends on N, is still under discussion; see Castellano and Pastor-Satorras (2007) and Hong, Ha, and Park (2007).

Giuraniuc *et al.* (2006) considered the contact process with a degree-dependent rate of emergence of particles assumed to be proportional to $(q_iq_j)^{-\mu}$, where μ is a tunable parameter, and q_i and q_j are degrees of neighboring vertices. Using a mean-field approximation that is equivalent to the annealed network approximation, they showed that this degree-dependent rate changes the critical behavior of the contact process in scale-free networks. The result is a shift the degree distribution exponent γ to $\gamma'=(\gamma-\mu)/(\gamma-1)$. This effect is similar to the Ising model with degree-dependent interactions in Sec. VI.C.5. For finite-size scaling in contact processes with this degree-dependent rate of emergence, see Karsai *et al.* (2006).

2. Reaction-diffusion processes

Reaction-diffusion processes on uncorrelated random complex networks were studied by Colizza *et al.* (2007). Consider the following process for particles of two types, A and B. In an initial state, particles are distributed randomly over vertices of a network. There may be an ar-

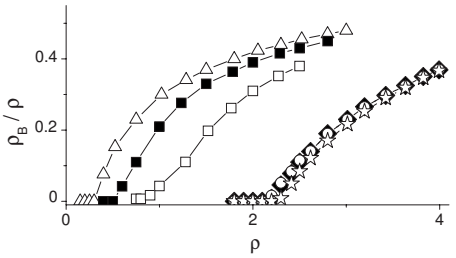

FIG. 35. Relative density of particles B vs the total density of A and B particles in the reaction-diffusion model in scale-free networks at $\mu/\lambda=2$. Rightmost curves (A particles are nondiffusing): stars, $N=10^4$, $\gamma=3$; closed diamonds, $N=10^4$, $\gamma=2.5$; open circles, $N=10^5$, $\gamma=2.5$. Leftmost curves (both A and B particles are diffusing, $\gamma=2.5$): open squares, $N=10^3$; closed squares, $N=10^4$; open triangles, $N=10^5$. Adapted from Colizza *et al.*, 2007.

bitrary number of these particles at any vertex. Suppose that only particles at the same vertex may react and transform to other particles. The rules of this transformation are the following:

(i) Each particle B can spontaneously turn into an A particle at the same vertex at a rate μ: $B \to A$.

(ii) Particles A and B can transform into two B particles at the same vertex at a rate λ: $A+B \to 2B$.

(iii) Particles B can hop to neighboring vertices at the unit rate.

These reactions preserve the total number of particles in the system. The steady state of this process depends strongly on a supposed behavior of particles A.

If A particles are nondiffusing and the total density of A and B particles ρ is smaller than the critical density $\rho_c=\mu/\lambda$, then B particles disappear in the limit $t\to\infty$ (this is the absorbing phase). At $\rho>\rho_c$, there is a nonzero density of B particles ρ_B in the steady state (this is the active phase); see Fig. 35. Colizza *et al.* (2007) showed that ρ_c and the critical behavior do not depend on the degree distribution.

If A particles can also hop, then the phase transition into the active phase occurs at a degree-dependent critical density $\rho_c=\langle q\rangle^2\mu/\langle q^2\rangle\lambda$. In networks with divergent $\langle q^2\rangle$, ρ_c is zero in the limit $N\to\infty$; see Fig. 35. A similar disappearance of the critical threshold was observed in percolation and the spread of diseases.

Network topology strongly affects the dynamics of the diffusion-annihilation process. This process is defined in the following way. Identical particles diffuse in a network. If two particles are at the same vertex, they annihilate ($A+A\to\emptyset$). Catanzaro *et al.* (2005) within the mean-field theory showed that in infinite uncorrelated random networks, the average density of particles $\rho(t)$ decreases as $t^{-\alpha}$ at long times, where the exponent $\alpha=1$ for a network with a finite second moment $\langle q^2\rangle$, and $\alpha=1/(\gamma-2)$ for an uncorrelated scale-free network with degree distribution exponent $2<\gamma<3$ (i.e., with divergent $\langle q^2\rangle$). However, in a finite scale-free network, there is a crossover to traditional mean field behavior $1/t$ at time $t>t_c(N)$, where the crossover time $t_c(N)$ increases with increasing N. Thus the non-mean-field behavior with $\alpha=1/(\gamma-2)$ may be observed only in a sufficiently large network [see ben-Avraham and Glasser (2007) for a discussion of kinetics of coalescence, $A+A\to A$, and annihilation, $A+A\to\emptyset$, beyond the mean-field approximation in the Bethe lattice]. This agrees with numerical simulations of Gallos and Argyrakis (2004) and Catanzaro *et al.* (2005).

B. Zero-range processes

The zero-range process describes nonequilibrium dynamics of condensation of interacting particles in lattices and networks. This process is closely related to the balls-in-boxes model (Bialas *et al.*, 1997) and equilibrium network ensembles (Burda *et al.*, 2001; Dorogovtsev *et al.*, 2003b; Angel *et al.*, 2005, 2006) discussed in Sec. IV.A. For a review on several applications of this model, see Evans and Hanney (2005).

In the zero-range process, identical particles hop between vertices on a graph with a rate $u(n)$, which depends on the number of particles n at the vertex of departure. The total number of particles is conserved. In fact, an interaction between particles on the same vertex is encoded in the function $u(n)$. The case $u(n)\propto n$ corresponds to noninteracting particles. If $u(n)$ increases faster than n, then we deal with local repulsion. If $u(n)$ decreases with n, then it assumes local attraction. Emergence of condensation depends on the hop rate $u(n)$ and the network structure.

The system evolves from an initial distribution of particles to a steady state. Under certain conditions, condensation of a finite fraction of particles occurs onto a single vertex. Note that this nonequilibrium phase transition occurs even in a one-dimensional lattice. In the steady state, the distribution of particles over vertices can be found exactly. The probability that vertices $i=1,2,\ldots,N$ are occupied by $n_1,n_2,\ldots,n_N$ particles is

$$\mathcal{P}(n_1,n_2,\ldots,n_N)=A\prod_{i=1}^{N} f_i(n_i), \tag{146}$$

where A is a normalization constant, the function $f_i(n)\equiv\Pi_{m=1}^{n}[\omega_i/u(m)]$ for $n\geqslant 1$, and $f_i(0)\equiv 1$ (Evans and Hanney, 2005). The parameters ω_i are the steady-state weights of a single random walker that moves on a given network. In simple terms, the frequency of visits of the walker to a vertex is proportional to its weight. The weights satisfy $\omega_i=\Sigma_j\,\omega_j T_{ji}$, where T_{ji} is a rate of particle hops from vertex j to neighboring vertex i. Using Eq. (146), one can find an exact mean occupation number of vertices.

First consider a homogeneous system where all vertices have the same degree. Condensation is absent if $u(n\to\infty)\to\infty$. In the steady state, all vertices have the same average occupation number (the so-called fluid phase). Condensation occurs if $u(n)$ decays asymptoti-

cally as $u(\infty)(1+b/n)$ with $b>2$. In this case, the steady state with condensate emerges when the concentration of particles ρ is larger than a critical concentration ρ_c determined by the function $u(n)$. In the condensed phase, a finite fraction of particles, $\rho-\rho_c$, occupies a single vertex chosen at random. All other vertices are occupied uniformly with the mean occupation number ρ_c. If $u(n\to\infty)=0$, then $\rho_c=0$.

The zero-range process in uncorrelated scale-free networks with degree distribution exponent $\gamma>2$ was studied by Noh (2005) and Noh *et al.* (2005). They considered the case in which the function $u(n)=n^{\delta}$. A particle can hop with the same probability to any nearest-neighboring vertex, i.e., the transition probability $T_{ij}=1/q_i$, where q_i is the degree of departure vertex i. In this case, $\omega_i=q_i$. It was shown that if $\delta>\delta_c=1/(\gamma-2)$, then the steady state is the fluid phase at any density of particles. If $\delta\leqslant\delta_c$, then the critical concentration $\rho_c=0$. At $\rho>0$, in the steady state, almost all particles are condensed not at a single vertex but a set of vertices with degrees exceeding $q_c\equiv[q_{\rm cut}(N)]^{1-\delta/\delta_c}$. These vertices form a vanishingly small fraction of vertices in the network as $N\to\infty$. Note that these results were obtained for the cutoff $q_{\rm cut}(N)=N^{1/(\gamma-1)}$ [see the discussion of $q_{\rm cut}(N)$ in Sec. II.E.4]. When $\delta=0$, then $q_c=q_{\rm cut}(N)$ and all particles condense at a vertex with the highest degree $q_{\rm cut}(N)$. See Tang *et al.* (2006) for specifics of condensation in a zero-range process in weighted scale-free networks.

The steady state in the zero-range process on a scale-free network is completely determined by the degree distribution. The topological structure plays no role (i.e., it does not matter whether vertices are arranged in a finite-dimensional system or form a small world). It is assumed that the network structure may influence relaxation dynamics of the model, unfortunately no exact results are known. Noh (2005) studied the evolution of an initial distribution of particles to the steady state and estimated the relaxation time τ. In an uncorrelated random scale-free network, the relaxation time is $\tau\sim N^z$, where $z=\gamma/(\gamma-1)-\delta$, while in clustered scale-free networks, this exponent is $z=1-\delta$. This estimate agrees with the numerical simulations by Noh (2005) and Noh *et al.* (2005). Note that the scaling relation $\tau\sim N^z$ is also valid for a d-dimensional lattice. In this case, the exponent z depends on both the dimension d and the probability distribution of hopping rates. In particular, $z=2$ for a $(d>2)$-regular lattice (Evans and Hanney, 2005).

In a finite network, the condensate at a given vertex exists a finite time $\tau_m(N)$. After "melting" at this vertex, the condensate appears at another vertex, then at another one, and so on. For a homogeneous network, such as a random regular graph, $\tau_m\sim N^{z'}\gg\tau\sim N^z$, where $z'>z$. Bogacz *et al.* (2007a, 2007b) and Waclaw *et al.* (2007) argued that in heterogeneous systems the typical melting time of the condensate $\tau_m(N)$ increases exponentially with N, i.e., $\tau_m(N)\sim e^{cN}$, in contrast to a homogeneous system. The zero-range process slowly relaxes to the condensed phase in comparison to the relaxation time to the equilibrium state in the ferromagnetic Ising model. (The relaxation time of the Ising model is finite at all temperatures except the critical one, at which it scales with N as N^s; see Sec. IX.B.) As soon as the condensate is formed, it exists for an exponentially long time at a vertex of the network: $\tau_m\sim e^{cN}\gg\tau\sim N^z$.

C. The voter model

According to Sood and Redner (2005), "the voter model is perhaps the simplest and most completely solved example of cooperative behavior." In this model, each vertex is in one of two states—spin up or spin down. In the vertex update version of the model, the evolution is defined as follows. At each time step, (i) choose a vertex at random and (ii) ascribe to this vertex the state of its randomly chosen neighbor.

The evolution in the voter model starts with some random configuration of up and down spins, say, with a fraction of n_0 spins up. One can see that this evolution is determined by random annihilation of chaotic interfaces between "domains" with up and down spins. In a finite system, there is always a chance that the system will reach an absorbing state, where all spins are up (or down). However, on the infinite regular lattices of dimensionality greater than 2, the voter model never reaches the absorbing states, staying in the active state forever. For the voter model on finite regular lattices of dimensionality greater than 2, the mean time to reach consensus is $\tau_N\sim N$ (ben-Avraham *et al.*, 1990; Krapivsky, 1992). Here N is the total number of vertices in a lattice.

On the other hand, the infinite one-dimensional voter model evolves to consensus. Castellano *et al.* (2003) and Vilone and Castellano (2004) studied the voter model on the Watts-Strogatz small-world networks and found that even a small concentration of shortcuts makes consensus unreachable in infinite networks. This is quite natural, since these networks are infinite-dimensional objects.

It is important that the average fraction of spins up n conserves in the voter model on regular lattices, i.e., $n(t)=n_0=$const. Here averaging is over all initial spin configurations and over all evolution histories. Suchecki *et al.* (2005a, 2005b) found that on random networks, $n(t)$ is not conserved. Instead, the following weighted quantity is conserved:

$$\tilde{n}=\sum_q \frac{qP(q)}{n(q)}\langle q\rangle, \tag{147}$$

where $n(q)$ is the average fraction of spins up among vertices of degree q. Thus, $\tilde{n}(t)=\tilde{n}_0=$const, where $\tilde{n}_0\equiv\tilde{n}(t=0)$. Note that $\tilde{n}$ is actually the probability that an end vertex of a randomly chosen edge is in state up.

Based on this conservation, Sood and Redner (2005) arrived at the following physical picture for the voter model on uncorrelated complex networks. Consensus is unreachable if these networks are infinite. In finite networks, the mean time to reach consensus is finite. The

evolution consists of two stages. The first is a short initial transient to an active state where, at any particular evolution history, the fraction of vertices of a given degree with spin up is approximately $\tilde{n}_0$. In the slow second stage, coarsening develops, and the system has an increasing chance to approach consensus. The mean time to reach consensus is

$$\tau_N = N\frac{\langle q\rangle^2}{\langle q^2\rangle}[(1-\tilde{n}_0)\ln(1-\tilde{n}_0)^{-1} + \tilde{n}_0 \ln \tilde{n}_0^{-1}]. \qquad (148)$$

The theory of Sood and Redner gives (a) $\tau_N \sim N$ for uncorrelated networks with a converging second moment of a degree distribution; (b) $\tau_N \sim N/\ln N$ in the case of the degree distribution $P(q) \sim q^{-3}$; and (c) τ_N growing slower than N if $\langle q^2\rangle$ diverges, i.e., if the degree distribution exponent is less than 3. In the last case, this size dependence (a power of N with exponent less than 1) is determined by a specific model-dependent cutoff of the degree distribution, $q_{\rm cut}(N)$.

Interestingly, in the second version of the voter model (edge update) the average fraction of up vertices is conserved as well as the mean magnetization. In the edge update voter model, at each time step an end vertex of a randomly chosen edge adopts the state of the second end. In this model, the evolution of the system on a complex network is qualitatively the same as on high-dimensional regular lattices, and $\tau_N \sim N$ (Suchecki *et al.*, 2005a, 2005b).

Other basic types of spin dynamics have also been widely discussed. Castellano *et al.* (2005) studied a difference between the voter dynamics and the Glauber-Metropolis zero-temperature dynamics on networks (Castellano and Pastor-Satorras, 2006b; Zhou and Lipowsky, 2005). In the Glauber-Metropolis dynamics applying the Ising model at zero temperature, at each time step, a randomly chosen spin gets an energetically favorable value, +1 or −1. In contrast to the evolution due to the interface annihilation in the voter model, in the Glauber-Metropolis dynamics domain walls shorten diminishing surface tension. Svenson (2001) showed numerically that, in infinite random networks, the Glauber-Metropolis dynamics of the Ising model at zero temperature does not reach the ground state. Häggström (2002) rigorously proved that this is true at least in the case of the Gilbert model of classical random graphs. Thus, this kind of dynamics can result in consensus only in finite networks, as in the voter model. Nonetheless, Castellano *et al.* found that the voter and Glauber-Metropolis dynamics provide markedly different relaxation of spin systems on random networks. For the Glauber-Metropolis dynamics, the time dependence of the probability that a system does not yet reach consensus essentially deviates from exponential relaxation, typical for the voter dynamics.

For detailed discussion of the voter model on complex networks in the context of opinion formation, see Wu and Huberman (2004). For other nonequilibrium phenomena in complex networks modeling social interactions, see Klemm *et al.* (2003), Antal *et al.* (2005), and Baronchelli *et al.* (2007).

A few numerical studies were devoted to nonequilibrium phase transitions in the ferromagnetic Ising model on directed complex networks with possible application to processes in social, economic, and biological systems. In the directed Ising model, interactions between spins are asymmetric and directed, and a Hamiltonian formulation is impossible. Each spin is affected only by those of its nearest-neighboring spins, which are connected to this spin by outgoing edges. Using a directed Watts-Strogatz network generated from a square lattice, Sánchez *et al.* (2002) found that a ferromagnetic phase transition in this system is continuous at a sufficiently small density of the shortcuts. This transition, however, becomes first order above a critical concentration of the shortcuts. Lima and Stauffer (2006) carried out simulations of the ferromagnetic Ising model on a directed Barabási-Albert network at $T=0$ and found that different dynamics algorithms lead to different final states of the spin system. These first investigations demonstrated a strong influence of a directed network structure on the nonequilibrium dynamics. However, these systems are not yet understood.

D. Coevolution models

We discussed systems in which a cooperative model does not influence its network substrate. Holme and Newman (2006) described an interesting contrasting situation, in which an evolving network and interacting agents on it strongly influence each other. The model of Holme and Newman, in essence, is an adaptive voter model and may be formulated as follows. There is a sparse network of N vertices with a mean degree $\langle q\rangle$. Each vertex may be in one of G states—opinions, where G is a large number (which is needed for a sharp phase transition). Vertices and connections evolve: at each time step, choose a random vertex i in state g_i. If the vertex is isolated, do nothing. Otherwise, (i) with probability φ, reattach the other end of a randomly chosen edge of vertex i to a randomly chosen vertex with the same opinion g_i; or (ii) with probability $1-\phi$, ascribe the opinion g_i to a randomly chosen nearest neighbor j of vertex i. Due to process (i), vertices with similar opinions become connected—agents influence the structure of the network. Due to process (ii), opinions of neighbors change—the network influences agents.

Suppose that the initial state is the classical random graph with vertices in random states. Let the mean degree be greater than 1, so that the giant connected component is present. This system evolves to a final state consisting of a set of connected components, with all vertices in each of the components being in coinciding states—internal consensus. Of course, vertices in different connected components may be in different states. In their simulation, Holme and Newman studied the structure of this final state at various values of the parameter ϕ. In more precise terms, they investigated the resulting

size distribution $P(s)$ of the connected components.

If $\phi=0$, the connections do not move, and the final network coincides with the original one, that is, with a network containing a giant connected component. This giant component is destroyed by process (i) if the probability ϕ is sufficiently high, and at $\phi\sim 1$, the network is segregated into a set of finite connected components, each one of about N/G vertices. It turns out that at the critical value $\phi_c=\phi_c(\langle q\rangle, N/G)$ there is a sharp transition, where the giant connected component disappears. At the critical point, $P(s)$ seems to have a power-law form with a nonstandard exponent. There is a principal difference from the usual emergence of the giant connected component in random networks—in this evolving system, the phase transition is nonequilibrium. In particular, this transition depends on the initial state of the system. We expect that models of this kind will attract much interest in the future; see Zimmermann *et al.* (2004), Caldarelli *et al.* (2006), Ehrhardt *et al.* (2006), Gil and Zanette (2006), Zanette (2007), Gross and Blasius (2008), and Kozma and Barrat (2008). Allahverdyan and Petrosyan (2006) and Biely *et al.* (2007) considered somewhat related problems where spins at vertices and edges interacted with each other.

XIII. SUMMARY AND OUTLOOK

A. Open problems

We indicate a few directions of particular interest among those discussed in this paper. The first one is the synchronization in the Kuramoto model on complex networks, for which there is no solid theory. The second direction is the coevolving networks and interacting systems defined on them (Holme and Newman, 2006; Pacheco *et al.*, 2006). We did not discuss a number of interesting NP optimization problems that were studied using tools of statistical physics but were considered only for classical random graphs. Among them, there were sparse graph error-correcting codes [see Montanari (2005), and references therein], phase transitions in random satisfiability problems (Mézard *et al.*, 2002; Mertens *et al.*, 2003; Achlioptas *et al.*, 2005; Krząkała *et al.*, 2007) and combinatorial auctions (Galla *et al.*, 2006). Note that the coloring graph problem and minimum vertex covers were also not analyzed for complex networks. Finally, we add the difficult but doable problem of finding a replica-symmetry breaking solution for a spin glass on a complex network.

Real-life networks are finite, loopy (clustered), and correlated. Most of them are out of equilibrium. A solid theory of correlation phenomena in complex networks must take into account finite-size effects, loops, degree correlations, and other structural peculiarities. We described two successful analytical approaches to cooperative phenomena in infinite networks. The first was based on the tree ansatz, and the second was the generalization of the Landau theory of phase transitions. What is beyond these approaches? Several first methodical studies aiming at strict accounting for loops were performed recently; see Montanari (2005), Montanari and Rizzo (2005), and Chertkov and Chernyak (2006a, 2006b). The approximations and loop expansions proposed were not applied to complex networks, and is a tool for future work. It is still unknown when and how loops change cooperative phenomena in complex networks. The tree ansatz usually fails in finite networks. In this respect, the problem of a finite-size network is closely related to the problem of loops. It is technically difficult to go beyond intuitive estimates of finite-size effects demonstrated in Sec. III.B.4 and the finite-size scaling conjecture. The strict statistical mechanics theory of finite networks is still not developed.

Despite some interesting results, cooperative models on growing networks are poorly understood. As a rule, it is still impossible to predict the type of critical phenomenon in an interacting system of this kind. The effect of structural correlations in a complex network on collective phenomena is also not well studied.

B. Conclusions

We have reviewed recent progress in critical phenomena in complex networks. In more precise terms, we have considered critical effects in a wide range of cooperative models placed on various networks and network models. We have demonstrated a number of diverse critical effects and phenomena, which greatly differ from those in lattices. It turns out, however, that each of these phenomena in networks, in principle, can be explained in the framework of a unified approach. This unified view has been presented in this paper.

We have shown that, in simple terms, the appearance of critical phenomena is determined by the combination of two factors—the small-world effect and a strong heterogeneity and complex architecture of networks. The compactness of networks leads to Gaussian critical fluctuations, and in this respect the theory of phase transitions in networks is even simpler than in low-dimensional lattices. On the other hand, the complex organization of connections makes these critical phenomena far more rich and strayed from those predicted by the traditional mean-field theories.

It was claimed that "the study of complex networks is still in its infancy" (Newman, 2003a). Now the time has come of age. Nonetheless, we have indicated a wide circle of open problems and challenging issues. We stress that in contrast to the impressive progress in understanding the basic principles and nature of the critical phenomena in networks, progress in the application of these ideas to real-world networks is rather modest. There is much to be done in this direction.

Complex networks are ultimately compact, maximally disordered, and heterogeneous substrates for interacting systems. These network systems are among the fundamental structures of nature. The phenomena and processes in these highly nontraditional systems differ remarkably from those in ordered and disordered lattices and fractals. This is why the study of these intriguing

effects will lead to a new understanding of a wide circle of natural, artificial, and social systems.

ACKNOWLEDGMENTS

We thank M. Alava, A.-L. Barabási, M. Bauer, O. Bénichou, G. Bianconi, M. Boguñá, B. Bollobás, S. Bornholdt, Z. Burda, S. Coulomb, D. Dhar, M. E. Fisher, M. Hase, S. Havlin, B. Kahng, T. Kaski, E. Khajeh, P. L. Krapivsky, F. Krząkała, A. Krzywicki, D. Krioukov, S. N. Majumdar, S. Maslov, D. Mukamel, M. E. J. Newman, J. D. Noh, J. G. Oliveira, M. Ostilli, J. Pacheco, H. Park, R. Pastor-Satorras, M. Peltomaki, A. M. Povolotsky, J. J. Ramasco, S. Redner, O. Riordan, G. J. Rodgers, M. Rosvall, A. N. Samukhin, B. N. Shalaev, K. Sneppen, B. Söderberg, B. Tadić, A. Vespignani, T. Vicsek, B. Waclaw, M. Weigt, L. Zdeborová, and A. Zyuzin for numerous helpful discussions, and conversations on the topic of this work. We particularly thank J. G. Oliveira for numerous comments, and remarks on the manuscript of this article. This work was supported by the POCI program, Projects No. FAT/46241/2002, No. MAT/46176/2003, No. FIS/61665/2004, and No. BIA-BCM/62662/2004, and by the DYSONET program.

REFERENCES

Acebrón, J. A., L. L. Bonilla, C. J. Pérez Vicente, F. Ritort, and R. Spigler, 2005, Rev. Mod. Phys. **77**, 137.
Achlioptas, D., A. Naor, and Y. Peres, 2005, Nature **435**, 759.
Aizenman, M., and J. L. Lebowitz, 1988, J. Phys. A **21**, 3801.
Albert, R., and A.-L. Barabási, 2002, Rev. Mod. Phys. **74**, 47.
Albert, R., H. Jeong, and A.-L. Barabási, 1999, Nature **401**, 130.
Albert, R., H. Jeong, and A.-L. Barabási, 2000, Nature **406**, 378.
Aleksiejuk, A., J. A. Holyst, and D. Stauffer, 2002, Physica A **310**, 260.
Allahverdyan, A. E., and K. G. Petrosyan, 2006, Europhys. Lett. **75**, 908.
Alvarez-Hamelin, J. I., L. Dall'Asta, A. Barrat, and A. Vespignani, 2006, Adv. Neural Inf. Process. Syst. **18**, 41.
Alvarez-Hamelin, J. I., L. Dall'Asta, A. Barrat, and A. Vespignani, 2008, Networks Heterog. Media **3**, 371.
Andrade, J. S., Jr., H. J. Herrmann, R. F. S. Andrade, and L. R. da Silva, 2005, Phys. Rev. Lett. **94**, 018702.
Andrade, R. F. S., and H. J. Herrmann, 2005, Phys. Rev. E **71**, 056131.
Angel, A. G., M. R. Evans, E. Levine, and D. Mukamel, 2005, Phys. Rev. E **72**, 046132.
Angel, A. G., T. Hanney, and M. R. Evans, 2006, Phys. Rev. E **73**, 016105.
Antal, T., P. L. Krapivsky, and S. Redner, 2005, Phys. Rev. E **72**, 036121.
Antoni, M., and S. Ruffo, 1995, Phys. Rev. E **52**, 2361.
Appel, K., and W. Haken, 1977a, Ill. J. Math. **21**, 429.
Appel, K., and W. Haken, 1977b, Ill. J. Math. **21**, 491.
Arenas, A., A. Díaz-Guilera, and R. Guimera, 2001, Phys. Rev. Lett. **86**, 3196.
Arenas A., A. Díaz-Guilera, and C. J. Pérez-Vicente, 2006a, Phys. Rev. Lett. **96**, 114102.
Arenas, A., A. Díaz-Guilera, and C. J. Perez-Vicente, 2006b, Physica D **224**, 27.
Atay, F. M., J. Jost, and A. Wende, 2004, Phys. Rev. Lett. **92**, 144101.
Baillie, C., W. Janke, D. Johnston, and P. Plecháč, 1995, Nucl. Phys. B **450**, 730.
Bakke, J. O. H., A. Hansen, and J. Kertész, 2006, Europhys. Lett. **76**, 717.
Barabási, A.-L., and R. Albert, 1999, Science **286**, 509.
Barabási, A.-L., E. Ravasz, and T. Vicsek, 2001, Physica A **299**, 559.
Barahona, M., and L. Pecora, 2002, Phys. Rev. Lett. **89**, 054101.
Baronchelli, A., L. Dall'Asta, A. Barrat, and V. Loreto, 2007, Phys. Rev. E **76**, 051102.
Barrat, A., and M. Weigt, 2000, Eur. Phys. J. B **13**, 547.
Barthel, W., and A. K. Hartmann, 2004, Phys. Rev. E **70**, 066120.
Barthelemy, M., A. Barrat, R. Pastor-Satorras, and A. Vespignani, 2004, Phys. Rev. Lett. **92**, 178701.
Barthelemy, M., A. Barrat, R. Pastor-Satorras, and A. Vespignani, 2005, J. Theor. Biol. **235**, 275.
Bartolozzi, M., T. Surungan, D. B. Leinweber, and A. G. Williams, 2006, Phys. Rev. B **73**, 224419.
Bauer, M., and D. Bernard, 2002, e-print arXiv:cond-mat/0206150.
Bauer, M., S. Coulomb, and S. N. Dorogovtsev, 2005, Phys. Rev. Lett. **94**, 200602.
Bauer, M., and O. Golinelli, 2001a, Eur. Phys. J. B **24**, 339.
Bauer, M., and O. Golinelli, 2001b, Phys. Rev. Lett. **86**, 2621.
Baxter, R. J., 1982, *Exactly Solved Models in Statistical Mechanics* (Academic, London).
Bedeaux, D., K. E. Shuler, and I. Oppenheim, 1970, J. Stat. Phys. **2**, 1.
ben-Avraham, D., D. B. Considine, P. Meakin, S. Redner, and H. Takayasu, 1990, J. Phys. A **23**, 4297.
ben-Avraham, D., and M. L. Glasser, 2007, J. Phys.: Condens. Matter **19**, 065107.
Bender, E. A., and E. R. Canfield, 1978, J. Comb. Theory, Ser. A **24**, 296.
Ben-Naim, E., and P. L. Krapivsky, 2004, Phys. Rev. E **69**, 050901(R).
Berezinskii, V. L., 1970, Zh. Eksp. Teor. Fiz. **59**, 907 [Sov. Phys. JETP **32**, 493 (1970)].
Berg, J., and M. Lässig, 2002, Phys. Rev. Lett. **89**, 228701.
Bernardo, M., F. Garofalo, and F. Sorrentino, 2007, Int. J. Bifurcation Chaos Appl. Sci. Eng. **17**, 7.
Bethe, H. A., 1935, Proc. R. Soc. London, Ser. A **150**, 552.
Bialas, P., L. Bogacz, B. Burda, and D. Johnston, 2000, Nucl. Phys. B **575**, 599.
Bialas, P., Z. Burda, and D. Johnston, 1997, Nucl. Phys. B **493**, 505.
Bialas, P., Z. Burda, J. Jurkiewicz, and A. Krzywicki, 2003, Phys. Rev. E **67**, 066106.
Bianconi, G., 2002, Phys. Lett. A **303**, 166.
Bianconi, G., and A.-L. Barabási, 2001, Phys. Rev. Lett. **86**, 5632.
Bianconi, G., and A. Capocci, 2003, Phys. Rev. Lett. **90**, 078701.
Bianconi, G., N. Gulbahce, and A. E. Motter, 2008, Phys. Rev. Lett. **100**, 118701.
Bianconi, G., and M. Marsili, 2005, J. Stat. Mech.: Theory Exp. (2005), P06005.

Biely, C., R. Hanel, and S. Thurner, 2007, e-print arXiv:0707.3085.
Binder, K., and A. P. Young, 1986, Rev. Mod. Phys. **58**, 801.
Boccaletti, S., V. Latora, Y. Moreno, M. Chavez, and D.-U. Hwang, 2006, Phys. Rep. **424**, 175.
Bogacz, L., Z. Burda, W. Janke, and B. Waclaw, 2007a, Chaos **17**, 026112.
Bogacz, L., Z. Burda, W. Janke, and B. Waclaw, 2007b, Proc. SPIE **6601**, 66010V.
Boguñá, M., and R. Pastor-Satorras, 2002, Phys. Rev. E **66**, 047104.
Boguñá, M., and R. Pastor-Satorras, 2003, Phys. Rev. E **68**, 036112.
Boguñá, M., R. Pastor-Satorras, and A. Vespignani, 2003a, Phys. Rev. Lett. **90**, 028701.
Boguñá, M., R. Pastor-Satorras, and A. Vespignani, 2003b, Lect. Notes Phys. **625**, 127.
Boguñá, M., R. Pastor-Satorras, and A. Vespignani, 2004, Eur. Phys. J. B **38**, 205.
Boguñá, M., and M. A. Serrano, 2005, Phys. Rev. E **72**, 016106.
Bollobás, B., 1980, Eur. J. Comb. **1**, 311.
Bollobás, B., 1984, in *Graph Theory, and Combinatorics: Proceedings of the Cambridge Combinatorial Conference in Honour of Paul Erdős*, edited by B. Bollobás (Academic, New York), p. 35.
Bollobás, B., and O. Riordan, 2003, in *Handbook of Graphs and Networks*, edited by S. Bornholdt and H. G. Schuster (Wiley-VCH, Weinheim), p. 1.
Bollobás, B., and O. Riordan, 2005, Random Struct. Algorithms **27**, 1.
Bonabeau E., 1995, J. Phys. Soc. Jpn. **64**, 327.
Borgs, C., J. T. Chayes, H. Kesten, and J. Spencer, 2001, Commun. Math. Phys. **224**, 153.
Brandes, U., D. Delling, M. Gaertler, R. Görke, M. Hoefer, Z. Nikoloski, and D. Wagner, 2006, e-print arXiv:physics/0608255.
Braunstein, A., R. Mulet, A. Pagnani, M. Weigt, and R. Zecchina, 2003, Phys. Rev. E **68**, 036702.
Braunstein, A., and R. Zecchina, 2004, J. Stat. Mech.: Theory Exp. (2004), P06007.
Braunstein, L. A., S. V. Buldyrev, R. Cohen, S. Havlin, and H. E. Stanley, 2003, Phys. Rev. Lett. **91**, 168701.
Braunstein L. A., S. V. Buldyrev, S. Sreenivasan, R. Cohen, S. Havlin, and H. E. Stanley, 2004, Lect. Notes Phys. **650**, 127.
Burda, Z., J. D. Correia, and A. Krzywicki, 2001, Phys. Rev. E **64**, 046118.
Burda, Z., D. Johnston, J. Jurkiewicz, M. Kaminski, M. A. Nowak, and G. Papp, 2002, Phys. Rev. E **65**, 026102.
Burda, Z., J. Jurkiewicz, and A. Krzywicki, 2004a, Phys. Rev. E **69**, 026106.
Burda, Z., J. Jurkiewicz, and A. Krzywicki, 2004b, Phys. Rev. E **70**, 026106.
Burda, Z., and A. Krzywicki, 2003, Phys. Rev. E **67**, 046118.
Caldarelli, G., 2007, *Scale-Free Networks: Complex Webs in Nature, and Technology*, Oxford Finance Series (Oxford University Press, Oxford).
Caldarelli, G., A. Capocci, P. De Los Rios, and M. A. Muñoz, 2002, Phys. Rev. Lett. **89**, 258702.
Caldarelli, G., A. Capocci, and D. Garlaschelli, 2006, e-print arXiv:cond-mat/0611201.
Callaway, D. S., J. E. Hopcroft, J. M. Kleinberg, M. E. J. Newman, and S. H. Strogatz, 2001, Phys. Rev. E **64**, 041902.
Callaway, D. S., M. E. J. Newman, S. H. Strogatz, and D. J. Watts, 2000, Phys. Rev. Lett. **85**, 5468.
Carmi, S., R. Cohen, and D. Dolev, 2006, Europhys. Lett. **74**, 1102.
Carmi, S., S. Havlin, S. Kirkpatrick, Y. Shavitt, and E. Shir, 2006, e-print arXiv:cond-mat/0601240.
Carmi, S., S. Havlin, S. Kirkpatrick, Y. Shavitt, and E. Shir, 2007, Proc. Natl. Acad. Sci. U.S.A. **104**, 11150.
Caruso, F., V. Latora, A. Pluchino, A. Rapisarda, and B. Tadic, 2006, Eur. Phys. J. B **50**, 243.
Caruso, F., A. Pluchino, V. Latora, S. Vinciguerra, and A. Rapisarda, 2007, Phys. Rev. E **75**, 055101(R).
Castellani, T., F. Krząkała, and F. Ricci-Tersenghi, 2005, Eur. Phys. J. B **47**, 99.
Castellano, C., V. Loreto, A. Barrat, F. Cecconi, and D. Parisi, 2005, Phys. Rev. E **71**, 066107.
Castellano, C., and R. Pastor-Satorras, 2006a, Phys. Rev. Lett. **96**, 038701.
Castellano, C., and R. Pastor-Satorras, 2006b, J. Stat. Mech.: Theory Exp. (2006), P05001.
Castellano, C., and R. Pastor-Satorras, 2007, Phys. Rev. Lett. **98**, 029802.
Castellano, C., and R. Pastor-Satorras, 2008, Phys. Rev. Lett. **100**, 148701.
Castellano, C., D. Vilone, and A. Vespignani, 2003, Europhys. Lett. **63**, 153.
Catanzaro, M., M. Boguñá, and R. Pastor-Satorras, 2005, Phys. Rev. E **71**, 056104.
Chalupa, J., P. L. Leath, and G. R. Reich, 1979, J. Phys. C **12**, L31.
Chatterjee, A., and P. Sen, 2006, Phys. Rev. E **74**, 036109.
Chavez, M., D.-U. Hwang, A. Amann, H. G. E. Hentschel, and S. Boccaletti, 2005, Phys. Rev. Lett. **94**, 218701.
Chavez, M., D.-U. Hwang, J. Martinerie, and S. Boccaletti, 2006, Phys. Rev. E **74**, 066107.
Chertkov, M., and V. Y. Chernyak, 2006a, J. Stat. Mech.: Theory Exp. (2006), P06009.
Chertkov, M., and V. Y. Chernyak, 2006b, e-print arXiv:cs.NI/0609154.
Chung, F., and L. Lu, 2002, Proc. Natl. Acad. Sci. U.S.A. **99**, 15879.
Chung, F., L. Lu, and V. Vu, 2003, Proc. Natl. Acad. Sci. U.S.A. **100**, 6313.
Chung, F. R. K., 1997, *Spectral Graph Theory* (American Mathematical Society, Providence, RI).
Clauset, A., M. E. J. Newman, and C. Moore, 2004, Phys. Rev. E **70**, 066111.
Cohen, R., D. ben-Avraham, and S. Havlin, 2002, Phys. Rev. E **66**, 036113.
Cohen, R., K. Erez, D. ben-Avraham, and S. Havlin, 2000, Phys. Rev. Lett. **85**, 4626.
Cohen, R., K. Erez, D. ben-Avraham, and S. Havlin, 2001, Phys. Rev. Lett. **86**, 3682.
Cohen, R., S. Havlin, and D. ben-Avraham, 2003a, in *Handbook of Graphs and Networks*, edited by S. Bornholdt and H. G. Schuster (Wiley-VCH, Weinheim), p. 85.
Cohen, R., S. Havlin, and D. ben-Avraham, 2003b, Phys. Rev. Lett. **91**, 247901.
Colizza, V., R. Pastor-Satorras, and A. Vespignani, 2007, Nat. Phys. **3**, 276.
Coolen, A. C. C., N. S. Skantzos, I. P. Castillo, C. J. P. Vicente, J. P. L. Hatchett, B. Wemmenhove, and T. Nikoletopoulos, 2005, J. Phys. A **38**, 8289.
Copelli, M., and P. R. A. Campos, 2007, Eur. Phys. J. B **56**, 273.

Coppersmith, D., D. Gamarnik, M. T. Hajiaghayi, and G. B. Sorkin, 2004, Random Struct. Algorithms **24**, 502.
Costin, O., and R. D. Costin, 1991, J. Stat. Phys. **64**, 193.
Costin, O., R. D. Costin, and C. P. Grünfeld, 1990, J. Stat. Phys. **59**, 1531.
Coulomb, M., and S. Bauer, 2003, Eur. Phys. J. B **35**, 377.
Danila, B., Y. Yu, S. Earl, J. A. Marsh, Z. Toroczkai, and K. E. Bassler, 2006, Phys. Rev. E **74**, 046114.
de Arcangelis, L., and H. Herrmann, 2002, Physica A **308**, 545.
Denker, M., M. Timme, M. Diesmann, F. Wolf, and T. Geisel, 2004, Phys. Rev. Lett. **92**, 074103.
Derényi, I., I. Farkas, G. Palla, and T. Vicsek, 2004, Physica A **334**, 583.
Derényi, I., G. Palla, and T. Vicsek, 2005, Phys. Rev. Lett. **94**, 160202.
Derrida, B., 1981, Phys. Rev. B **24**, 2613.
Dezsõ, Z., and A.-L. Barabási, 2002, Phys. Rev. E **65**, 055103.
Domb, C., 1960, Adv. Phys. **9**, 245.
Dorogovtsev, S. N., 2003, Phys. Rev. E **67**, 045102(R).
Dorogovtsev, S. N., A. V. Goltsev, and J. F. F. Mendes, 2002a, Phys. Rev. E **65**, 066122.
Dorogovtsev, S. N., A. V. Goltsev, and J. F. F. Mendes, 2002b, Phys. Rev. E **66**, 016104.
Dorogovtsev, S. N., A. V. Goltsev, and J. F. F. Mendes, 2004, Eur. Phys. J. B **38**, 177.
Dorogovtsev, S. N., A. V. Goltsev, and J. F. F. Mendes, 2005, Phys. Rev. E **72**, 066130.
Dorogovtsev, S. N., A. V. Goltsev, and J. F. F. Mendes, 2006a, Phys. Rev. Lett. **96**, 040601.
Dorogovtsev, S. N., A. V. Goltsev, and J. F. F. Mendes, 2006b, Physica D **224**, 7.
Dorogovtsev, S. N., A. V. Goltsev, and J. F. F. Mendes, 2007, e-print arXiv:0705.0010.
Dorogovtsev, S. N., A. V. Goltsev, J. F. F. Mendes, and S. N. Samukhin, 2003, Phys. Rev. E **68**, 046109.
Dorogovtsev, S. N., and J. F. F. Mendes, 2001, Phys. Rev. E **63**, 056125.
Dorogovtsev, S. N., and J. F. F. Mendes, 2002, Adv. Phys. **51**, 1079.
Dorogovtsev, S. N., and J. F. F. Mendes, 2003, *Evolution of Networks: From Biological Nets to the Internet and WWW* (Oxford University Press, Oxford).
Dorogovtsev, S. N., J. F. F. Mendes, A. M. Povolotsky, and A. N. Samukhin, 2005, Phys. Rev. Lett. **95**, 195701.
Dorogovtsev, S. N., J. F. F. Mendes, and A. N. Samukhin, 2000, Phys. Rev. Lett. **85**, 4633.
Dorogovtsev, S. N., J. F. F. Mendes, and A. N. Samukhin, 2001a, Phys. Rev. E **64**, 025101(R).
Dorogovtsev, S. N., J. F. F. Mendes, and A. N. Samukhin, 2001b, Phys. Rev. E **64**, 066110.
Dorogovtsev, S. N., J. F. F. Mendes, and A. N. Samukhin, 2001c, Phys. Rev. E **63**, 062101.
Dorogovtsev, S. N., J. F. F. Mendes, and A. N. Samukhin, 2003a, Nucl. Phys. B **653**, 307.
Dorogovtsev, S. N., J. F. F. Mendes, and A. N. Samukhin, 2003b, Nucl. Phys. B **666**, 396.
Doye, J. P. K., and C. P. Massen, 2005, Phys. Rev. E **71**, 016128.
Durrett, R., 2006, *Random Graph Dynamics* (Cambridge University Press, Cambridge).
Echenique, P., J. Gómez-Gardeñes, and Y. Moreno, 2005, Europhys. Lett. **71**, 325.
Eggarter, T. P., 1974, Phys. Rev. B **9**, 2989.
Ehrhardt, G. C. M. A., and M. Marsili, 2005, J. Stat. Mech.: Theory Exp. (2005), P02006.
Ehrhardt, G. C. M. A., M. Marsili, and F. Vega-Redondo, 2006, Phys. Rev. E **74**, 036106.
Erdős, P., and A. Rényi, 1959, Publ. Math. (Debrecen) **6**, 290.
Evans, M. R., and T. Hanney, 2005, J. Phys. A **38**, R195.
Falk, H., 1975, Phys. Rev. B **12**, 5184.
Farkas, I., I. Derenyi, G. Palla, and T. Vicsek, 2004, Lect. Notes Phys. **650**, 163.
Fernholz, D., and V. Ramachandran, 2004, UTCS Technical Report TR04-13 (unpublished).
Fortuin, C. M., and P. W. Kasteleyn, 1972, Physica (Amsterdam) **57**, 536.
Freeman, W. T., E. C. Pasztor, and O. T. Carmichael, 2000, Int. J. Comput. Vis. **40**, 25.
Frey, B. J., 1998, *Graphical Models for Machine Learning and Digital Communication* (MIT, Cambridge).
Frieze, A. M., 1990, Discrete Math. **81**, 171.
Fronczak, A., and P. Fronczak, 2007, e-print arXiv:0709.2231.
Gade, P. M., and C.-K. Hu, 2000, Phys. Rev. E **62**, 6409.
Galla, T., M. Leone, M. Marsili, M. Sellitto, M. Weigt, and R. Zecchina, 2006, Phys. Rev. Lett. **97**, 128701.
Gallos, L. K., and P. Argyrakis, 2004, Phys. Rev. Lett. **92**, 138301.
Gallos, L. K., R. Cohen, P. Argyrakis, A. Bunde, and S. Havlin, 2005, Phys. Rev. Lett. **94**, 188701.
Gallos, L. K., F. Liljeros, P. Argyrakis, A. Bunde, and S. Havlin, 2007, Phys. Rev. E **75**, 045104(R).
Gallos, L. K., C. Song, S. Havlin, and H. A. Makse, 2007, Proc. Natl. Acad. Sci. U.S.A. **104**, 7746.
Garey, M. A., and D. S. Johnson, 1979, *Computers and Intractability* (Freeman, New York).
Gil, S., and D. H. Zanette, 2006, Phys. Lett. A **356**, 89.
Gilbert, E. N., 1959, Ann. Math. Stat. **30**, 1141.
Gitterman, M., 2000, J. Phys. A **33**, 8373.
Giuraniuc, C. V., J. P. L. Hatchett, J. O. Indekeu, M. Leone, I. Pérez Castillo, B. Van Schaęybroeck, and C. Vanderzande, 2005, Phys. Rev. Lett. **95**, 098701.
Giuraniuc, C. V., J. P. L. Hatchett, J. O. Indekeu, M. Leone, I. Perez Castillo, B. Van Schaeybroeck, and C. Vanderzande, 2006, Phys. Rev. E **74**, 036108.
Goh, K.-I., B. Kahng, and D. Kim, 2001, Phys. Rev. Lett. **87**, 278701.
Goh, K.-I., D.-S. Lee, B. Kahng, and D. Kim, 2003, Phys. Rev. Lett. **91**, 148701.
Goh, K.-I., D.-S. Lee, B. Kahng, and D. Kim, 2005, Physica A **346**, 011665.
Goh, K.-I., G. Salvi, B. Kahng, and D. Kim, 2006, Phys. Rev. Lett. **96**, 018701.
Goltsev, A. V., S. N. Dorogovtsev, and J. F. F. Mendes, 2003, Phys. Rev. E **67**, 026123.
Goltsev, A. V., S. N. Dorogovtsev, and J. F. F. Mendes, 2006, Phys. Rev. E **73**, 056101.
Gómez-Gardeñes, J., Y. Moreno, and A. Arenas, 2007a, Phys. Rev. Lett. **98**, 034101.
Gómez-Gardeñes, J., Y. Moreno, and A. Arenas, 2007b, Phys. Rev. E **75**, 066106.
Gourley, S., and N. F. Johnson, 2006, Physica A **363**, 82.
Grassberger P., 1983, Math. Biosci. **63**, 157.
Grassberger, P., and A. de la Torre, 1979, Ann. Phys. (N.Y.) **122**, 373.
Grinstein, G., and R. Linsker, 2005, Proc. Natl. Acad. Sci. U.S.A. **102**, 9948.
Gross, T., and B. Blasius, 2008, J. R. Soc., Interface **5**, 259.

Guardiola, X., A. Díaz-Guilera, M. Llas, and C. J. Pérez, 2000, Phys. Rev. E **62**, 5565.
Guimerà, R., A. Díaz-Guilera, F. Vega-Redondo, A. Cabrales, and A. Arenas, 2002, Phys. Rev. Lett. **89**, 248701.
Guimerà, R., M. Sales-Pardo, and L. A. N. Amaral, 2004, Phys. Rev. E **70**, 025101.
Ha, M., H. Hong, and H. Park, 2007, Phys. Rev. Lett. **98**, 029801.
Häggström O., 2002, Physica A **310**, 275.
Harris, A. B., 1975, Phys. Rev. B **12**, 203.
Harris, T. E., 1974, Ann. Probab. **2**, 969.
Hartmann, A. K., and M. Weigt, 2005, *Phase Transitions in Combinatorial Optimization Problems: Basics, Algorithms and Statistical Mechanics* (Wiley-VCH, Berlin).
Hastings, M. B., 2003, Phys. Rev. Lett. **91**, 098701.
Hastings, M. B., 2006, Phys. Rev. Lett. **96**, 148701.
Helbing, D., J. Siegmeier, and S. Lämmer, 2007, Networks Heterog. Media **2**, 193.
Herrero, C. P., 2002, Phys. Rev. E **65**, 066110.
Herrero, C. P., 2004, Phys. Rev. E **69**, 067109.
Hinczewski, M., and A. N. Berker, 2006, Phys. Rev. E **73**, 066126.
Hinrichsen, H., 2000, Adv. Phys. **49**, 815.
Holme, P., F. Liljeros, C. R. Edling, and B. J. Kim, 2003, Phys. Rev. E **68**, 056107.
Holme, P., and M. E. J. Newman, 2006, Phys. Rev. E **74**, 056108.
Hong, H., H. Chaté, H. Park, and L.-H. Tang, 2007, Phys. Rev. Lett. **99**, 184101.
Hong, H., M. Y. Choi, and B. J. Kim, 2002, Phys. Rev. E **65**, 026139.
Hong, H., M. Ha, and H. Park, 2007, Phys. Rev. Lett. **98**, 258701.
Hong, H., B. J. Kim, and M. Y. Choi, 2002, Phys. Rev. E **66**, 018101.
Hong, H., B. J. Kim, M. Y. Choi, and H. Park, 2004, Phys. Rev. E **69**, 067105.
Hong, H., H. Park, and M. Y. Choi, 2004, Phys. Rev. E **70**, 045204(R).
Hong, H., H. Park, and M. Y. Choi, 2005, Phys. Rev. E **72**, 036217.
Hong, H., H. Park, and L.-H. Tang, 2007, Phys. Rev. E **76**, 066104.
Huang, L., K. Park, Y.-C. Lai, L. Yang, and K. Yang, 2006, Phys. Rev. Lett. **97**, 164101.
Ichinomiya, T., 2004, Phys. Rev. E **70**, 026116.
Ichinomiya, T., 2005, Phys. Rev. E **72**, 016109.
Iglói, F., and L. Turban, 2002, Phys. Rev. E **66**, 036140.
Ihler, A. T., J. W. Fischer, and A. S. Willsky, 2005, J. Mach. Learn. Res. **6**, 905.
Janson, S., 2007, e-print arXiv:0708.4404.
Jeong, D., H. Hong, B. J. Kim, and M. Y. Choi, 2003, Phys. Rev. E **68**, 027101.
Johnston, D. A., and P. Plecháč, 1998, J. Phys. A **31**, 475.
Jost, J., and M. P. Joy, 2001, Phys. Rev. E **65**, 016201.
Jung, S., S. Kim, and B. Kahng, 2002, Phys. Rev. E **65**, 056101.
Kalapala, V., and C. Moore, 2002, http://www.cs.unm.edu/~treport/tr/02-08/maxcut.ps.gz
Kalisky, T., and R. Cohen, 2006, Phys. Rev. E **73**, 035101.
Kappen, H., 2002, in *Modelling Biomedical Signals*, edited by G. Nardulli and S. Stramaglia (World Scientific, Singapore), pp. 3–27.
Karsai, M., J.-C. A. d'Auriac, and F. Iglói, 2007, Phys. Rev. E **76**, 041107.
Karsai, M., R. Juhász, and F. Iglói, 2006, Phys. Rev. E **73**, 036116.
Kasteleyn, P. W., and C. M. Fortuin, 1969, J. Phys. Soc. Jpn. Suppl. **26**, 11.
Kenah, E., and J. Robins, 2007, Phys. Rev. E **76**, 036113.
Khajeh, E., S. N. Dorogovtsev, and J. F. F. Mendes, 2007, Phys. Rev. E **75**, 041112.
Kikuchi, R., 1951, Phys. Rev. **81**, 988.
Kim, B. J., 2004, Phys. Rev. E **69**, 045101.
Kim, B. J., H. Hong, P. Holme, G. S Jeon, P. Minnhagen, and M. Y. Choi, 2001, Phys. Rev. E **64**, 056135.
Kim, D.-H., and A. E. Motter, 2007, Phys. Rev. Lett. **98**, 248701.
Kim, D.-H., G. J. Rodgers, B. Kahng, and D. Kim, 2005, Phys. Rev. E **71**, 056115.
Kim, J., P. L. Krapivsky, B. Kahng, and S. Redner, 2002, Phys. Rev. E **66**, 055101.
Kinouchi, O., and M. Copelli, 2006, Nat. Phys. **2**, 348.
Kirkpatrick, S., 2005, http://www.cs.huji.ac.il/~kirk/Jellyfish_Dimes.ppt
Kleinberg, J., 1999, Cornell Computer Science Technical Report 99–1776 (unpublished).
Kleinberg J., 2000, Nature **406**, 845.
Klemm, K., V. M. Eguíluz, R. Toral, and M. San Miguel, 2003, Phys. Rev. E **67**, 026120.
Kori, H., and A. S. Mikhailov, 2004, Phys. Rev. Lett. **93**, 254101.
Kori, H., and A. S. Mikhailov, 2006, Phys. Rev. E **74**, 066115.
Kosterlitz, J. M., and D. J. Thouless, 1973, J. Phys. C **6**, 1181.
Kozma, B., and A. Barrat, 2007, Phys. Rev. E **77**, 016102.
Kozma, B., M. B. Hastings, and G. Korniss, 2004, Phys. Rev. Lett. **92**, 108701.
Krapivsky, P. L., 1992, Phys. Rev. A **45**, 1067.
Krapivsky, P. L., and B. Derrida, 2004, Physica A **340**, 714.
Krapivsky, P. L., and S. Redner, 2002, J. Phys. A **35**, 9517.
Krapivsky, P. L., S. Redner, and F. Leyvraz, 2000, Phys. Rev. Lett. **85**, 4629.
Krivelevich, M., and B. Sudakov, 2003, Combinatorics, Probab. Comput. **12**, 61.
Krząkała, F., A. Montanari, F. Ricci-Tersenghi, G. Semerjian, and L. Zdeborova, 2007, Proc. Natl. Acad. Sci. U.S.A. **104**, 10318.
Krząkała, F., A. Pagnani, and M. Weigt, 2004, Phys. Rev. E **70**, 046705.
Kulkarni, R. V., E. Almaas, and D. Stroud, 1999, Phys. Lett. A **263**, 341.
Kumpula, J. M., J. Saramaki, K. Kaski, and J. Kertesz, 2007, Eur. Phys. J. B **56**, 41.
Kuramoto, Y., 1984, *Chemical Oscillations, Waves and Turbulence* (Springer, New York).
Kwon, O., and H.-T. Moon, 2002, Phys. Lett. A **298**, 319.
Lago-Fernández, L. F., R. Huerta, F. Corbacho, and J. A. Sigüenza, 2000, Phys. Rev. Lett. **84**, 2758.
Lahtinen, J., J. Kertész, and K. Kaski, 2005, Physica A **349**, 535.
Lancaster, D., 2002, J. Phys. A **35**, 1179.
Lee, D.-S., 2005, Phys. Rev. E **72**, 026208.
Lee, D.-S., K.-I. Goh, B. Kahng, and D. Kim, 2004a, Physica A **338**, 84.
Lee, D.-S., K.-I. Goh, B. Kahng, and D. Kim, 2004b, J. Korean Phys. Soc. **44**, 633.
Lee, D.-S., K.-I. Goh, B. Kahng, and D. Kim, 2004c, Nucl.

Phys. B **696**, 351.
Lee, E. J., K.-I. Goh, B. Kahng, and D. Kim, 2005, Phys. Rev. E **71**, 056108.
Lee, J.-S., K.-I. Goh, B. Kahng, and D. Kim, 2006, Eur. Phys. J. B **49**, 231.
Lee, K. E., B. H. Hong, and J. W. Lee, 2005, e-print arXiv:cond-mat/0510067.
Leland, W. E., M. S. Taqqu, W. Willinger, and D. W. Wilson, 1994, IEEE/ACM Trans. Netw. **2**, 1.
Leone, M., A. Vázquez, A. Vespignani, and R. Zecchina, 2002, Eur. Phys. J. B **28**, 191.
Li, G., L. A. Braunstein, S. V. Buldyrev, S. Havlin, and H. E. Stanley, 2007, Phys. Rev. E **75**, 045103.
Liers, F., M. Palassini, A. K. Hartmann, and M. Jünger, 2003, Phys. Rev. B **68**, 094406.
Lima, F. W. S., and D. Stauffer, 2006, Physica A **359**, 423.
Lind, P. G., J. A. C. Gallas, and H. J. Herrmann, 2004, Phys. Rev. E **70**, 056207.
Liu, Z., W. Ma, H. Zhang, Y. Sun, and P. M. Hui, 2006, Physica A **370**, 843.
Lopes, J. V., Y. G. Pogorelov, J. M. B. L. dos Santos, and R. Toral, 2004, Phys. Rev. E **70**, 026112.
López, E., R. Parshani, R. Cohen, S. Carmi, and S. Havlin, 2007, Phys. Rev. Lett. **99**, 188701.
Lübeck, S., and H.-K. Janssen, 2005, Phys. Rev. E **72**, 016119.
Luczak, T., 1991, Combinatorica **11**, 45.
Luijten, E., and H. W. J. Blöte, 1997, Phys. Rev. B **56**, 8945.
Lyons, R., 1989, Commun. Math. Phys. **125**, 337.
Maslov, S., and K. Sneppen, 2002, Science **296**, 910.
Masuda, N., K.-I. Goh, and B. Kahng, 2005, Phys. Rev. E **72**, 066106.
Matsuda, H., 1974, Prog. Theor. Phys. **51**, 1053.
May, R. M., and A. L. Lloyd, 2001, Phys. Rev. E **64**, 066112.
McEliece, R. J., D. J. C. MacKay, and J. F. Cheng, 1998, IEEE J. Sel. Areas Commun. **16**, 140.
McGraw, P., and M. Menzinger, 2007, Phys. Rev. E **75**, 027104.
Medvedyeva, K., P. Holme, P. Minnhagen, and B. J. Kim, 2003, Phys. Rev. E **67**, 036118.
Melin, R., J. C. Angles d'Auriac, P. Chandra, and B. Doucot, 1996, J. Phys. A **29**, 5773.
Mertens, S., M. Mézard, and R. Zecchina, 2003, Random Struct. Algorithms **28**, 340.
Mézard, M., T. Mora, and R. Zecchina, 2005, Phys. Rev. Lett. **94**, 197205.
Mézard, M., and G. Parisi, 2001, Eur. Phys. J. B **20**, 217.
Mézard, M., G. Parisi, and M. A. Virasoro, 1987, *Spin Glass Theory and Beyond* (World Scientific, Singapore).
Mézard, M., G. Parisi, and R. Zecchina, 2002, Science **297**, 812.
Mézard, M., and Tarzia, 2007, e-print arXiv:0707.0189.
Mézard, M., and R. Zecchina, 2002, Phys. Rev. E **66**, 056126.
Miller, J. C., 2007, Phys. Rev. E **76**, 010101(R).
Molloy, M., and B. A. Reed, 1995, Random Struct. Algorithms **6**, 161.
Molloy, M., and B. A. Reed, 1998, Combinatorics, Probab. Comput. **7**, 295.
Montanari, A., 2005, e-print arXiv:cond-mat/0512296.
Montanari, A., and T. Rizzo, 2005, J. Stat. Mech.: Theory Exp. (2005), P10011.
Mooij, J. M., and H. J. Kappen, 2005, J. Stat. Mech.: Theory Exp. (2005), P11012.
Moore, C., and M. E. J. Newman, 2000a, Phys. Rev. E **61**, 5678.
Moore, C., and M. E. J. Newman, 2000b, Phys. Rev. E **62**, 7059.
Moreno, Y., and A. F. Pacheco, 2004, Europhys. Lett. **68**, 603.
Moreno, Y., R. Pastor-Satorras, A. Vázquez, and A. Vespignani, 2003, Europhys. Lett. **62**, 292.
Moreno, Y., R. Pastor-Satorras, and A. Vespignani, 2002, Eur. Phys. J. B **26**, 521.
Moreno, Y., and A. Vazquez, 2002, Europhys. Lett. **57**, 765.
Moreno, Y., and A. Vázquez, 2003, Eur. Phys. J. B **31**, 265.
Moreno, Y., M. Vazquez-Prada, and A. F. Pacheco, 2004, Physica A **343**, 279.
Motter, A. E., 2004, Phys. Rev. Lett. **93**, 098701.
Motter, A. E., 2007, New J. Phys. **9**, 182.
Motter, A. E., and Y.-C. Lai, 2002, Phys. Rev. E **66**, 065102.
Motter, A. E., C. Zhou, and J. Kurths, 2005a, Phys. Rev. E **71**, 016116.
Motter, A. E., C. Zhou, and J. Kurths, 2005b, Europhys. Lett. **69**, 334.
Motter, A. E., C. Zhou, and J. Kurths, 2005c, in *Science of Complex Networks: From Biology to the Internet and WWW*, edited by J. F. F Mendes *et al.*, AIP Conf. Proc. No. 776 (AIP, Melville, NY), p. 201.
Mukamel, D., 1974, Phys. Lett. **50A**, 339.
Mulet, R., A. Pagnani, M. Weigt, and R. Zecchina, 2002, Phys. Rev. Lett. **89**, 268701.
Muller-Hartmann, E., and J. Zittartz, 1974, Phys. Rev. Lett. **33**, 893.
Nâsell, I., 2002, Math. Biosci. **179**, 1.
Newman, M. E. J., 2000, J. Stat. Phys. **101**, 819.
Newman, M. E. J., 2002a, Phys. Rev. E **66**, 016128.
Newman, M. E. J., 2002b, Phys. Rev. Lett. **89**, 208701.
Newman, M. E. J., 2003a, SIAM Rev. **45**, 167.
Newman, M. E. J., 2003b, Phys. Rev. E **68**, 026121.
Newman, M. E. J., 2003c, in *Handbook of Graphs and Networks: From the Genome to the Internet*, edited by S. Bornholdt and H. G. Schuster (Wiley-VCH, Berlin), p. 35.
Newman, M. E. J., 2003d, Phys. Rev. E **67**, 026126.
Newman, M. E. J., 2007, Phys. Rev. E **76**, 045101.
Newman, M. E. J., and M. Girvan, 2004, Phys. Rev. E **69**, 026113.
Newman, M. E. J., I. Jensen, and R. M. Ziff, 2002, Phys. Rev. E **65**, 021904.
Newman, M. E. J., S. H. Strogatz, and D. J. Watts, 2001, Phys. Rev. E **64**, 026118.
Newman, M. E. J., and D. J. Watts, 1999a, Phys. Rev. E **60**, 7332.
Newman, M. E. J., and D. J. Watts, 1999b, Phys. Lett. A **263**, 341.
Nikoletopoulos, T., A. C. C. Coolen, I. Pérez Castillo, N. S. Skantzos, J. P. L. Hatchett, and B. Wemmenhove, 2004, J. Phys. A **37**, 6455.
Nishikawa, T., and A. E. Motter, 2006a, Phys. Rev. E **73**, 065106.
Nishikawa, T., and A. E. Motter, 2006b, Physica D **224**, 77.
Nishikawa, T., A. E. Motter, Y.-C. Lai, and F. C. Hoppensteadt, 2003, Phys. Rev. Lett. **91**, 014101.
Noh, J. D., 2005, Phys. Rev. E **72**, 056123.
Noh, J. D., 2007, Phys. Rev. E **76**, 026116.
Noh, J. D., G. M. Shim, and H. Lee, 2005, Phys. Rev. Lett. **94**, 198701.
Oh, E., D.-S. Lee, B. Kahng, and D. Kim, 2007, Phys. Rev. E **75**, 011104.
Oh, E., K. Rho, H. Hong, and B. Kahng, 2005, Phys. Rev. E **72**, 047101.
Ohira, T., and R. Sawatari, 1998, Phys. Rev. E **58**, 193.
Ostilli, M., 2006a, J. Stat. Mech.: Theory Exp. (2006), P10004.

Ostilli, M., 2006b, J. Stat. Mech.: Theory Exp. (2006), P10005.
Ozana M., 2001, Europhys. Lett. **55**, 762.
Pacheco, J. M., A. Traulsen, and M. A. Nowak, 2006, Phys. Rev. Lett. **97**, 258103.
Pagnani, A., G. Parisi, and M. Ratieville, 2003, Phys. Rev. E **67**, 026116.
Palla, G., I. Derényi, I. Farkas, and T. Vicsek, 2004, Phys. Rev. E **69**, 046117.
Palla, G., I. Derényi, and T. Vicsek, 2007, J. Stat. Phys. **128**, 219.
Parisi, G., and T. Rizzo, 2006, e-print arXiv:cond-mat/0609777.
Parisi, G., and F. Slanina, 2006, J. Stat. Mech.: Theory Exp. (2006), L003.
Park, J., and M. E. J. Newman, 2004a, Phys. Rev. E **70**, 066146.
Park, J., and M. E. J. Newman, 2004b, Phys. Rev. E **70**, 066117.
Pastor-Satorras, R., and A. Vespignani, 2001, Phys. Rev. Lett. **86**, 3200.
Pastor-Satorras, R., and A. Vespignani, 2002a, Phys. Rev. E **65**, 035108.
Pastor-Satorras, R., and A. Vespignani, 2002b, Phys. Rev. E **65**, 036104.
Pastor-Satorras, R., and A. Vespignani, 2003, in *Handbook of Graphs and Networks: From the Genome to the Internet*, edited by S. Bornholdt and H. G. Schuster (Wiley-VCH, Berlin), p. 111.
Pastor-Satorras, R., and A. Vespignani, 2004, *Evolution and Structure of the Internet: A Statistical Physics Approach* (Cambridge University Press, Cambridge).
Pearl, J., 1988, *Probabilistic Reasoning in Intelligent Systems: Networks of Plausible Inference* (Morgan Kaufmann, San Francisco).
Pecora, L. M., and T. L. Carroll, 1998, Phys. Rev. Lett. **80**, 2109.
Peierls, R., 1936, Proc. Cambridge Philos. Soc. **32**, 477.
Pękalski, A., 2001, Phys. Rev. E **64**, 057104.
Petermann, T., and P. De Los Rios, 2004, Phys. Rev. E **69**, 066116.
Pikovsky, A. S., M. G. Rosenblum, and J. Kurths, 2001, *Synchronization: A Universal Concept in Nonlinear Sciences* (Cambridge University Press, Cambridge).
Pittel, B., J. Spencer, and N. Wormald, 1996, J. Comb. Theory, Ser. B **67**, 111.
Pretti, M., and A. Pelizzola, 2003, J. Phys. A **36**, 11201.
Radicchi, F., and H. Meyer-Ortmanns, 2006, Phys. Rev. E **73**, 036218.
Reichardt, J., and S. Bornholdt, 2004, Phys. Rev. Lett. **93**, 218701.
Reichardt, J., and S. Bornholdt, 2006, Phys. Rev. E **74**, 016110.
Restrepo, J. G., E. Ott, and B. R. Hunt, 2005, Phys. Rev. E **71**, 036151.
Rizzo, T., B. Wemmenhove, and H. J. Kappen, 2007, Phys. Rev. E **76**, 011102.
Rosvall, M., P. Minnhagen, and K. Sneppen, 2004, Phys. Rev. E **71**, 066111.
Roy, S., and S. M. Bhattacharjee, 2006, Phys. Lett. A **352**, 13.
Rozenfeld, H. D., and D. ben-Avraham, 2007, Phys. Rev. E **75**, 061102.
Sánchez, A. D., J. M. López, and M. A. Rodríguez, 2002, Phys. Rev. Lett. **88**, 048701.
Scalettar, R. T., 1991, Physica A **170**, 282.
Schwartz, J. M., A. J. Liu, and L. Q. Chayes, 2006, Europhys. Lett. **73**, 560566.
Schwartz, N., R. Cohen, D. ben-Avraham, A.-L. Barabási, and S. Havlin, 2002, Phys. Rev. E **66**, 015104.
Serrano, M. A., and M. Boguna, 2006a, Phys. Rev. Lett. **97**, 088701.
Serrano, M. A., and M. Boguna, 2006b, Phys. Rev. E **74**, 056114.
Serrano, M. A., and M. Boguna, 2006c, Phys. Rev. E **74**, 056115.
Serrano, M. A., and P. De Los Rios, 2007, Phys. Rev. E **76**, 056121.
Seyed-allaei, H., G. Bianconi, and M. Marsili, 2006, Phys. Rev. E **73**, 046113.
Skantzos, N. S., I. P. Castillo, and J. P. L. Hatchett, 2005, Phys. Rev. E **72**, 066127.
Skantzos, N. S., and J. P. L. Hatchett, 2007, Physica A **381**, 202.
Soderberg, B., 2002, Phys. Rev. E **66**, 066121.
Solé, R. V., and S. Valverde, 2001, Physica A **289**, 595.
Solomonoff, R., and A. Rapoport, 1951, Bull. Math. Biophys. **13**, 107.
Song, C., L. K. Gallos, S. Havlin, and H. A. Makse, 2007, J. Stat. Mech.: Theory Exp. (2007), P03006.
Song, C., S. Havlin, and H. A. Makse, 2005, Nature (London) **433**, 392.
Song, C., S. Havlin, and H. A. Makse, 2006, Nat. Phys. **2**, 275.
Sood, V., and S. Redner, 2005, Phys. Rev. Lett. **94**, 178701.
Stosic, T., B. D. Stosic, and I. P. Fittipaldi, 1998, J. Magn. Magn. Mater. **177**, 185.
Strauss, D., 1986, SIAM Rev. **28**, 513.
Strogatz, S. H., 2000, Physica D **143**, 1.
Strogatz, S. H., 2003, *Sync: The Emerging Science of Spontaneous Order* (Hyperion, New York).
Suchecki, K., V. M. Eguíluz, and M. San Miguel, 2005a, Europhys. Lett. **69**, 228.
Suchecki, K., V. M. Eguíluz, and M. San Miguel, 2005b, Phys. Rev. E **72**, 036132.
Svenson, P., 2001, Phys. Rev. E **64**, 036122.
Svenson, P., and M. G. Nordahl, 1999, Phys. Rev. E **59**, 3983.
Szabó, G., M. J. Alava, and J. Kertész, 2003, Phys. Rev. E **67**, 056102.
Tadić, B., G. J. Rodgers, and S. Thurner, 2006, Int. J. Bifurcation Chaos Appl. Sci. Eng. **17**, 2363.
Tadić, B., and S. Thurner, 2004, Physica A **332**, 566.
Tadić, B., S. Thurner, and G. J. Rodgers, 2004, Phys. Rev. E **69**, 036102.
Tanaka, H.-A., A. J. Lichtenberg, and S. Oishi, 1997, Phys. Rev. Lett. **78**, 2104.
Tanaka, K., 2002, J. Phys. A **35**, R81.
Tang, M., Z. Liu, and J. Zhou, 2006, Phys. Rev. E **74**, 036101.
Thouless, D. J., 1986, Phys. Rev. Lett. **56**, 1082.
Thouless, D. J., P. W. Anderson, and R. G. Palmer, 1977, Philos. Mag. **35**, 593.
Timme, M., 2006, Europhys. Lett. **76**, 367.
Timme, M., F. Wolf, and T. Geisel, 2004, Phys. Rev. Lett. **92**, 074101.
Toroczkai, Z., and K. E. Bassler, 2004, Nature **428**, 716.
Vázquez, A., 2006a, Phys. Rev. Lett. **96**, 038702.
Vázquez, A., 2006b, Phys. Rev. E **74**, 056101.
Vázquez, A., and Y. Moreno, 2003, Phys. Rev. E **67**, 015101(R).
Vázquez, A., and M. Weigt, 2003, Phys. Rev. E **67**, 027101.
Viana, L., and A. J. Bray, 1985, J. Phys. C **18**, 3037.
Vilone, D., and C. Castellano, 2004, Phys. Rev. E **69**, 016109.
von Heimburg, J., and H. Thomas, 1974, J. Phys. C **7**, 3433.
Waclaw, B., L. Bogacz, Z. Burda, and W. Janke, 2007, Phys. Rev. E **76**, 046114.

Waclaw, B., and I. M. Sokolov, 2007, Phys. Rev. E **75**, 056114.
Walsh T., 1999, in *Proceedings of the 16th International Joint Conference on Artificial Intelligence*, edited by T. Dean (Morgan Kaufmann, San Francisco), p. 1172.
Wang, W.-X., B.-H. Wang, C.-Y. Yin, Y.-B. Xie, and T. Zhou, 2006, Phys. Rev. E **73**, 026111.
Wang, X. F., and G. Chen, 2002, Int. J. Bifurcation Chaos Appl. Sci. Eng. **12**, 187.
Warren, C. P., L. M. Sander, and I. M. Sokolov, 2003, Physica A **325**, 1.
Watts, D. J., 1999, *Small Worlds: The Dynamics of Networks between Order and Randomness* (Princeton University Press, Princeton, NJ).
Watts, D. J., 2002, Proc. Natl. Acad. Sci. U.S.A. **99**, 5766.
Watts, D. J., and S. H. Strogatz, 1998, Nature **393**, 440.
Weigt, M., and A. K. Hartmann, 2000, Phys. Rev. Lett. **84**, 6118.
Weigt, M., and A. K. Hartmann, 2001, Phys. Rev. E **63**, 056127.
Weigt, M., and H. Zhou, 2006, Phys. Rev. E **74**, 046110.
Willinger, W., R. Govindan, S. Jamin, V. Paxson, and S. Shenker, 2002, Proc. Natl. Acad. Sci. U.S.A. **99**, 2573.
Wu, A.-C., X.-J. Xu, and Y.-H. Wang, 2007, Phys. Rev. E **75**, 032901.
Wu, F., and B. A. Huberman, 2004, e-print arXiv:cond-mat/0407252.
Wu, F. Y., 1982, Rev. Mod. Phys. **54**, 235.
Wu, Z., C. Lagorio, L. A. Braunstein, R. Cohen, S. Havlin, and H. E. Stanley, 2007, Phys. Rev. E **75**, 066110.
Yamada, H., 2002, Prog. Theor. Phys. **108**, 13.
Yedidia, J. S., W. T. Freeman, and Y. Weiss, 2001, in *Advances in Neural Information Processing Systems*, edited by T. K. Leen, T. G. Dietterich, and V. Tresp (MIT, Cambridge), Vol. 13, pp. 689–695.
Zanette, D. H., 2007, e-print arXiv:0707.1249.
Zdeborová, L., and F. Krząkała, 2007, Phys. Rev. E **76**, 031131.
Zhang, H., Z. Liu, M. Tang, and P. M. Hui, 2007, Phys. Lett. A **364**, 177.
Zhang, X., and M. A. Novotny, 2006, Braz. J. Phys. **36**, 664.
Zhou, C., A. E. Motter, and J. Kurths, 2006, Phys. Rev. Lett. **96**, 034101.
Zhou, H., 2003, Eur. Phys. J. B **32**, 265.
Zhou, H., 2005, Phys. Rev. Lett. **94**, 217203.
Zhou, H., and R. Lipowsky, 2005, Proc. Natl. Acad. Sci. U.S.A. **102**, 10052.
Zimmermann, M. G., Eguíluz V. M., and M. San Miguel, 2004, Phys. Rev. E **69**, 065102.